

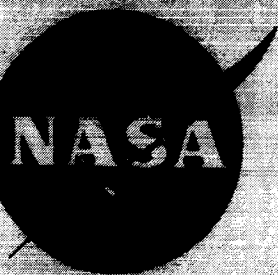
580

NASA TM X-491

NASA TM X-491

CLASSIFICATION CHANGED  
**UNCLASSIFIED**

78 Authority of P 71-617 Date 5 OCT 1971



# TECHNICAL MEMORANDUM

X-491

SUMMARY OF WIND-TUNNEL INVESTIGATIONS OF THE  
STATIC LONGITUDINAL STABILITY CHARACTERISTICS  
OF THE PRODUCTION MERCURY CONFIGURATIONS  
AT MACH NUMBERS FROM 0.05 TO 20

By Steve W. Brown and William C. Moseley, Jr.

Space Task Group  
Langley Field, Va.

Declassified by authority of NASA  
Classification Change Notices No. 215  
Dated \*\*31 DEC 1971

NATIONAL AERONAUTICS AND SPACE ADMINISTRATION  
WASHINGTON

February 1961

REF ID: A6512

DECLASSIFIED

NATIONAL AERONAUTICS AND SPACE ADMINISTRATION

TECHNICAL MEMORANDUM X-491

SUMMARY OF WIND-TUNNEL INVESTIGATIONS OF THE  
STATIC LONGITUDINAL STABILITY CHARACTERISTICS  
OF THE PRODUCTION MERCURY CONFIGURATIONS  
AT MACH NUMBERS FROM 0.05 TO 20\*

By Steve W. Brown and William C. Moseley, Jr.

ABSTRACT

Investigations were conducted in various NASA and AEDC wind tunnels. The test Reynolds numbers generally approximated the estimated Mercury flight Reynolds numbers. Results indicated that the escape configuration is statically stable near an angle of attack of  $0^{\circ}$ , the exit configuration is statically unstable, and the reentry configuration is statically stable.

---

\* Title, Unclassified.

REF ID: A6512  
DECLASSIFIED

NATIONAL AERONAUTICS AND SPACE ADMINISTRATION

TECHNICAL MEMORANDUM X-491

SUMMARY OF WIND-TUNNEL INVESTIGATIONS OF THE  
STATIC LONGITUDINAL STABILITY CHARACTERISTICS  
OF THE PRODUCTION MERCURY CONFIGURATIONS  
AT MACH NUMBERS FROM 0.05 TO 20\*

By Steve W. Brown and William C. Moseley, Jr.

SUMMARY

Wind-tunnel investigations have been made to determine the static longitudinal stability characteristics of the Mercury capsule configurations. These tests were conducted on the escape, exit, and reentry configurations of the production version of the Mercury capsule at the NASA Langley and Ames Research Centers and at the USAF Arnold Engineering and Development Center.

The test results indicate that the production escape configuration (capsule plus escape tower) is statically stable near an angle of attack of  $0^\circ$  throughout the Mach number range from 0 to 6.80. The production exit configuration (capsule with small end forward) is statically unstable throughout the Mach number range from 0 to 6.82. The desired instability was obtained by the addition of the destabilizer flap. This instability assures that the capsule would enter the earth's atmosphere from orbital flight with heat shield forward. (The exit configuration without flap is neutrally stable or slightly stable over a limited angle-of-attack range near  $0^\circ$  for Mach numbers greater than about 4.) The reentry configuration (capsule with blunt end forward) is statically stable throughout the Mach number range from 0 to 20.

INTRODUCTION

Numerous wind-tunnel investigations have been made by the National Aeronautics and Space Administration during the various stages of development of the Project Mercury capsule. Different shapes of blunt nonlifting

---

\*Title, Unclassified.

bodies were tested in an effort to find the one best suited for the requirements of a manned orbital vehicle. (See refs. 1 to 12.) From these early studies evolved the present production Mercury configurations.

The Mercury configurations are defined as the escape, exit, and reentry configurations. The capsule with the escape tower attached is referred to as the escape configuration. With the small end forward and tower removed, the capsule is referred to as the exit configuration, whereas with the blunt end forward the capsule is known as the reentry configuration. Some results of the early wind-tunnel tests on the Mercury configurations are given in references 13 to 17. During the development of the production Mercury configurations, many minor modifications and refinements were made to the configurations. See for example, refs. 18 to 20.) The purpose of this paper is to present the results of wind-tunnel investigations made at the Langley and Ames Research Centers and the Arnold Engineering and Development Center (AEDC) to determine the static longitudinal stability of the production Mercury configurations. Also included are results for the exit configuration without the destabilizer flap. Tests were made at Mach numbers from 0.05 to 20 for a range of Reynolds numbers.

#### SYMBOLS

General arrangement of the configurations showing positive directions of forces and moments is given in figure 1. The symbols and coefficients used in the presentation are defined as follows:

$C_A$  axial-force coefficient,  $\frac{\text{Total axial force}}{qS}$

$C_D$  drag coefficient,  $C_A \cos \alpha + C_N \sin \alpha$

$C_{D,\alpha=0}$  drag coefficient at  $\alpha = 0^\circ$

$C_L$  lift coefficient,  $C_N \cos \alpha - C_A \sin \alpha$

$C_{L_\alpha}$  lift-curve slope per degree at  $\alpha \approx 0^\circ$ ,  $\frac{\partial C_L}{\partial \alpha}$

$C_m$  pitching-moment coefficient,  $\frac{\text{Pitching moment}}{qSd}$

REF ID: A6512

3

$C_{m_\alpha}$	pitching-moment-curve slope per degree at $\alpha \approx 0^\circ$ , $\frac{\partial C_m}{\partial \alpha}$
$C_N$	normal-force coefficient, $\frac{\text{Normal force}}{qS}$
$C_{N_\alpha}$	normal-force-curve slope per degree at $\alpha \approx 0^\circ$ , $\frac{\partial C_N}{\partial \alpha}$
d	capsule maximum diameter, ft
M	free-stream Mach number
p	free-stream static pressure, lb/sq ft
q	free-stream dynamic pressure, $0.7pM^2$ , lb/sq ft
R	Reynolds number (based on capsule maximum diameter)
S	capsule cross-sectional area at station of maximum diameter, sq ft
$\alpha$	angle of attack of model center line, deg

#### TEST FACILITIES

The aerodynamic tests on the production Mercury configurations were conducted in the following NASA and AEDC facilities. Except where otherwise noted, the models were sting-mounted on an internal electrical strain-gage balance.

##### Low Subsonic

The tests at low subsonic speeds were made in the Langley free-flight tunnel which has an octagonal test section with a maximum diameter of 12 feet and is housed in a steel sphere. The tunnel operates at a stagnation pressure of 1 atmosphere over a Mach number range from 0 to 0.1.

##### Transonic

The Langley 8-foot transonic pressure tunnel is a single-return, closed-circuit, pressure-type tunnel capable of operating from  $1/4$  to 1 atmosphere and over a Mach number range from 0.3 to 1.14. The test section is rectangular in cross section and has a cross-sectional area of approximately 50 square feet. The upper and lower walls of the test

section are slotted to permit continuous operation through the transonic speed range.

The AEDC 16-foot transonic circuit of the propulsion wind tunnel is a continuous-flow closed-circuit facility capable of operation from a pressure level which approaches a vacuum to a stagnation pressure of 2.5 atmospheres and over a Mach number range from 0.5 to 1.6. The test section is 16 feet square (in cross section) and 40 feet long. The walls of the test section are perforated and enclosed in a large plenum chamber. A pumping system connected to the plenum chamber, together with the perforated walls, provides a means of unchoking the test section when it is operating at or near sonic speeds and for the attenuation of disturbance waves when it is operating above sonic speeds. (See ref. 21.)

#### Supersonic

The 9- by 7-foot supersonic test section of the Ames Unitary Plan wind tunnel is of the asymmetric sliding-block type in which the variation of the test-section Mach number from 1.4 to 2.6 is achieved by translating in the streamwise direction the fixed contour block which forms the floor of the nozzle. The stagnation pressure can be varied from about 2 to 30 lb/sq in. abs. (See ref. 22.)

The Langley Unitary Plan wind tunnel is of the asymmetric sliding-block, closed-working-section type. The low range test section has a Mach number range from 1.5 to 2.9 and the high range test section, from 2.3 to 5. The working sections are 4 feet high, 4 feet wide, and approximately 7 feet long. The maximum stagnation pressure is approximately 60 lb/sq in. abs for the low range test section and approximately 150 lb/sq in. abs for the high range test section. (See ref. 22.)

#### Hypersonic

One of the tunnels used for the tests at hypersonic speeds was a 2-foot low-density hypersonic tunnel at the Langley Research Center which is a continuous-flow, two-dimensional, closed-circuit, ejector-type tunnel. The operating pressure can be varied from 1/4 to 4 atmospheres and Mach number, from 3 to 7.

The Langley 20-inch hypersonic tunnel is of the continuous blow-down type and is designed to operate at a Mach number of 6. The tunnel has a stagnation-pressure range from 300 lb/sq in. abs to 400 lb/sq in. abs.

The Langley 11-inch hypersonic tunnel is an intermittent blow-down-type tunnel and was designed to operate at Mach numbers of 7 and 10.

This tunnel utilizes interchangeable test sections and is capable of operating from a pressure level of about 5 atmospheres to 45 atmospheres. (See refs. 24 and 25.)

The AEDC tunnel HS-2 is a 50-inch-diameter, arc-driven, Hotshot type tunnel. Air, initially confined to an arc chamber by a diaphragm located near the throat of an attached convergent-divergent nozzle, is heated and compressed by an electric-arc discharge and expanded by the conical nozzle to the test section and vacuum tank. A useful run duration of about 20 milliseconds is obtained. (See ref. 25.) The tunnel HS-2 operates at Mach numbers from 9.9 to 20.

The Ames pressurized ballistic range and the Ames supersonic free-flight tunnel launch the model as a projectile down an instrumented range of recording stations. Analysis of a series of records obtained at these stations determine the model characteristics during flight. The ballistic range is equipped with 24 spark-shadowgraph stations located at various intervals along its 203-foot length. Chronographs record the time intervals between shadowgraphs taken as the model passes each station. The wind tunnel is similar to the range except that the models are fired through a counter-current airstream. The test section of this wind tunnel is equipped with 9 spark-shadowgraph stations spaced at 3-foot intervals. (See refs. 17 and 26.)

#### MODEL DESCRIPTION

The general dimensions and various components of the production Mercury configurations are presented in figure 2. The models were made principally of steel and aluminum except the model tested in the free-flight tunnel, which was constructed of wood.

#### Escape Configuration

Some of the escape models tested did not have all the components of the production version. The minor components, which were expected to have small effects on the aerodynamic characteristics, were not on some of the small models. The  $\frac{1}{4}$ -scale model tested in the Langley free-flight tunnel, the  $\frac{1}{9}$ -scale model tested in the Langley 8-foot transonic pressure tunnel, and the 5.37-percent-scale model tested in a 2-foot low-density tunnel at the Langley Research Center did not have the igniter-cable conduits and junction boxes, the igniter-cable-fairing strap turnbuckles, and the ramp at the base of the rocket. Also the 5.37-percent-scale model did not have the tangential igniter-cable fairings and igniter-cable junction boxes.

The  $\frac{1}{9}$ -scale model tested in both the Ames and Langley Unitary Plan wind tunnels did not have the igniter-cable-fairing strap turnbuckles. One version of the  $\frac{1}{9}$ -scale escape model tested in Langley Unitary Plan wind tunnel had a full-scale parachute-housing diameter of 30 inches.

#### Exit and Reentry Configurations

Most exit models tested were scale models of the production exit configuration shown in figure 2. The model tested in the Langley 20-inch hypersonic tunnel had a full-scale parachute-housing diameter of 30 inches instead of 32 inches. In addition to the models tested with a destabilizer flap, tests were made in the 20-inch hypersonic and 8-foot transonic pressure tunnels for models without destabilizer flaps and with a parachute-housing diameter of 30 inches.

The reentry models tested were scale models of the basic capsule with a parachute-housing diameter of 30 inches and without the destabilizer flap on the face of the antenna housing.

#### TEST CONDITIONS AND ACCURACY

A comparison of the test Reynolds numbers with typical flight Reynolds numbers is given in figure 3. The test Reynolds numbers generally approximated the flight Reynolds numbers with the exception of the high Reynolds numbers of the exit phase. The test conditions are summarized in table I.

The available accuracy estimates for the test data are given in table II.

#### PRESENTATION OF RESULTS

The results of the investigation are presented in the following figures:

#### Figure

Variation of aerodynamic characteristics with angle of attack  
for escape configuration . . . . . 4 to 8

## Figure

Effect of Reynolds number on the longitudinal aerodynamic characteristics of the production escape configuration at $M = 2.5$ . . . . .	9
Variation of aerodynamic characteristics with angle of attack for exit configuration . . . . .	10 to 14
Variation of aerodynamic characteristics with angle of attack for reentry configuration . . . . .	15 to 19
Summary of longitudinal stability characteristics for -	
Escape configuration . . . . .	20
Exit configuration . . . . .	21
Reentry configuration . . . . .	22
Variation of aerodynamic characteristics with angle of attack and Mach number for -	
Escape configuration . . . . .	23
Reentry configuration (with destabilizer flap) . . . . .	24
Reentry configuration (without destabilizer flap) . . . . .	25

## DISCUSSION

## General Comments

For some Mach numbers of the tests made in the Langley 8-foot transonic pressure tunnel of the escape configuration, the Reynolds number was not held constant throughout the range of angle of attack. It was necessary to lower the dynamic pressure at the higher angles of attack because of balance load limitations. The Reynolds numbers for the different angle-of-attack ranges are noted in the figures. Two escape configurations were tested in the Langley Unitary Plan wind tunnel. The production escape configuration (with the full-scale parachute-housing diameter of 32 inches) was tested only for the positive angle-of-attack range. The other configuration, which had a full-scale parachute-housing diameter of 30 inches, was tested for both the positive and negative angle-of-attack ranges.

Summary data from the Ames pressurized ballistic range, the Ames supersonic free-flight tunnel, and the AEDC tunnel HS-2 are included on the summary plot for the reentry configuration (fig. 22). The data is

presented only in summary form because the tests in these facilities were conducted over a limited angle-of-attack range. In correlating the summary data of tunnel HS-2, it might be well to point out that the estimated accuracy of the data was on the order of  $\pm 15$  percent.

The data of figures 23, 24, and 25 are comprehensive plots of the variation of the aerodynamic characteristics of the escape and reentry configurations with angle of attack and Mach number. (Figures 23, 24, and 25 can be found in a pocket at the back of the report.) Also given in tables III, IV, and V are tabulations of the aerodynamic data determined from the faired plots of figures 23, 24, and 25. It has been necessary to extrapolate and estimate over considerable portions of the angle-of-attack range.

#### Escape Configuration

The production escape configuration is statically stable at  $\alpha \approx 0^\circ$ , the trim point. This is shown by the pitching-moment coefficient curves in figure 4. For subsonic, transonic, and low supersonic Mach numbers ( $M = 0.05$  to  $1.80$ ) the configuration is stable over a limited angle-of-attack range ( $\alpha = 0^\circ$  to  $20^\circ$  at  $M = 0.05$  and  $\alpha = 0^\circ$  to  $25^\circ$  at  $M = 1.80$ ). For the high supersonic and the hypersonic Mach numbers ( $M = 2.01$  to  $6.80$ ), the configuration is stable up to the maximum test angle of attack ( $\alpha \approx 25^\circ$ ).

In developing the production Mercury capsule, several modifications have been made to the escape configuration. The modifications, except for the addition of the  $45^\circ$  flow separator, had only small effects on the stability. The flow separator causes a substantial increase in the stability of the escape configuration. (See ref. 19.) At angle of attack, the flow separator creates unsymmetrical flow separation over the capsule in the pitch plane. This unsymmetrical flow separation affects a rearward shift of the center of pressure and hence an increase in the stability of the configuration. The flow separator caused a greater increase in the stability at the subsonic and transonic Mach numbers than it did at the higher Mach numbers. This increase can be seen by the curve for  $C_m \alpha$  in figure 20 where the basic and production

configurations are compared (refs. 13, 15, and 19). The basic configuration (which did not have a flow separator) had marginal stability at the subsonic and transonic Mach numbers. (See ref. 13.) The (d) parts of figures 4 to 8 show data at supersonic speeds for both the 30- and 32-inch parachute housings. Although there was some effect of increasing the housing size the effect was generally small.

The variations of the normal-force coefficient and the lift coefficient with angle of attack are generally linear only up to  $\alpha \approx 5^\circ$ .

(See figs. 5 and 7.) The normal-force-curve slope and the lift-curve slope at  $\alpha = 0^\circ$  are both positive, and they vary slightly with Mach number. (See fig. 20.)

The axial-force coefficient and the drag coefficient for the escape configuration have a nonlinear variation with angle of attack. (See figs. 6 and 8.) The drag coefficient at  $\alpha = 0^\circ$  ( $C_{D,\alpha=0}$ ) increases with increasing Mach number in the subsonic and transonic regions to a maximum near  $M = 1$ , whereas at the supersonic and hypersonic Mach numbers it decreases with increasing Mach number. (See fig. 20.)

The longitudinal aerodynamic characteristics of the production escape configuration were not affected by variation in Reynolds number from  $3.3 \times 10^6$  to  $9 \times 10^6$  at  $M = 2.5$ . (See fig. 9.)

#### Exit Configuration

The production exit configuration is statically unstable throughout the test Mach number and angle-of-attack ranges. (See fig. 10.) This desired instability was obtained by the addition of the destabilizer flap. The instability assures that the capsule will enter the earth's atmosphere from orbital flight with the heat shield forward. The exit configuration without the flap became neutrally stable or slightly stable over a limited angle-of-attack range near  $0^\circ$  for Mach numbers greater than about 4. (See fig. 10.) The effect of the destabilizer flap was an incremental shift in the pitching-moment-coefficient curve near  $\alpha = 0^\circ$ . This shift eliminated the trim point near  $\alpha = 0^\circ$ . The production exit models were tested with the destabilizer flap rotated  $180^\circ$  in roll from its normal location during exit. (See fig. 2 for normal location.)

The variations of the normal-force coefficient and the lift coefficient with angle of attack are generally linear over a limited angle-of-attack range near  $\alpha = 0^\circ$ . (See figs. 11 and 13.) The normal-force-curve slope and the lift-curve slope at  $\alpha = 0^\circ$  are both positive and they are generally constant with Mach number. (See fig. 21.)

The axial-force coefficient and the drag coefficient have a nonlinear variation with angle of attack. (See figs. 12 and 14.) The plot of  $C_{D,\alpha=0}$  against Mach number for the exit configuration (fig. 21) is similar to that for the escape configuration.

### Reentry Configuration

The reentry data presented in this paper are for the basic Mercury reentry configuration which had a full-scale parachute-housing diameter of 30 inches (refs. 13 and 15 to 17). The production Mercury capsule has not been tested in the reentry mode. However, the small increase in parachute-housing diameter should have little or no effect on the stability of the reentry model. The effect of the destabilizer flap on the reentry stability is unknown but the effect is expected to be small.

The reentry configuration is statically stable throughout the test Mach number and angle-of-attack ranges. (See fig. 15.) The variation of  $C_m$  with angle of attack is linear over a limited angle-of-attack range near  $\alpha = 0^\circ$ . The summary plot (fig. 22) shows that  $C_{M_\alpha}$  is negative and generally constant throughout the Mach number range investigated.

The variations of the normal-force coefficient and the lift coefficient with angle of attack are linear over a limited angle-of-attack range near  $\alpha = 0^\circ$ . (See figs. 16 and 18.) In the subsonic and transonic Mach number ranges, the normal-force coefficient is zero or slightly negative up to  $\alpha \approx 10^\circ$ . The summary plot (fig. 22) shows  $C_{N_\alpha}$  has slight negative values at subsonic and transonic speeds and becomes slightly positive at supersonic and hypersonic speeds. The lift-curve slope at  $\alpha = 0^\circ$  is negative and generally constant with Mach number throughout the test Mach number range. The negative lift coefficient and hence negative lift-curve slope at low positive angles of attack is the result of the reentry configuration having a relatively low normal force and a high axial force. The negative lift-curve slope (or low normal force) is desirable, because the resultant force vector of lift and drag rotates with angle of attack so as to be primarily in the axial direction and the astronaut is positioned to withstand high axial loads. On the other hand, the negative lift-curve slope has an undesirable effect since it contributes to capsule dynamic instability.

The axial-force coefficient and the drag coefficient have a non-linear variation with angle of attack. (See figs. 17 and 19.) With increase in Mach number,  $C_{D,\alpha=0}$  increases up to about  $M \approx 4$ , and above this Mach number it remains constant.

REF ID: A6572  
[REDACTED] DECLASSIFIED

11

#### SUMMARY OF RESULTS

Tests have been conducted over a Mach number range of 0.05 to 20 to determine the static stability characteristics of the production Mercury escape, exit, and reentry configurations. The results are summarized as follows:

1. The production escape configuration is statically stable near an angle of attack of  $0^{\circ}$  throughout the Mach number range from 0 to 6.80.
2. The production exit configuration is statically unstable throughout the Mach number range from 0 to 6.82. The desired instability was obtained by the addition of the destabilizer flap. This instability assures that the capsule would enter the earth's atmosphere from orbital flight with the heat shield forward. (The exit configuration without flap is neutrally stable or slightly stable over a limited angle-of-attack range near  $0^{\circ}$  for Mach numbers greater than about 4.)
3. The reentry configuration tested is statically stable throughout the Mach number range from 0 to 20.

Goddard Space Flight Center, Space Task Group,  
National Aeronautics and Space Administration,  
Langley Field, Va., October 3, 1960.

[REDACTED]

## REFERENCES

1. Faget, Maxime A., Garland, Benjamine J., and Buglia, James J.: Preliminary Studies of Manned Satellites - Wingless Configuration: Nonlifting. NACA RM L58E07a, 1958.
2. Carter, Howard S., Kolenkiewicz, Ronald, and English, Roland D.: Principal Results From Wind-Tunnel Stability Tests of Several Proposed Space Capsule Models up to an Angle of Attack of  $33^{\circ}$ . NASA TM X-21, 1959.
3. Lichtenstein, Jacob H., Fisher, Lewis R., Scher, Stanley H., and Lawrence, George F.: Some Static, Oscillatory, and Free-Body Tests of Blunt Bodies at Low Subsonic Speeds. NASA MEMO 2-22-59L, 1959.
4. Pearson, Albin O.: Wind-Tunnel Investigation at Mach Numbers From 0.40 to 1.14 of the Static Aerodynamic Characteristics of a Non-lifting Vehicle Suitable for Reentry. NASA MEMO 4-13-59L, 1959.
5. Turner, Kenneth L., and Shaw, David S.: Wind-Tunnel Investigation at Mach Numbers From 1.60 to 4.50 of the Static-Stability Characteristics of Two Nonlifting Vehicles Suitable for Reentry. NASA MEMO 3-2-59L, 1959.
6. Fisher, Lewis R., Keith, Arvid L., Jr., and DiCamillo, Joseph R.: Aerodynamic Characteristics of Some Families of Blunt Bodies at Transonic Speeds. NASA MEMO 10-28-58L, 1958.
7. Letko, William: Experimental Investigation at a Mach Number of 3.11 of the Lift, Drag, and Pitching-Moment Characteristics of a Number of Blunt Low-Fineness-Ratio Bodies. NASA MEMO 1-18-59L, 1959.
8. Penland, Jim A., and Armstrong, William O.: Preliminary Aerodynamic Data Pertinent to Manned Satellite Reentry Configurations. NACA RM L58E13a, 1958.
9. Scallion, William I.: Full-Scale Wind-Tunnel Investigation of the Low-Speed Static Aerodynamic Characteristics of a Model of a Reentry Capsule. NASA TM X-220, 1959.
10. Pearson, Albin O.: Wind-Tunnel Investigation at Mach Numbers From 0.20 to 1.17 of the Static Aerodynamic Characteristics of a Possible Reentry Capsule. NASA TM X-262, 1960.

REF ID: A6516

REF ID: A6516

13

11. Shaw, David S., and Turner, Kenneth L.: Wind-Tunnel Investigation of Static Aerodynamic Characteristics of a 1/9-Scale Model of a Possible Reentry Capsule at Mach Numbers From 2.29 to 4.65. NASA TM X-233, 1959.
12. Spencer, Bernard, Jr.: An Investigation of the Aerodynamic Characteristics at Subsonic Speeds of a Nonlifting-Type Space-Capsule Model Simulating Escape and Reentry Configurations. NASA TM X-228, 1960.
13. Pearson, Albin O.: Wind-Tunnel Investigation at Mach Numbers From 0.50 to 1.14 of the Static Aerodynamic Characteristics of a Model of a Project Mercury Capsule. NASA TM X-292, 1960.
14. Rittenhouse, Lewis E., and Kaupp, Harry, Jr.: Transonic Wind Tunnel Tests To Determine Some Aerodynamic Characteristics of Two Proposed Escape Configurations for Project Mercury. AEDC-TN-59-76 (Contract No. AF 40(600)-800), Arnold Eng. Dev. Center, July 1959.
15. Shaw, David S. and Turner, Kenneth L.: Wind-Tunnel Investigation of Static Aerodynamic Characteristics of a 1/9-Scale Model of a Project Mercury Capsule at Mach Numbers From 1.60 to 4.65. NASA TM X-291, 1960.
16. Wallace, A. R., and Swain, W. N.: Static Stability, Heat Transfer, and Pressure Distribution Tests of NASA-McDonnell Mercury Models at Mach Numbers 17 to 21. AEDC-TN-59-157 (Contract No. AF 40(600)-800), Arnold Eng. Dev. Center, Jan. 1960.
17. Sommer, Simon C., Short, Barbara J., and Compton, Dale L.: Free-Flight Measurements of Static and Dynamic Stability of Models of the Project Mercury Re-Entry Capsule at Mach Numbers 3 and 9.5. NASA TM X-373, 1960.
18. Rittenhouse, Lewis E., and Kaupp, Harry, Jr.: Experimentally Determined Static Stability and Drag Characteristics for NASA's Project Mercury Manned Orbital Capsule at Transonic Speeds. AEDC-TN-59-130 (Contract No. AF 40(600)-800), Arnold Eng. Dev. Center, Oct. 1959.
19. Rittenhouse, Lewis E., and Kaupp, Harry, Jr.: The Effects of Several External Modifications on the Static Stability Characteristics of the NASA Project Mercury Escape Configuration at Transonic Speeds. AEDC-TN-60-50 (Contract No. AF 40(600)-800), Arnold Eng. Dev. Center, Mar. 1960.
20. Pearson, Albin O.: Wind-Tunnel Investigation at Mach Numbers From 3.0 to 6.8 of the Static Aerodynamic Characteristics of Modified Project Mercury Exit and Escape Configurations. NASA TM X-324, 1960.

21. Anon.: Propulsion Wind Tunnel. Vol. 3 of Test Facilities Handbook, second ed., Arnold Eng. Dev. Center, Jan. 1959.
22. Anon.: Manual for Users of the Unitary Plan Wind Tunnel Facilities of the National Advisory Committee for Aeronautics. NACA, 1956.
23. McLellan, Charles H., Williams, Thomas W., and Beckwith, Ivan E.: Investigation of the Flow Through a Single-Stage Two-Dimensional Nozzle in the Langley 11-Inch Hypersonic Tunnel. NACA TN 2223, 1950.
24. McLellan, Charles H., Williams, Thomas W., and Bertram, Mitchell H.: Investigation of a Two-Step Nozzle in the Langley 11-Inch Hypersonic Tunnel. NACA TN 2171, 1950.
25. Anon.: Gas Dynamics Facility. Vol. 4 of Test Facilities Handbook, second ed., Arnold Eng. Dev. Center, Jan. 1959.
26. Seiff, Alvin: A Free-Flight Wind Tunnel for Aerodynamic Testing at Hypersonic Speeds. NACA Rep. 1222, 1955. (Supersedes NACA RM A52A24.)

DECLASSIFIED

15

2W

TABLE I.- TEST CONDITIONS

Facility	Configuration	Mach number	Stagnation pressure, lb/sq in. abs	Dynamic pressure, lb/sq ft	Stagnation temperature, °F	Reynolds number
Langley free-flight tunnel	Escape and reentry, $\frac{1}{4}$ -scale model	0.05	14.7	3.7	75	$0.60 \times 10^6$
Langley 8-foot transonic pressure tunnel	Escape, $\frac{1}{9}$ -scale model	0.30 .50 .80 1.00 1.14	14.8 14.7 14.7 8.7 8.3  14.7 7.0 5.6  14.7 6.4 4.9	126.0 313 623 367 352  784 372 296  860 375 288	125 125 125 125 125	$1.21 \times 10^6$ 1.89 2.58 1.52 1.46  2.81 1.32 1.06  2.87 1.25 .97
	Exit, $\frac{1}{9}$ -scale model	0.50 .80 1.00 1.14	14.7 14.7 14.7 13.5 14.7	313 623 784 719 860	125 125 125 125	$1.89 \times 10^6$ 2.58 2.81 2.59 2.87
	Exit without destabilizer flap, $\frac{1}{7}$ -scale model	0.50 .80 1.00 1.14	14.7 14.7 14.7 14.7	312 623 783 858	125 125 125 125	$2.42 \times 10^6$ 3.30 3.61 3.68
	Reentry, $\frac{1}{7}$ -scale model	0.50 .60 .70 .80 .90 .95 .98 1.00 1.03 1.14	14.7 14.7 14.7 14.7 14.7 14.7 14.7 14.7 14.7 14.7	312 418 524 623 710 750 770 783 801 858	125 125 125 125 125 125 125 125 125 125	$2.42 \times 10^6$ 2.77 3.06 3.30 3.50 3.56 3.60 3.61 3.62 3.68
AEDC 16-foot transonic circuit	Escape and exit, 32-percent scale model	0.50 .70 .90 1.14 1.30 1.50	16.05 12.7 11.2 10.6 10.6 10.4 11.35	340 450 540 619 652 645 700	120 120 120 120 120 120 140	$6.0 \times 10^6$ 6.0 6.0 6.0 6.0 6.0 6.0
Ames Unitary Plan wind tunnel	Escape, $\frac{1}{9}$ -scale model	1.55 1.80 2.01 2.50	---	---	---	$2.4 \times 10^6$ 2.4 3.3 3.1
	Escape, 32-percent scale model	2.50	---	---	---	$3.3 \times 10^6$ 6.0 9.0

TABLE I.- TEST CONDITIONS - Concluded

Facility	Configuration	Mach number	Stagnation pressure, lb/sq in. abs	Dynamic pressure, lb/sq ft	Stagnation temperature, °F	Reynolds number
Langley Unitary Plan wind tunnel	Escape, $\frac{1}{9}$ -scale model	2.50	{ 21 38	785 1385	{ 150	$\{ 2.50 \times 10^6$ $4.40$
		2.87	{ 26 54	712 1480	{ 150	$\{ 2.50$ $5.21$
		3.94	48	540	175	2.50
		4.65	65	412	175	2.50
		2.30	18	798	150	$2.45 \times 10^6$
	Exit, $\frac{1}{9}$ -scale model	2.87	24	680	150	2.39
		3.94	42	475	175	2.20
		1.60	14.6	885	125	$2.69 \times 10^6$
		2.06	16.2	805	150	2.50
2-foot low-density hypersonic tunnel	Reentry, $\frac{1}{9}$ -scale model	2.87	{ 24.7 38.0	678 1051	{ 150	$\{ 2.39$ $3.67$
		3.94	55.8	624	175	2.20
		4.65	55.0	343	175	2.05
		3.15	14.97	326	263	$0.75 \times 10^6$
		3.92	14.88	169	280	.51
	Exit, 5.37-percent scale model	4.72	24.49	145	310	.35
		5.73	39.60	110	332	.39
		6.80	56.92	77	327	.29
		3.02	14.41	350	262	$0.80 \times 10^6$
		3.96	15.02	165	265	.50
Langley 20-inch hypersonic tunnel	Exit, 5.37-percent scale model	4.70	24.61	148	282	.36
		5.75	40.16	110	310	.40
	Reentry, 5.37-percent scale model	6.82	56.15	75	332	.29
		5.98	267	622	410	$1.60 \times 10^6$
Langley 11-inch hypersonic tunnel	Reentry 3.20-percent scale model	5.98	295	687	410	$1.80 \times 10^6$
		6.66	132	171	675	$0.20 \times 10^6$
Ames pressurized ballistic range	Reentry, 2.21-percent scale model	9.60	412	113	1200	.13
		3.0	11.8	---	---	$2.2 \times 10^6$
Ames supersonic free-flight tunnel	Reentry, 0.60-percent scale model	9.5	---	---	---	$1.4 \times 10^6$
		14.0	---	---	---	1.9
AEDC tunnel HS-2	Reentry, 5.24-percent scale model	19.0	---	0.05	---	$0.06 \times 10^6$

REF ID: A6572  
REF ID: A6572

17

TABLE II.- ACCURACIES

Facility	Configuration	M	$\alpha$ , deg	$C_m$	$C_N$	$C_A$	$C_L$	$C_D$	Accuracy of -	
									$C_m$	$C_N$
Langley 8-foot transonic pressure tunnel	Escape	0.3	$\pm 0.01$	$\pm 0.2$	$\pm 0.03$	$\pm 0.15$	$\pm 0.15$	$\pm 0.15$	$\pm 0.15$	$\pm 0.15$
		.5	$\pm .01$	$\pm .2$	$\pm .016$	$\pm .06$	$\pm .06$	$\pm .06$	$\pm .06$	$\pm .06$
		1.14	$\pm .004$	$\pm .2$	$\pm .016$	$\pm .06$	$\pm .06$	$\pm .06$	$\pm .06$	$\pm .06$
	Exit	0.5	$\pm 0.01$	$\pm 0.2$	$\pm 0.016$	$\pm 0.06$	$\pm 0.06$	$\pm 0.06$	$\pm 0.06$	$\pm 0.06$
		1.14	$\pm .004$	$\pm .2$	$\pm .006$	$\pm .02$	$\pm .02$	$\pm .02$	$\pm .02$	$\pm .02$
	Reentry	0.5	$\pm 0.01$	$\pm 0.2$	$\pm 0.008$	$\pm 0.04$	$\pm 0.04$	$\pm 0.04$	$\pm 0.04$	$\pm 0.04$
AEDC 16-foot transonic circuit	Escape and exit	0.5	$\pm 0.003$	$\pm 0.1$	$\pm 0.007$	$\pm 0.011$	$\pm 0.018$	$\pm 0.011$	$\pm 0.017$	$\pm 0.017$
		1.5	$\pm .005$	$\pm .1$	$\pm .003$	$\pm .005$	$\pm .01$	$\pm .005$	$\pm .005$	$\pm .009$
Langley Unitary Plan Wind tunnel	Escape, exit and reentry	2.3	$\pm 0.05$	$\pm 0.1$	$\pm 0.005$	$\pm 0.024$	$\pm 0.021$	$\pm 0.024$	$\pm 0.021$	$\pm 0.021$
Langley 11-inch hypersonic tunnel	Reentry	6.66	$\pm 0.03$	$\pm 0.1$	$\pm 0.007$	$\pm 0.02$	$\pm 0.008$	$\pm 0.020$	$\pm 0.008$	$\pm 0.008$
Ames Unitary Plan Wind tunnel	Escape, $\frac{1}{9}$ -scale model	9.6	$\pm .03$	$\pm .1$	$\pm .007$	$\pm .02$	$\pm .008$	$\pm .020$	$\pm .008$	$\pm .008$
2-foot low-density tunnel	Escape, 32-percent scale model	1.55 to 2.5	---	---	$\pm .05$	$\pm .007$	$\pm .0035$	$\pm .007$	$\pm .0035$	$\pm .0035$
	Escape and exit	3.02 to 6.82	$\pm 0.1$	$\pm 0.2$	$\pm 0.02$	$\pm 0.04$	$\pm 0.03$	$\pm 0.04$	$\pm 0.03$	$\pm 0.03$

TABLE III.- AERODYNAMIC COEFFICIENTS FOR ESCAPE CONFIGURATION

(a) C<sub>III</sub>

~~UNCLASSIFIED~~

TABLE III. - AERODYNAMIC COEFFICIENTS FOR ESCAPE CONFIGURATION - Continued

(b) CT

$\alpha$ , deg	$C_L$ at -							$C_L$ at +						
	M = 0	M = 0.5	M = 0.7	M = 0.9	M = 1.0	M = 1.15	M = 1.5	M = 2	M = 3	M = 5	M = 7	M = 9.6		
0	0	0	0	0	0	0	0	0	0	0	0	0	0	0
5	.09	.09	.045	.11	.09	.07	.1	.16	.18	.21	.21	.21	.21	.21
10	.17	.17	.21	.17	.16	.14	.2	.25	.30	.33	.33	.33	.33	.33
15	.22	.21	.31	.21	.25	.18	.28	.34	.39	.42	.42	.42	.42	.42
20	.29	.30	.36	.30	.28	.23	.36	.44	.48	.48	.48	.48	.48	.48
25	.36	.36	.39	.39	.37	.35	.44	.55	.55	.52	.52	.52	.52	.52
30	.42	.41	.45	.45	.43	.48	.56	.58	.57	.56	.56	.56	.56	.56
35	.47	.48	.51	.51	.48	.64	.68	.72	.7	.51	.51	.51	.51	.51
40	.49	.50	.55	.55	.48	.76	.72	.72	.66	.44	.44	.44	.44	.44
45	.55	.55	.61	.61	.64	.83	.79	.79	.66	.59	.59	.59	.59	.59
50	.59	.59	.65	.65	.79	.78	.76	.76	.66	.48	.48	.48	.48	.48
55	.62	.62	.66	.66	.66	.66	.52	.46	.39	.3	.3	.3	.3	.3
60	.38	.56	.7	.55	.53	.52	.38	.35	.3	.21	.21	.21	.21	.21
65	.15	.44	.4	.44	.34	.34	.23	.22	.18	.12	.12	.12	.12	.12
70	.1	.33	.3	.3	.23	.15	.08	.05	.02	.01	.01	.01	.01	.01
75	.1	.2	.18	.05	.06	.05	.06	.07	.08	.09	.09	.09	.09	.09
80	.09	.38	.38	.27	.24	.21	.16	.14	.15	.17	.17	.17	.17	.17
85	.08	.38	.44	.39	.35	.28	.22	.19	.21	.21	.21	.21	.21	.21
90	.08	.34	.47	.47	.45	.38	.32	.24	.27	.27	.27	.27	.27	.27
95	.085	.35	.49	.49	.48	.41	.35	.28	.28	.28	.28	.28	.28	.28
100	.1	.36	.48	.48	.47	.42	.36	.29	.27	.27	.27	.27	.27	.27
105	.13	.32	.49	.45	.38	.36	.3	.28	.28	.28	.28	.28	.28	.28
110	.14	.36	.45	.45	.39	.32	.29	.29	.29	.29	.29	.29	.29	.29
115	.14	.38	.49	.49	.43	.36	.32	.27	.27	.25	.25	.25	.25	.25
120	.09	.09	.2	.3	.26	.26	.21	.19	.18	.18	.18	.18	.18	.18
125	.02	.02	.1	.18	.22	.19	.14	.12	.11	.11	.11	.11	.11	.11
130	.06	.08	.0	.08	.08	.08	.04	.04	.04	.03	.03	.03	.03	.03
135	.13	.13	.13	.13	.13	.13	.1	.04	.04	.12	.12	.12	.12	.12
140	.18	.18	.18	.18	.14	.13	.1	.17	.17	.12	.12	.12	.12	.12
145	.22	.23	.2	.2	.18	.18	.17	.17	.17	.21	.21	.21	.21	.21
150	.24	.26	.25	.24	.24	.24	.25	.25	.25	.28	.28	.28	.28	.28
155	.28	.28	.28	.28	.28	.28	.28	.28	.28	.33	.33	.33	.33	.33
160	.29	.29	.29	.29	.28	.28	.28	.28	.28	.34	.34	.34	.34	.34
165	.28	.28	.28	.28	.27	.27	.28	.28	.28	.32	.32	.32	.32	.32
170	.22	.24	.24	.24	.22	.22	.22	.22	.22	.25	.25	.25	.25	.25
175	.14	.14	.14	.14	.12	.12	.12	.12	.12	.14	.14	.14	.14	.14

TABLE III. - AERODYNAMIC COEFFICIENTS FOR ESCAPE CONFIGURATION - Continued

(c)  $C_D$ 

$\alpha$ , deg	$C_D$ at -											
	M = 0	M = 0.5	M = 0.7	M = 0.9	M = 1.0	M = 1.15	M = 1.5	M = 2	M = 3	M = 5	M = 7	M = 9.6
0	0.63	0.64	0.64	0.72	0.92	0.99	0.93	0.78	0.66	0.46	0.23	0.18
5	0.66	0.66	0.7	0.76	0.99	1.03	0.99	0.82	0.5	0.32	.3	.2
10	0.7	.75	.75	.82	1.03	1.03	1.05	0.88	.75	.57	.42	.4
15	.73	.73	.78	.82	1.03	1.03	1.1	0.98	.85	.68	.54	.5
20	.75	.75	.8	.84	1.03	1.03	1.12	1.07	.96	.82	.67	.6
25	.78	.78	.82	.92	1.05	1.05	1.12	1.12	1.08	.96	.86	.78
30	.84	.85	.87	.97	1.08	1.18	1.24	1.19	1.11	.98	.9	.85
35	.86	.9	.92	.98	1.16	1.27	1.46	1.42	1.4	1.26	1.02	.96
40	.88	.92	.92	.98	1.06	1.31	1.32	1.6	1.58	1.42	1.16	1.1
45	.92	.97	.97	1.06	1.44	1.56	1.72	1.74	1.74	1.58	1.31	1.24
50	.98	1.03	1.16	1.16	1.44	1.85	1.85	1.85	1.73	1.58	1.45	1.41
55	1.02	1.08	1.28	1.28	1.62	1.81	1.94	1.94	1.82	1.7	1.6	1.55
60	1.04	1.12	1.37	1.57	1.66	1.86	1.92	2.0	2.06	2.02	1.8	1.73
65	1.05	1.15	1.41	1.6	1.68	1.92	2.0	2.08	2.08	1.98	1.88	1.82
70	1.06	1.16	1.42	1.62	1.7	1.92	2.0	2.08	2.09	2.05	1.95	1.88
75	1.08	1.15	1.59	1.64	1.74	2.11	2.11	2.09	2.09	2.05	1.98	1.89
80	1.1	1.15	1.58	1.54	1.64	1.8	2.16	2.16	2.07	2.01	1.94	1.87
85	1.05	.99	1.28	1.64	1.64	1.8	2.1	2.04	1.97	1.97	1.85	1.79
90	.96	.95	1.26	1.63	1.78	2.02	1.98	1.93	1.93	1.87	1.8	1.75
95	.92	.93	1.24	1.6	1.74	1.96	1.92	1.85	1.85	1.74	1.66	1.64
100	.9	.92	1.2	1.55	1.69	1.88	1.81	1.78	1.74	1.67	1.58	1.55
105	.9	.9	1.13	1.48	1.63	1.81	1.74	1.72	1.68	1.6	1.54	1.51
110	.9	.88	1.07	1.4	1.56	1.74	1.74	1.72	1.61	1.53	1.45	1.42
115	.88	.86	1.03	1.35	1.49	1.68	1.68	1.67	1.67	1.61	1.53	1.49
120	.86	.85	1.0	1.3	1.43	1.61	1.61	1.62	1.57	1.47	1.37	1.36
125	.86	.85	1.	1.26	1.38	1.54	1.54	1.59	1.55	1.43	1.33	1.32
130	.87	.84	1.	1.24	1.33	1.46	1.46	1.57	1.55	1.43	1.33	1.32
135	.89	.85	1.	1.22	1.32	1.42	1.42	1.57	1.55	1.46	1.36	1.35
140	.92	.88	1.	1.22	1.31	1.4	1.4	1.57	1.55	1.48	1.38	1.37
145	.95	.92	1.01	1.22	1.31	1.4	1.4	1.58	1.56	1.48	1.38	1.37
150	.97	.94	1.02	1.22	1.31	1.4	1.4	1.59	1.56	1.46	1.36	1.35
155	.98	.95	1.03	1.22	1.31	1.4	1.4	1.61	1.56	1.46	1.36	1.35
160	1.0	.98	1.04	1.22	1.31	1.4	1.4	1.62	1.56	1.46	1.36	1.35
165	1.01	.99	1.04	1.22	1.31	1.4	1.4	1.62	1.56	1.46	1.36	1.35
170	1.02	1.0	1.04	1.22	1.31	1.4	1.4	1.62	1.56	1.46	1.36	1.35
175	1.02	1.01	1.04	1.22	1.31	1.4	1.4	1.62	1.56	1.46	1.36	1.35
180	1.02	1.02	1.04	1.22	1.31	1.4	1.4	1.62	1.56	1.46	1.36	1.35

TABLE III.- AERODYNAMIC COEFFICIENTS FOR ESCAPE CONFIGURATION - Continued

(d)  $C_N$ 

$\alpha$ , deg	$C_N$ at -								$M = 9.6$			
	$M = 0$	$M = 0.5$	$M = 0.7$	$M = 0.9$	$M = 1.0$	$M = 1.15$	$M = 1.5$	$M = 2$	$M = 3$	$M = 5$	$M = 7$	
0	0	.147	.106	0	.176	0	.151	0	.159	0	.19	0
5	.147	.289	.298	.310	.336	.310	.350	.327	.353	.36	.21	.22
10	.289	.421	.434	.444	.459	.446	.524	.520	.51	.55	.36	.36
15	.421	.529	.538	.565	.569	.615	.592	.704	.683	.66	.52	.52
20	.529	.656	.656	.7	.742	.779	.772	.872	.910	.83	.65	.65
25	.656										.77	
30	.784	.780	.825	.918	.975	.906	1.105	1.097	1.05	.97	.87	
35	.878	.909	.970	1.129	1.206	1.270	1.572	1.277	1.2	1.08	1.03	.98
40	.941	1.013	1.113	1.343	1.414	1.521	1.580	1.552	1.39	1.20	1.12	1.07
45	1.004	1.117	1.301	1.520	1.690	1.739	1.697	1.51	1.32	1.24	1.18	
50	1.066	1.207	1.377	1.611	1.696	1.806	1.841	1.796	1.63	1.45	1.32	
55	1.099	1.240	1.485	1.612	1.706	1.861	1.888	1.853	1.71	1.56	1.43	
60	1.091	1.250	1.536	1.635	1.703	1.871	1.922	1.924	1.8	1.66	1.6	1.55
65	1.015	1.241	1.523	1.450	1.692	1.884	1.964	1.978	1.87	1.75	1.69	1.63
70	1.962	1.220	1.471	1.625	1.676	1.921	1.982	1.981	2.07	1.83	1.76	1.72
75	1.017	1.163	1.389	1.592	1.696	2.025	2.003	1.962	1.96	1.89	1.8	1.77
80	1.068	1.998	1.254	1.568	1.721	2.091	2.011	1.955	1.97	1.88	1.84	1.78
85	1.039	.955	1.237	1.600	1.764	2.068	2.013	1.946	1.96	1.84	1.82	1.76
90	.96	.95	1.26	1.63	1.78	2.02	1.98	1.93	1.9	1.8	1.75	
95	.924	.957	1.278	1.636	1.769	1.983	1.937	1.88	1.84	1.76	1.67	
100	.904	.969	1.265	1.668	1.737	1.914	1.872	1.83	1.76	1.68	1.58	
105	.905	.952	1.218	1.516	1.673	1.841	1.797	1.783	1.75	1.69	1.57	
110	.894	.916	1.159	1.463	1.599	1.721	1.715	1.68	1.6	1.60	1.49	
115	.857	.855	1.060	1.364	1.503	1.658	1.628	1.57	1.49	1.34	1.26	
120	.790	.781	.966	1.276	1.388	1.524	1.508	1.45	1.36	1.19	1.09	
125	.716	.691	.877	1.155	1.257	1.571	1.583	1.54	1.25	1.06	.99	
130	.628	.592	.766	1.001	1.083	1.195	1.241	1.21	1.11	.84	.87	
135	.537	.509	.651	.834	.933	1.032	1.089	1.07	.98	.81	.63	
140	.433	.428	.526	.685	.765	.869	.917	.92	.84	.69	.58	
145	.365	.359	.415	.552	.612	.656	.734	.75	.66	.55	.44	
150	.277	.245	.294	.402	.447	.484	.553	.57	.5	.41	.32	
155	.160	.148	.182	.262	.300	.358	.377	.4	.34	.28	.22	
160	.069	.053	.093	.135	.166	.197	.231	.24	.2	.16	.12	
165	.009	.014	.008	.045	.078	.092	.110	.12	.1	.06	.04	
170	-.040	-.063	-.016	-.005	-.011	-.017	-.035	.04	.03	0	-.02	
175	-.051	-.029	-.043	-.005	-.007	0	-.002	.01	0	-.02	-.11	
180	0	0	0	0	0	0	0	0	0	0	0	

TABLE III. - AERODYNAMIC COEFFICIENTS FOR ESCAPE CONFIGURATION - Concluded

22

(e)  $C_A$ 

$\alpha$ , deg	C <sub>A</sub> at -							M = 9.6			
	M = 0	M = 0.5	M = 0.7	M = 0.9	M = 1.0	M = 1.15	M = 1.5	M = 2	M = 3	M = 5	M = 7
0	0.63	0.64	0.64	0.72	0.92	0.90	0.78	0.46	0.30	0.23	0.18
5	.65	.65	.69	.75	.98	.92	.81	.49	.32	.28	.18
10	.66	.66	.71	.78	.99	.95	.85	.52	.41	.34	.34
15	.65	.64	.69	.73	.94	.97	.87	.57	.42	.38	.40
20	.61	.60	.65	.69	.87	.96	.88	.62	.49	.47	.42
25	.55	.55	.58	.67	.80	.88	.83	.77	.64	.56	.49
30	.52	.52	.53	.59	.69	.78	.79	.74	.68	.57	.45
35	.43	.46	.44	.48	.57	.63	.77	.78	.70	.61	.53
40	.36	.35	.35	.39	.47	.55	.76	.76	.69	.64	.57
45	.30	.25	.20	.33	.55	.57	.72	.76	.72	.69	.62
50	.25	.16	.16	.32	.41	.52	.68	.74	.74	.72	.66
55	.21	.11	.11	.35	.39	.50	.69	.74	.72	.73	.67
60	.23	.08	.08	.31	.37	.48	.67	.71	.69	.72	.68
65	.51	.06	.04	.07	.28	.50	.66	.67	.68	.68	.67
70	.46	.10	.11	.27	.37	.54	.64	.67	.73	.68	.67
75	.38	.10	.19	.40	.59	.59	.60	.61	.60	.62	.62
80	.28	.56	.61	.55	.55	.55	.52	.49	.49	.50	.56
85	.17	.44	.55	.44	.44	.49	.46	.40	.36	.37	.46
90	.08	.34	.47	.45	.38	.32	.25	.24	.24	.27	.37
95	.01	.27	.38	.34	.26	.18	.11	.09	.10	.13	.24
100	-.06	.19	.26	.26	.12	.05	.04	.05	.05	.03	.10
105	-.11	.08	.18	.05	-.05	-.17	-.17	-.16	-.14	-.09	-.02
110	-.18	-.06	0	-.07	-.17	-.28	-.32	-.30	-.22	-.19	-.14
115	-.25	-.20	-.16	-.23	-.30	-.42	-.46	-.44	-.35	-.31	-.27
120	-.35	-.35	-.33	-.39	-.26	-.12	-.05	-.05	-.05	-.03	-.02
125	-.46	-.46	-.49	-.58	-.61	-.73	-.80	-.74	-.62	-.58	-.55
130	-.61	-.60	-.64	-.86	-.85	-.74	-.96	-.97	-.79	-.75	-.81
135	-.72	-.69	-.76	-.89	-.93	-.98	-.1.13	-.1.14	-.1.08	-.98	-.94
140	-.82	-.79	-.86	-.1.02	-.1.07	-.1.10	-.1.28	-.1.29	-.1.23	-.1.15	-.1.16
145	-.90	-.89	-.94	-.1.10	-.1.17	-.1.25	-.1.41	-.1.43	-.1.37	-.1.27	-.1.26
150	-.96	-.94	-.98	-.1.01	-.1.18	-.1.25	-.1.34	-.1.32	-.1.25	-.1.24	-.1.24
155	-.96	-.01	-.02	-.1.05	-.1.22	-.1.31	-.1.39	-.1.35	-.1.32	-.1.28	-.1.42
160	-.96	-.04	-.05	-.1.07	-.1.25	-.1.34	-.1.42	-.1.42	-.1.35	-.1.33	-.1.47
165	-.96	-.04	-.03	-.1.07	-.1.25	-.1.34	-.1.42	-.1.42	-.1.35	-.1.33	-.1.49
170	-.96	-.03	-.02	-.1.05	-.1.06	-.1.24	-.1.33	-.1.32	-.1.25	-.1.22	-.1.50
175	-.96	-.02	-.02	-.1.05	-.1.06	-.1.23	-.1.32	-.1.31	-.1.25	-.1.22	-.1.51
180	-.96	-.02	-.02	-.1.04	-.1.04	-.1.22	-.1.30	-.1.30	-.1.24	-.1.22	-.1.53

REF ID: A6573  
RECLASSIFIED

TABLE IV. - AERODYNAMIC COEFFICIENTS FOR REENTRY CONFIGURATION WITH DESTABILIZER FLAP

(a)  $c_m$

$\alpha$ , deg	C <sub>m</sub> at -													
	M = 0	M = 0.5	M = 0.7	M = 0.9	M = 1.0	M = 1.1	M = 1.3	M = 1.6	M = 2.0	M = 3.0	M = 5.0	M = 7.0	M = 9.6	M = 20.0
-0	0	0	0	0	0	0	0	0	0	0	0	0	0	0
-5	.01	.01	.01	.01	.01	.01	.01	.01	.01	.01	.02	.02	.012	.012
-10	.02	.02	.02	.02	.02	.02	.02	.02	.02	.02	.035	.035	.03	.03
-15	.03	.03	.03	.03	.03	.03	.03	.03	.03	.03	.055	.055	.045	.045
-20	.045	.045	.045	.045	.045	.048	.048	.048	.048	.048	.065	.065	.06	.06
-25	.055	.055	.055	.055	.055	.058	.058	.058	.058	.058	.075	.075	.075	.075
-30	.11	.13	.15	.17	.192	.192	.188	.188	.188	.188	.102	.102	.1	.1
-35	.16	.16	.16	.17	.175	.175	.175	.175	.175	.175	.125	.125	.125	.125
-40	.18	.18	.17	.17	.165	.165	.162	.162	.162	.162	.152	.152	.155	.155
-45	.17	.17	.15	.15	.155	.155	.152	.152	.152	.152	.178	.178	.18	.18
-50	.15	.15	.13	.13	.145	.145	.145	.145	.145	.145	.205	.205	.2	.2
-55	.13	.13	.13	.13	.145	.145	.145	.145	.145	.145	.225	.225	.225	.225
-60	.12	.115	.13	.16	.194	.194	.192	.192	.192	.192	.24	.24	.238	.238
-65	.108	.11	.13	.165	.2	.2	.205	.205	.205	.205	.245	.245	.245	.245
-70	.095	.1	.125	.125	.17	.17	.21	.21	.21	.21	.245	.245	.245	.245
-75	.09	.1	.125	.125	.175	.175	.22	.22	.22	.22	.248	.248	.248	.248
-80	.085	.1	.125	.125	.185	.185	.225	.225	.225	.225	.25	.25	.25	.25
-85	.08	.1	.13	.13	.19	.19	.235	.235	.235	.235	.252	.252	.25	.25
-90	.078	.1	.13	.195	.245	.245	.245	.245	.245	.245	.268	.268	.258	.258
-95	.065	.093	.12	.19	.255	.255	.255	.255	.255	.255	.27	.27	.262	.262
-100	.055	.088	.105	.185	.235	.235	.25	.25	.25	.25	.265	.265	.265	.265
-105	.16	.163	.175	.175	.22	.22	.264	.264	.264	.264	.276	.276	.265	.265
-110	.23	.188	.235	.235	.25	.25	.285	.285	.285	.285	.29	.29	.268	.268
-115	.265	.24	.25	.27	.288	.288	.29	.29	.29	.29	.295	.295	.27	.27
-120	.275	.238	.26	.297	.31	.31	.302	.302	.302	.302	.268	.268	.25	.25
-125	.275	.24	.295	.342	.34	.34	.298	.298	.298	.298	.265	.265	.255	.255
-130	.26	.245	.31	.367	.36	.35	.33	.33	.33	.33	.225	.225	.205	.205
-135	.25	.245	.304	.36	.357	.358	.31	.31	.31	.31	.238	.238	.17	.17
-140	.253	.232	.28	.32	.32	.32	.308	.308	.308	.308	.195	.195	.145	.145
-145	.245	.212	.245	.275	.28	.28	.27	.27	.27	.27	.172	.172	.125	.125
-150	.19	.19	.21	.25	.25	.25	.22	.22	.22	.22	.158	.158	.1	.1
-155	.173	.17	.18	.19	.19	.19	.18	.18	.18	.18	.12	.12	.07	.07
-160	.155	.152	.157	.15	.152	.15	.15	.15	.15	.15	.103	.103	.05	.05
-165	.132	.125	.125	.115	.115	.115	.11	.11	.11	.11	.088	.088	.035	.035
-170	.105	.1	.095	.088	.088	.08	.08	.08	.08	.08	.065	.065	.03	.03
-175	.063	.065	.065	.065	.065	.06	.05	.05	.05	.05	.048	.048	.04	.04
-180	.055	.055	.055	.055	.055	.05	.05	.05	.05	.05	.04	.04	.045	.045

TABLE IV. - AERODYNAMIC COEFFICIENTS FOR REENTRY CONFIGURATION WITH DESTABILIZER FLAP - Continued

(b)  $c_T$

UNCLASSIFIED

25

TABLE IV. - AERODYNAMIC COEFFICIENTS FOR REENTRY CONFIGURATION WITH DESTABILIZER FLAP - Continued

(c)  $c_D$

TABLE IV. - AERODYNAMIC COEFFICIENTS FOR REENTRY CONFIGURATION WITH DESTABILIZER FLAP - Continued

(d)  $C_N$

$\alpha_i$ , deg	C <sub>N</sub> at -										M = 20.0			
	M = 0	M = 0.5	M = 0.7	M = 0.9	M = 1.0	M = 1.1	M = 1.3	M = 1.6	M = 2.0	M = 3.0	M = 5.0	M = 7.0	M = 9.6	M = 20.0
0	0	0	0	0	0	0	0	0	0	0	0	0	0	0
-5	.01	.01	.01	.01	.01	.01	.01	.01	.02	.02	.03	.03	.03	.03
-10	.01	.01	.01	.01	.01	.01	.01	.01	.01	.01	.01	.01	.01	.01
-15	.01	.01	.01	.01	.01	.01	.01	.01	.01	.01	.01	.01	.01	.01
-20	.04	.03	.03	.03	.03	.03	.03	.03	.04	.04	.04	.04	.04	.04
-25	.09	.08	.08	.08	.08	.08	.08	.08	.09	.09	.09	.09	.09	.09
-30	.15	.12	.12	.12	.12	.12	.12	.12	.13	.13	.13	.13	.13	.13
-35	.24	.23	.23	.23	.23	.23	.23	.23	.24	.24	.24	.24	.24	.24
-40	.32	.30	.30	.30	.30	.30	.30	.30	.31	.31	.31	.31	.31	.31
-45	.40	.37	.38	.38	.38	.38	.38	.38	.39	.39	.39	.39	.39	.39
-50	.48	.43	.47	.47	.47	.47	.47	.47	.48	.48	.48	.48	.48	.48
-55	.53	.49	.55	.55	.55	.55	.55	.55	.56	.56	.56	.56	.56	.56
-60	.55	.54	.59	.59	.59	.59	.59	.59	.60	.60	.60	.60	.60	.60
-65	.58	.58	.67	.67	.67	.67	.67	.67	.68	.68	.68	.68	.68	.68
-70	.61	.72	.72	.72	.72	.72	.72	.72	.73	.73	.73	.73	.73	.73
-75	.53	.53	.76	.76	.76	.76	.76	.76	.77	.77	.77	.77	.77	.77
-80	.52	.67	.80	.80	.80	.80	.80	.80	.81	.81	.81	.81	.81	.81
-85	.50	.70	.87	.87	.87	.87	.87	.87	.88	.88	.88	.88	.88	.88
-90	.51	.74	.9	.9	.9	.9	.9	.9	.98	.98	.98	.98	.98	.98
-95	.53	.77	.91	.91	.91	.91	.91	.91	.98	.98	.98	.98	.98	.98
-100	.59	.81	.92	.92	.92	.92	.92	.92	.98	.98	.98	.98	.98	.98
-105	.65	.86	.95	.95	.95	.95	.95	.95	.98	.98	.98	.98	.98	.98
-110	.72	.84	.91	.91	.91	.91	.91	.91	.98	.98	.98	.98	.98	.98
-115	.79	.91	.91	.91	.91	.91	.91	.91	.98	.98	.98	.98	.98	.98
-120	.90	.95	.95	.95	.95	.95	.95	.95	.98	.98	.98	.98	.98	.98
-125	.97	.87	.95	.95	.95	.95	.95	.95	.98	.98	.98	.98	.98	.98
-130	.96	.86	.95	.95	.95	.95	.95	.95	.98	.98	.98	.98	.98	.98
-135	.94	.84	.91	.91	.91	.91	.91	.91	.98	.98	.98	.98	.98	.98
-140	.91	.85	.85	.85	.85	.85	.85	.85	.98	.98	.98	.98	.98	.98
-145	.72	.85	.73	.73	.73	.73	.73	.73	.98	.98	.98	.98	.98	.98
-150	.64	.67	.74	.74	.74	.74	.74	.74	.98	.98	.98	.98	.98	.98
-155	.57	.6	.65	.65	.65	.65	.65	.65	.98	.98	.98	.98	.98	.98
-160	.49	.5	.53	.53	.53	.53	.53	.53	.98	.98	.98	.98	.98	.98
-165	.41	.41	.54	.54	.54	.54	.54	.54	.98	.98	.98	.98	.98	.98
-170	.31	.3	.32	.32	.32	.32	.32	.32	.98	.98	.98	.98	.98	.98
-175	.20	.2	.21	.21	.21	.21	.21	.21	.98	.98	.98	.98	.98	.98
-180	.06	.06	.06	.06	.06	.06	.06	.06	.98	.98	.98	.98	.98	.98

DECLASSIFIED

27

TABLE IV. - AERODYNAMIC COEFFICIENTS FOR REENTRY CONFIGURATION WITH DESTABILIZER FLAP - Concluded

(e)  $C_A$ 

$\alpha$ , deg	M = 0	$C_A$ at -								M = 2.0	M = 3.0	M = 4.0	M = 5.0	M = 6.0	M = 7.0	M = 8.0	M = 9.0	M = 10.0
		M = 0.5	M = 0.7	M = 0.9	M = 1.0	M = 1.1	M = 1.3	M = 1.5	M = 1.6									
0	1.00	1.02	1.10	1.23	1.34	1.4	1.46	1.49	1.53	1.60	1.65	1.69	1.75	1.80	1.85	1.90	1.95	1.50
-5	1.02	1.03	1.11	1.24	1.33	1.4	1.45	1.48	1.51	1.59	1.53	1.46	1.40	1.35	1.30	1.25	1.18	1.48
-10	1.02	1.01	1.11	1.25	1.35	1.4	1.46	1.49	1.52	1.60	1.52	1.45	1.41	1.39	1.33	1.25	1.45	1.45
-15	1.01	1.02	1.09	1.23	1.33	1.4	1.44	1.48	1.50	1.56	1.45	1.41	1.39	1.31	1.21	1.26	1.31	1.39
-20	.99	1.00	1.06	1.19	1.31	1.38	1.42	1.45	1.47	1.51	1.38	1.37	1.31	1.26	1.26	1.26	1.26	1.26
-25	.97	.96	1.04	1.17	1.31	1.38	1.42	1.41	1.43	1.45	1.30	1.28	1.28	1.26	1.26	1.26	1.26	1.26
-30	.94	.95	1.00	1.12	1.29	1.37	1.41	1.41	1.44	1.49	1.33	1.29	1.21	1.19	1.19	1.19	1.19	1.19
-35	.87	.87	.85	.98	1.16	1.23	1.29	1.29	1.29	1.30	1.21	1.21	1.07	1.08	1.08	1.08	1.08	1.08
-40	.79	.79	.79	.85	.95	1.16	1.19	1.16	1.16	1.16	1.05	1.05	1.09	1.07	1.07	1.07	1.07	1.07
-45	.68	.71	.78	.87	.95	1.03	1.04	1.03	1.03	1.03	.97	.92	.85	.84	.83	.83	.83	.83
-50	.57	.60	.65	.73	.88	.9	.88	.88	.88	.83	.72	.61	.71	.70	.69	.69	.69	.69
-55	.46	.45	.49	.56	.73	.75	.75	.75	.75	.67	.56	.66	.57	.54	.53	.53	.53	.53
-60	.35	.35	.34	.45	.58	.59	.59	.59	.59	.51	.48	.52	.45	.39	.40	.40	.40	.40
-65	.25	.25	.21	.31	.41	.44	.44	.44	.44	.36	.34	.36	.31	.27	.28	.28	.28	.28
-70	.15	.15	.11	.15	.26	.28	.26	.26	.26	.23	.22	.21	.16	.15	.15	.15	.15	.15
-75	.05	.05	.01	.05	.09	.1	.09	.09	.09	.09	.09	.09	0	0	.02	.02	.02	.02
-80	-.05	-.08	-.07	-.03	-.08	-.06	-.06	-.06	-.06	-.05	-.04	-.04	-.07	-.12	-.17	-.17	-.17	-.17
-85	-.12	-.16	-.23	-.28	-.25	-.24	-.24	-.24	-.24	-.16	-.18	-.18	-.22	-.22	-.25	-.25	-.25	-.25
-90	-.16	-.25	-.32	-.41	-.38	-.37	-.37	-.37	-.37	-.28	-.28	-.28	-.31	-.26	-.3	-.3	-.3	-.3
-95	-.21	-.29	-.39	-.48	-.51	-.51	-.51	-.51	-.51	-.41	-.41	-.41	-.37	-.30	-.27	-.27	-.27	-.27
-100	-.25	-.32	-.37	-.48	-.57	-.57	-.57	-.57	-.57	-.52	-.52	-.52	-.45	-.34	-.44	-.44	-.44	-.44
-105	-.09	-.26	-.35	-.48	-.56	-.6	-.6	-.6	-.6	-.57	-.57	-.57	-.49	-.38	-.47	-.47	-.47	-.47
-110	-.09	-.18	-.3	-.47	-.56	-.56	-.56	-.56	-.56	-.55	-.55	-.55	-.54	-.52	-.47	-.5	-.5	-.5
-115	.09	-.13	-.22	-.42	-.48	-.48	-.48	-.48	-.48	-.54	-.54	-.54	-.57	-.56	-.54	-.54	-.54	-.54
-120	.05	-.15	-.15	-.2	-.39	-.45	-.47	-.47	-.47	-.51	-.57	-.64	-.62	-.58	-.55	-.55	-.55	-.55
-125	-.01	-.19	-.2	-.2	-.38	-.47	-.47	-.47	-.47	-.51	-.58	-.67	-.66	-.61	-.55	-.55	-.55	-.55
-130	-.09	-.18	-.25	-.35	-.47	-.51	-.49	-.49	-.49	-.57	-.59	-.71	-.69	-.62	-.47	-.47	-.47	-.47
-135	-.18	-.25	-.25	-.19	-.33	-.47	-.46	-.46	-.46	-.56	-.63	-.73	-.69	-.65	-.5	-.52	-.52	-.52
-140	-.29	-.29	-.26	-.26	-.37	-.54	-.54	-.54	-.54	-.66	-.66	-.72	-.69	-.57	-.52	-.52	-.52	-.52
-145	-.37	-.34	-.34	-.32	-.38	-.57	-.57	-.57	-.57	-.65	-.65	-.68	-.68	-.62	-.52	-.52	-.52	-.52
-150	-.42	-.41	-.41	-.48	-.66	-.74	-.72	-.72	-.72	-.74	-.74	-.74	-.69	-.58	-.52	-.52	-.52	-.52
-155	-.47	-.45	-.45	-.48	-.73	-.75	-.79	-.79	-.79	-.86	-.86	-.82	-.73	-.67	-.56	-.52	-.52	-.52
-160	-.50	-.5	-.54	-.54	-.8	-.85	-.84	-.84	-.84	-.91	-.91	-.89	-.82	-.71	-.63	-.52	-.52	-.52
-165	-.53	-.52	-.52	-.57	-.7	-.84	-.88	-.88	-.88	-.95	-.95	-.95	-.88	-.76	-.59	-.49	-.49	-.49
-170	-.56	-.54	-.58	-.74	-.88	-.9	-.9	-.9	-.9	-.98	-.98	-.98	-.84	-.72	-.51	-.41	-.41	-.41
-175	-.57	-.57	-.56	-.75	-.88	-.9	-.9	-.9	-.9	-.98	-.98	-.98	-.85	-.72	-.51	-.31	-.29	-.29
-180	-.56	-.56	-.55	-.72	-.88	-.9	-.9	-.9	-.9	-.98	-.98	-.98	-.85	-.72	-.51	-.28	-.26	-.26

TABLE V.—AERODYNAMIC COEFFICIENTS FOR REENTRY CONFIGURATION WITHOUT DESTABILIZER FLAP

(a) C<sub>m</sub>

REF CLASSIFIED

TABLE V.- AERODYNAMIC COEFFICIENTS FOR REENTRY CONFIGURATION WITHOUT DESTABILIZER FLAP - Continued

(b) c<sub>T</sub>

$\alpha$ , deg	C <sub>L</sub> at -							C <sub>L</sub> at +						
	M = 0	M = 0.5	M = 0.7	M = 0.9	M = 1.0	M = 1.1	M = 1.2	M = 1.6	M = 2.0	M = 3.0	M = 5.0	M = 7.0	M = 9.6	M = 20.0
0	0	0	0	0	0	0	0	0	0	0	0	0	0	0
5	-1.10	-1.19	-1.26	-1.30	-1.22	-1.23	-1.22	-1.12	-1.12	-1.11	-1.10	-1.10	-1.10	-1.10
10	-1.19	-1.26	-1.30	-1.33	-1.32	-1.32	-1.32	-1.23	-1.23	-1.22	-1.20	-1.20	-1.20	-1.20
15	-1.25	-1.30	-1.35	-1.37	-1.39	-1.40	-1.40	-1.32	-1.32	-1.30	-1.29	-1.29	-1.28	-1.28
20	-1.30	-1.35	-1.37	-1.40	-1.42	-1.42	-1.40	-1.34	-1.34	-1.30	-1.29	-1.29	-1.24	-1.24
25	-1.33	-1.35	-1.39	-1.41	-1.42	-1.42	-1.40	-1.34	-1.34	-1.30	-1.29	-1.29	-1.24	-1.24
30	-1.35	-1.35	-1.36	-1.38	-1.40	-1.40	-1.40	-1.34	-1.34	-1.30	-1.29	-1.29	-1.24	-1.24
35	-1.30	-1.28	-1.28	-1.30	-1.32	-1.32	-1.30	-1.26	-1.26	-1.23	-1.22	-1.22	-1.20	-1.20
40	-1.26	-1.28	-1.28	-1.30	-1.32	-1.32	-1.30	-1.26	-1.26	-1.23	-1.22	-1.22	-1.20	-1.20
45	-1.20	-1.24	-1.24	-1.28	-1.30	-1.30	-1.30	-1.26	-1.26	-1.23	-1.22	-1.22	-1.20	-1.20
50	-1.15	-1.18	-1.18	-1.20	-1.20	-1.20	-1.20	-1.16	-1.16	-1.14	-1.14	-1.14	-1.12	-1.12
55	-1.08	-1.08	-1.10	-1.10	-1.12	-1.12	-1.12	-1.12	-1.12	-1.05	-1.03	-1.03	-1.00	-1.00
60	-1.02	-1.01	0	0	-0.94	-0.94	-0.94	-0.96	-0.96	-0.91	-0.86	-0.86	-0.80	-0.80
65	0	0.06	0.08	0.08	0.05	0.05	0.05	0.02	0.02	0.11	0.13	0.13	0.09	0.09
70	0.04	0.11	0.17	0.17	0.16	0.16	0.16	0.10	0.10	0.17	0.17	0.17	0.16	0.16
75	0.10	0.16	0.25	0.25	0.25	0.25	0.25	0.20	0.20	0.23	0.23	0.23	0.20	0.20
80	0.14	0.20	0.30	0.30	0.30	0.30	0.30	0.27	0.27	0.27	0.27	0.27	0.25	0.25
85	0.16	0.22	0.38	0.38	0.38	0.38	0.38	0.32	0.32	0.32	0.32	0.32	0.30	0.30
90	0.16	0.23	0.42	0.42	0.42	0.42	0.42	0.38	0.38	0.38	0.38	0.38	0.36	0.36
95	0.16	0.23	0.42	0.42	0.42	0.42	0.42	0.38	0.38	0.38	0.38	0.38	0.36	0.36
100	0.14	0.20	0.28	0.28	0.28	0.28	0.28	0.22	0.22	0.25	0.25	0.25	0.22	0.22
105	0.10	0.05	0.05	0.05	0.05	0.05	0.05	0.02	0.02	0.07	0.07	0.07	0.06	0.06
110	-0.37	-0.31	-0.21	-0.21	-0.21	-0.21	-0.21	-0.15	-0.15	-0.13	-0.13	-0.13	-0.05	-0.05
115	-0.47	-0.44	-0.31	-0.31	-0.31	-0.31	-0.31	-0.26	-0.26	-0.23	-0.23	-0.23	-0.16	-0.16
120	-0.52	-0.52	-0.50	-0.49	-0.49	-0.49	-0.49	-0.38	-0.38	-0.32	-0.32	-0.32	-0.26	-0.26
125	-0.56	-0.55	-0.58	-0.54	-0.54	-0.54	-0.54	-0.46	-0.46	-0.39	-0.39	-0.39	-0.34	-0.34
130	-0.55	-0.55	-0.62	-0.62	-0.62	-0.62	-0.62	-0.56	-0.56	-0.51	-0.51	-0.51	-0.43	-0.43
135	-0.51	-0.53	-0.66	-0.66	-0.66	-0.66	-0.66	-0.60	-0.60	-0.51	-0.51	-0.51	-0.46	-0.46
140	-0.44	-0.46	-0.63	-0.63	-0.63	-0.63	-0.63	-0.56	-0.56	-0.49	-0.49	-0.49	-0.46	-0.46
145	-0.36	-0.41	-0.55	-0.55	-0.55	-0.55	-0.55	-0.41	-0.41	-0.32	-0.32	-0.32	-0.45	-0.45
150	-0.37	-0.40	-0.58	-0.58	-0.58	-0.58	-0.58	-0.46	-0.46	-0.36	-0.36	-0.36	-0.40	-0.40
155	-0.30	-0.37	-0.50	-0.50	-0.50	-0.50	-0.50	-0.30	-0.30	-0.21	-0.21	-0.21	-0.31	-0.31
160	-0.24	-0.25	-0.38	-0.38	-0.38	-0.38	-0.38	-0.20	-0.20	-0.19	-0.19	-0.19	-0.28	-0.28
165	-0.22	-0.22	-0.28	-0.28	-0.28	-0.28	-0.28	-0.14	-0.14	-0.14	-0.14	-0.14	-0.22	-0.22
170	-0.19	-0.17	-0.18	-0.18	-0.18	-0.18	-0.18	-0.11	-0.11	-0.13	-0.13	-0.13	-0.10	-0.10
175	-0.11	-0.09	-0.09	-0.09	-0.09	-0.09	-0.09	-0.06	-0.06	-0.07	-0.07	-0.07	-0.08	-0.08

0317122A1030

30

TABLE V. - AERODYNAMIC COEFFICIENTS FOR REENTRY CONFIGURATION WITHOUT DESTABILIZER FLAP - Continued

(e)  $C_D$ 

$\alpha$ , deg	$C_D$ at -										$M = 20.0$			
	$M = 0$	$M = 0.5$	$M = 0.7$	$M = 0.9$	$M = 1.0$	$M = 1.1$	$M = 1.2$	$M = 1.6$	$M = 2.0$	$M = 3.0$	$M = 5.0$	$M = 7.0$	$M = 9.6$	$M = 20.0$
0	1.00	1.02	1.10	1.23	1.34	1.40	1.44	1.49	1.53	1.60	1.55	1.49	1.48	1.48
5	1.01	1.02	1.08	1.23	1.33	1.38	1.42	1.47	1.51	1.59	1.53	1.46	1.44	1.44
10	1.01	.98	1.06	1.23	1.33	1.36	1.39	1.45	1.47	1.54	1.51	1.42	1.39	1.36
15	.95	.95	1.01	1.14	1.26	1.26	1.32	1.37	1.44	1.48	1.48	1.34	1.34	1.36
20	.92	.92	.97	1.10	1.25	1.25	1.33	1.38	1.37	1.36	1.40	1.25	1.24	1.27
25	.89	.88	.92	1.05	1.25	1.25	1.34	1.37	1.37	1.32	1.30	1.14	1.14	1.20
30	.85	.84	.84	1.02	1.22	1.22	1.31	1.31	1.25	1.18	1.21	1.03	1.04	1.12
35	.81	.80	.80	.84	1.20	1.20	1.23	1.24	1.19	1.12	1.13	.96	.96	1.03
40	.77	.76	.82	.94	1.16	1.16	1.19	1.21	1.15	1.08	1.08	.87	.89	.96
45	.73	.72	.78	.91	1.12	1.12	1.16	1.18	1.12	.95	1.05	.85	.84	.84
50	.69	.66	.72	.91	1.10	1.14	1.14	1.17	1.10	.95	1.03	.85	.81	.81
55	.65	.63	.68	.90	1.09	1.09	1.14	1.16	1.08	1.06	1.03	.86	.82	.82
60	.61	.61	.69	.88	1.08	1.15	1.17	1.17	1.10	1.09	1.05	.90	.81	.84
65	.55	.61	.70	.89	1.09	1.16	1.16	1.18	1.14	1.12	1.09	.95	.88	.88
70	.52	.63	.72	.82	1.09	1.12	1.12	1.17	1.10	1.09	1.05	.93	.84	.84
75	.50	.64	.74	.86	1.06	1.18	1.18	1.21	1.12	1.08	1.05	.90	.81	.81
80	.49	.62	.73	.86	1.01	1.21	1.24	1.28	1.20	1.27	1.26	1.11	1.07	1.06
85	.48	.60	.70	.90	1.04	1.24	1.24	1.30	1.21	1.32	1.31	1.18	1.14	1.13
90	.48	.61	.64	.87	1.02	1.24	1.24	1.32	1.33	1.36	1.37	1.25	1.21	1.20
95	.47	.61	.67	.87	1.02	1.24	1.24	1.32	1.30	1.36	1.37	1.25	1.21	1.20
100	.49	.64	.67	.87	1.04	1.25	1.25	1.34	1.39	1.44	1.40	1.20	1.27	1.26
105	.51	.51	.70	.84	1.07	1.25	1.25	1.38	1.43	1.48	1.44	1.34	1.33	1.32
110	.55	.55	.78	.91	1.10	1.26	1.26	1.40	1.45	1.50	1.46	1.46	1.36	1.36
115	.62	.62	.83	.94	1.12	1.27	1.27	1.37	1.43	1.50	1.46	1.47	1.36	1.37
120	.71	.71	.86	.96	1.14	1.28	1.28	1.35	1.40	1.47	1.45	1.46	1.34	1.35
125	.75	.86	.97	1.16	1.30	1.30	1.35	1.40	1.44	1.40	1.44	1.40	1.35	1.35
130	.75	.84	.84	1.14	1.31	1.31	1.36	1.40	1.40	1.39	1.35	1.35	1.23	1.24
135	.73	.80	.92	.92	1.15	1.27	1.27	1.38	1.43	1.48	1.44	1.44	1.35	1.36
140	.71	.77	.84	.84	1.16	1.26	1.26	1.35	1.40	1.46	1.42	1.42	1.34	1.35
145	.68	.73	.78	.93	1.06	1.15	1.15	1.25	1.30	1.37	1.34	1.34	1.28	1.29
150	.66	.70	.72	.86	1.03	1.03	1.03	1.08	1.07	1.10	1.06	1.06	1.06	1.06
155	.63	.68	.81	.93	.93	.94	.94	.98	1.02	1.02	.94	.95	.82	.84
160	.61	.62	.66	.66	.90	.94	.94	.98	.96	.98	.83	.70	.59	.55
165	.59	.59	.74	.74	.92	.92	.92	.92	.90	.88	.74	.60	.49	.45
170	.58	.58	.68	.68	.72	.72	.72	.72	.70	.66	.63	.50	.37	.37
175	.56	.56	.66	.66	.66	.66	.66	.66	.66	.62	.56	.30	.29	.30
180	.60	.60	.67	.67	.77	.77	.77	.77	.75	.75	.75	.22	.23	.23

DECLASSIFIED

TABLE V.- AERODYNAMIC COEFFICIENTS FOR REENTRY CONFIGURATION WITHOUT DESTABILIZER FLAP - Continued

(d) C<sub>IV</sub>



REF ID: A6512  
DECLASSIFIED

33

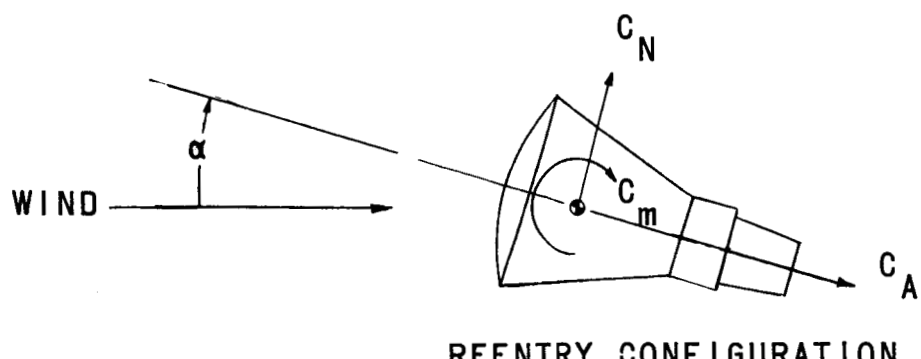
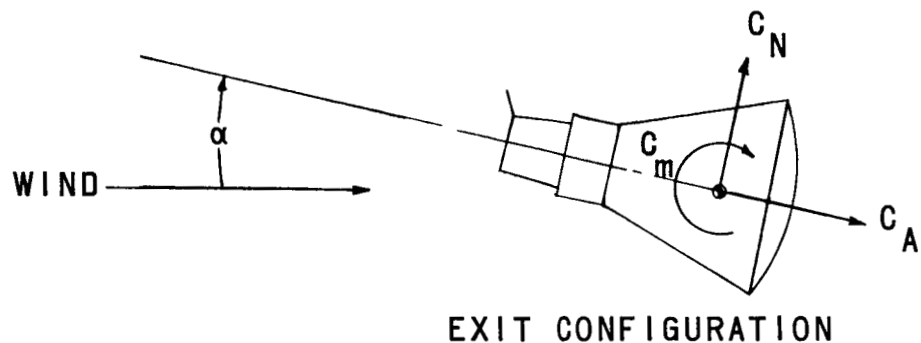
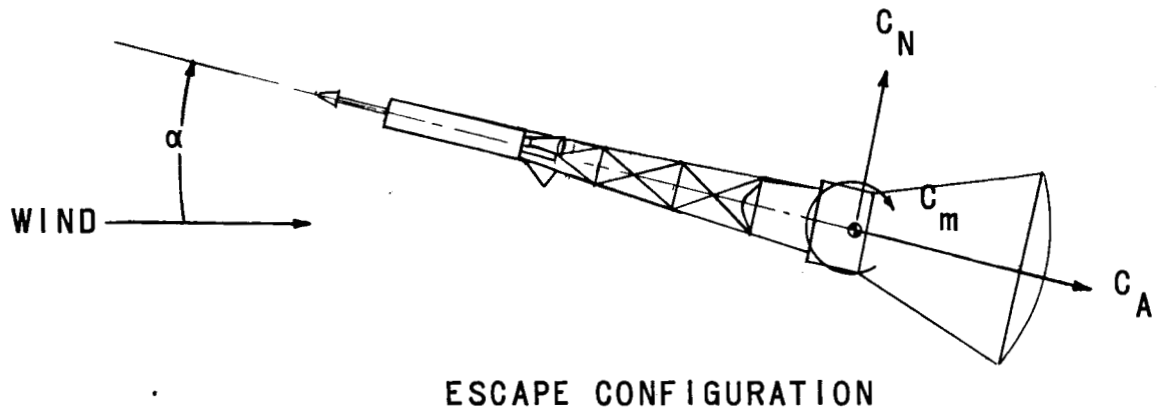


Figure 1.- General arrangement of the configurations showing positive directions of forces and moments.

0317122A1030

34

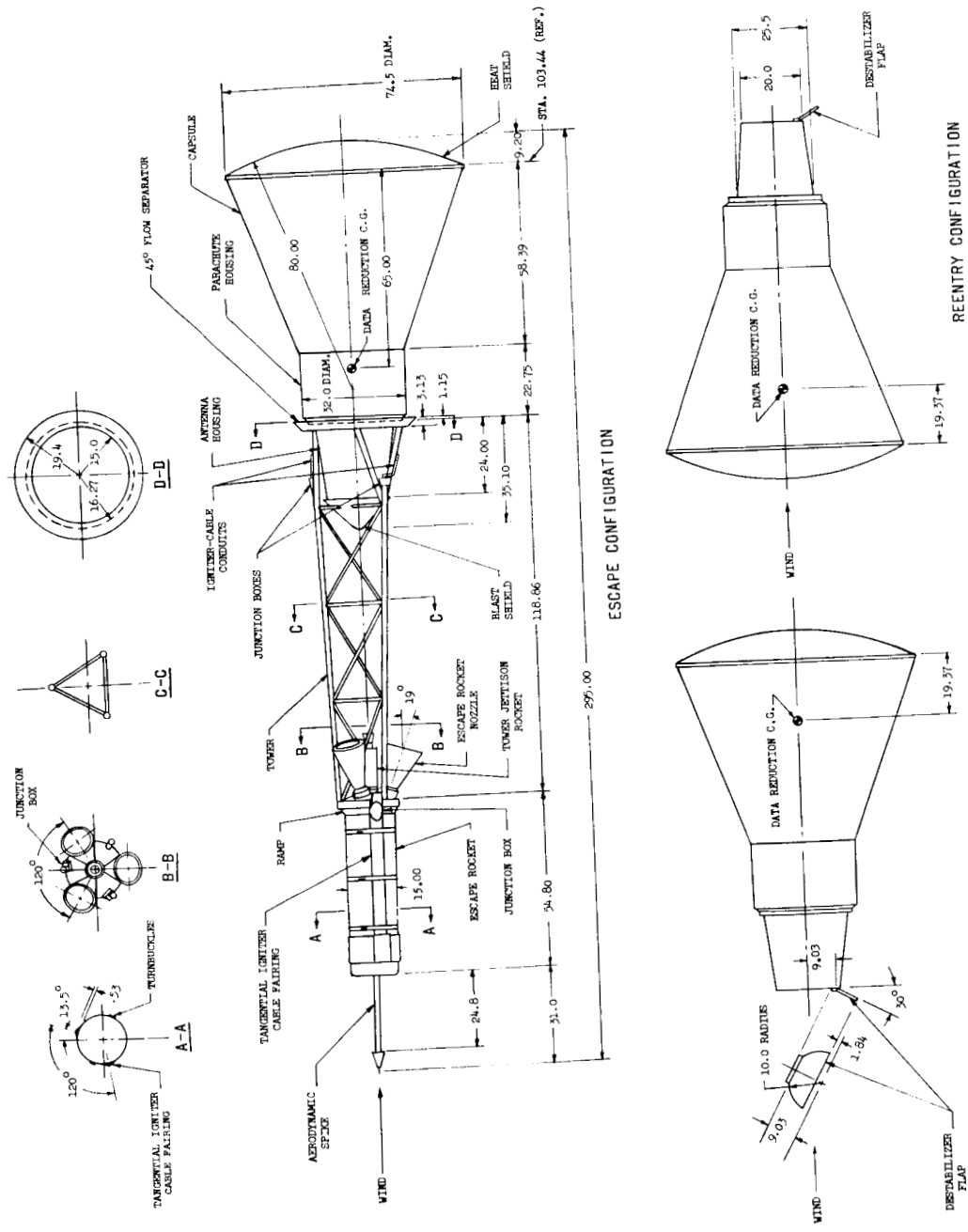


Figure 2.- General dimensions of the production Mercury configurations. All dimensions are in inches unless otherwise noted.

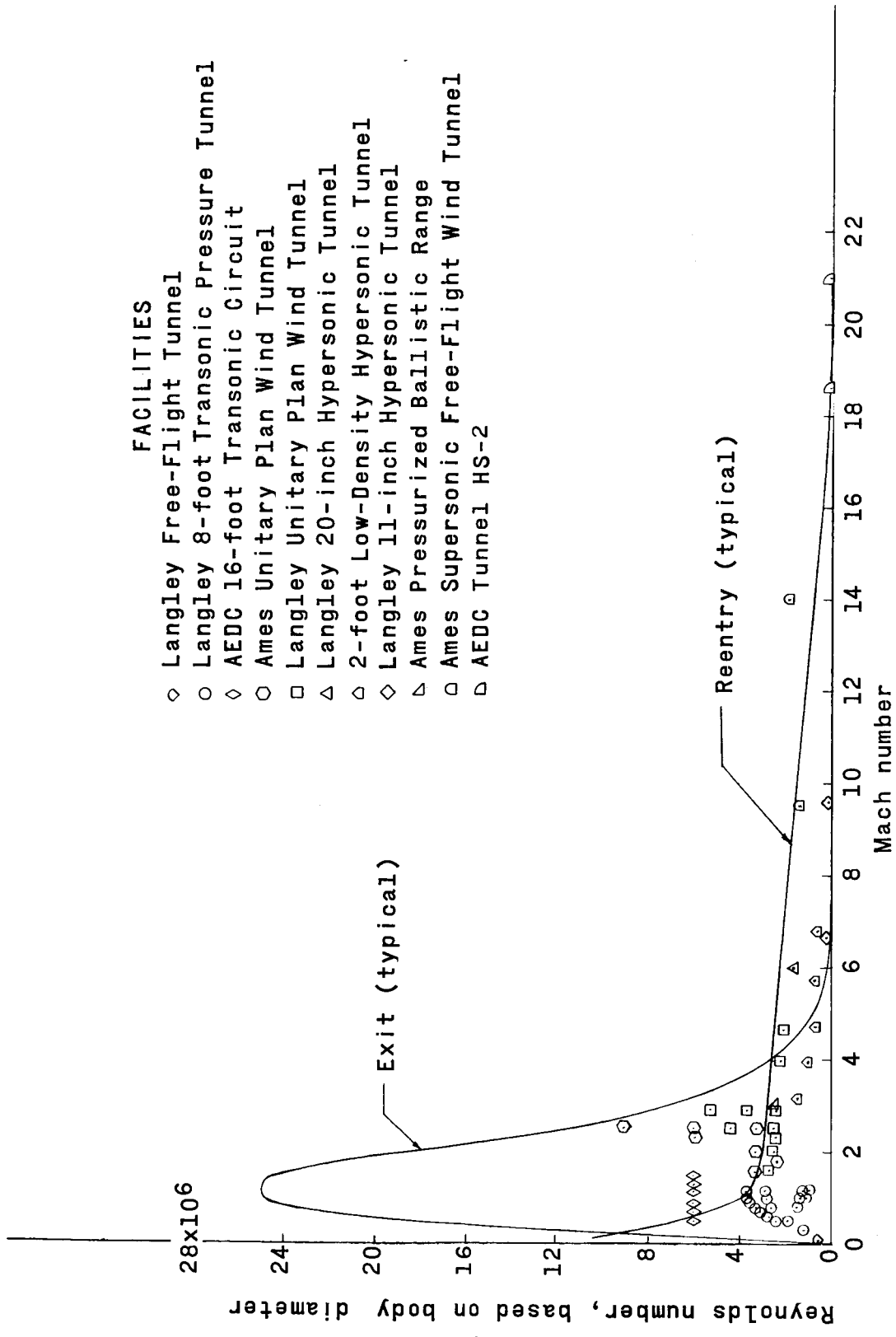


Figure 3.- Comparison of typical flight and wind-tunnel Reynolds numbers.

03171220.1030

36

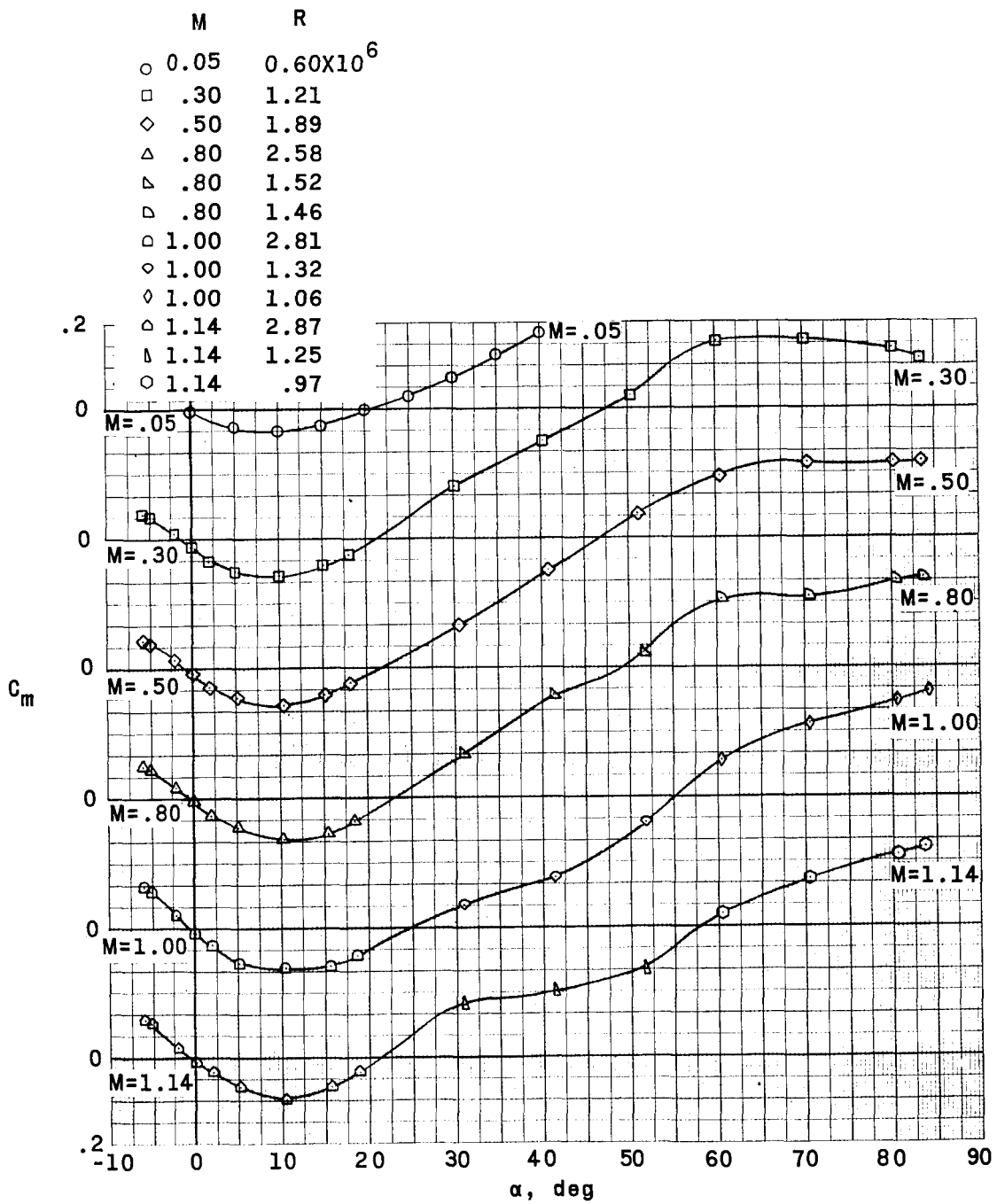
(a)  $M = 0.05$  to  $1.14$ .

Figure 4.- Variation of pitching-moment coefficient with angle of attack.  
Escape configuration.

REF ID: A6512

REF ID: A6512  
CLASSIFIED

37

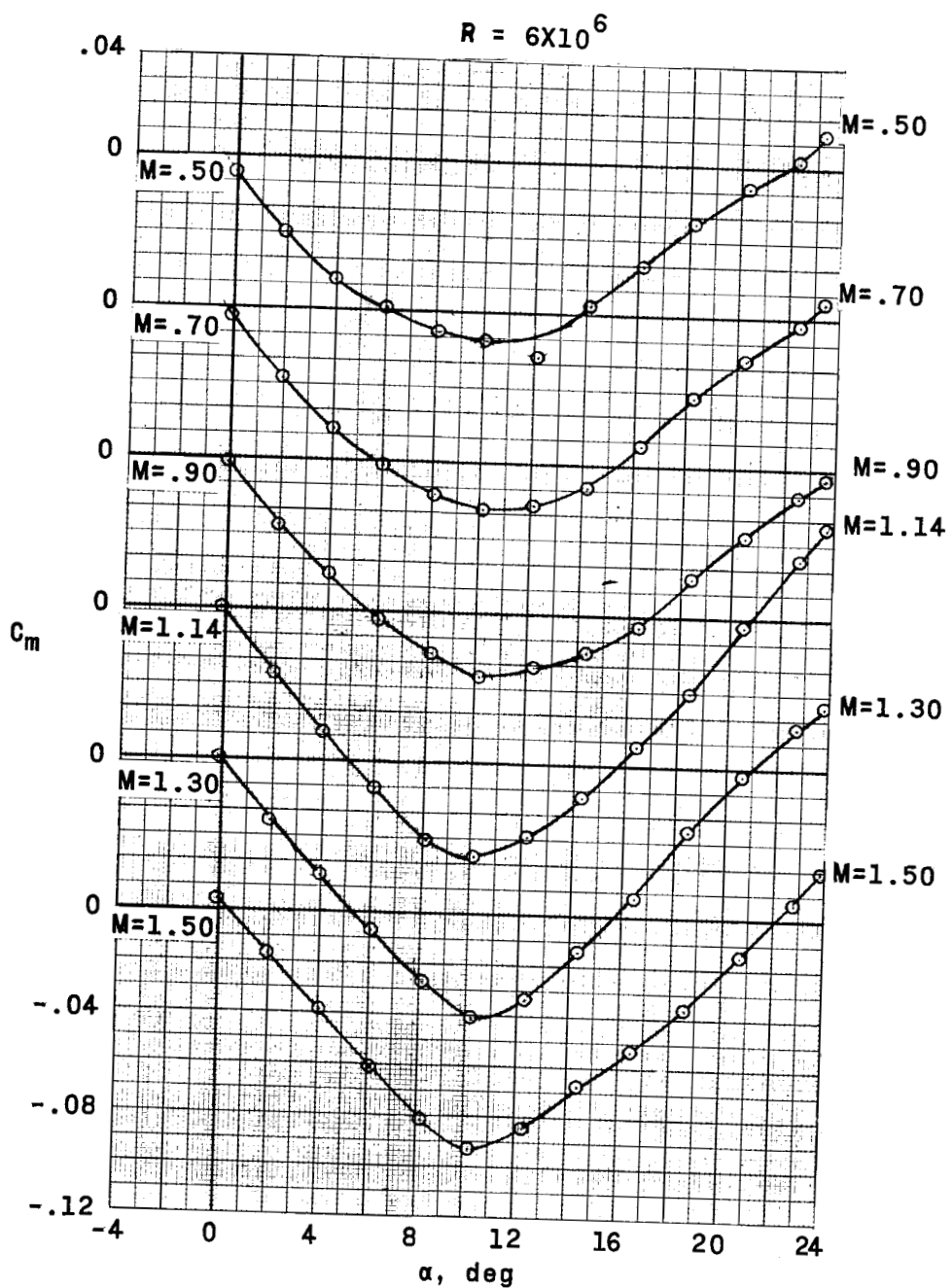
(b)  $M = 0.50$  to  $1.50$ .

Figure 4.- Continued.

037122A.1630

38

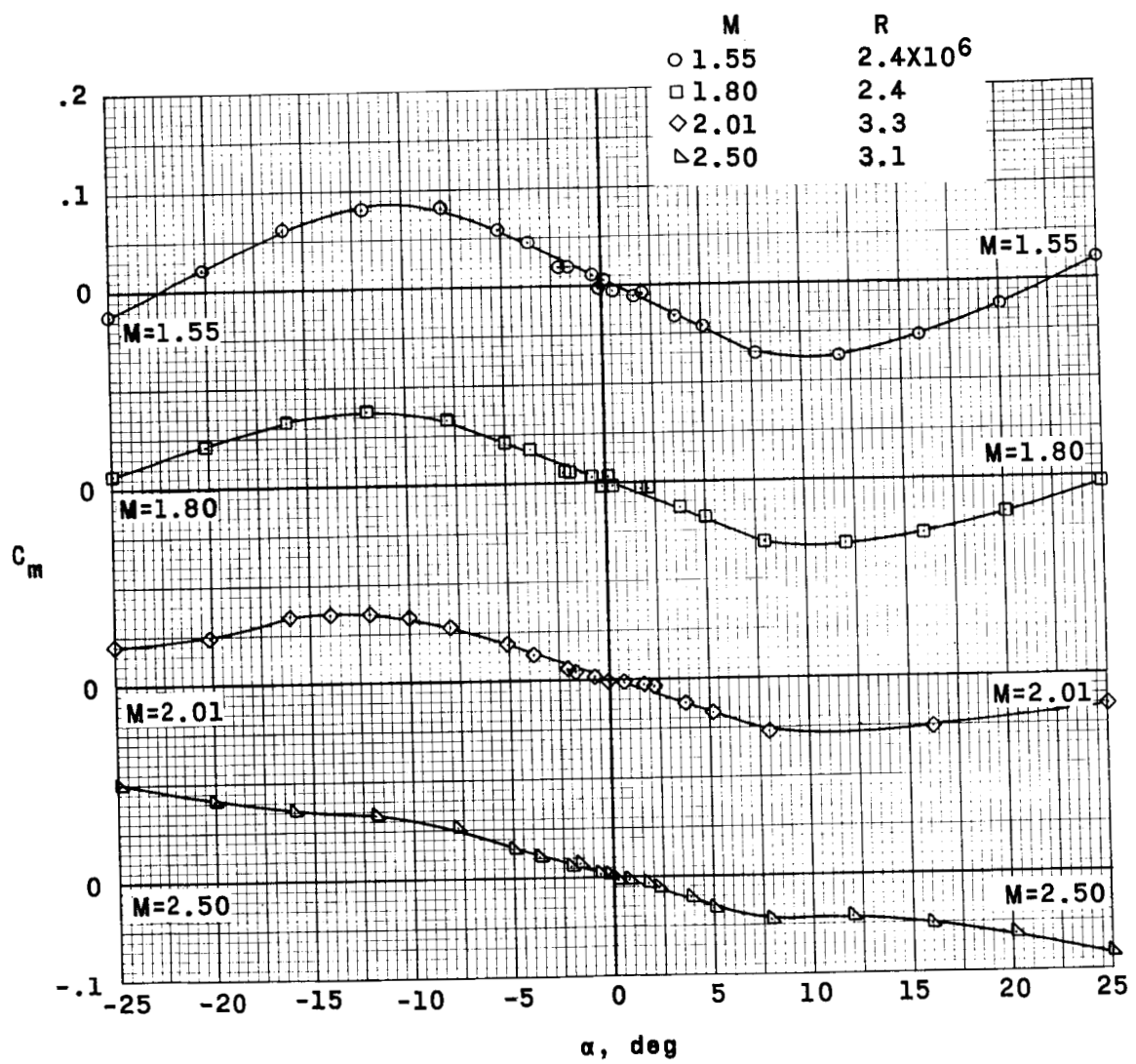
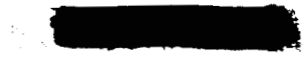
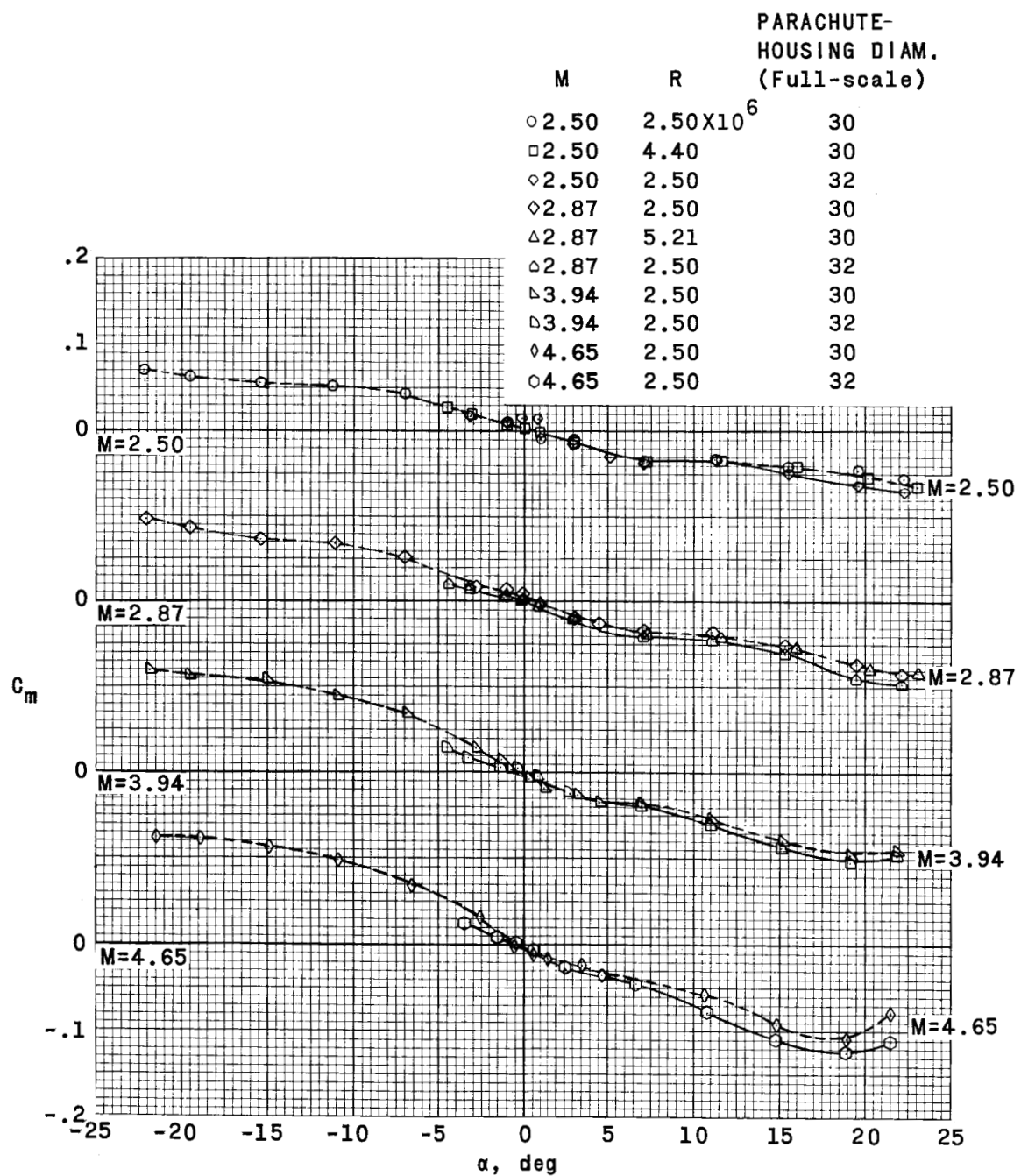
(c)  $M = 1.55$  to  $2.50$ .

Figure 4.- Continued.



REF ID: A6542  
CLASSIFIED 39



(d)  $M = 2.50$  to  $4.65$ .

Figure 4.- Continued.

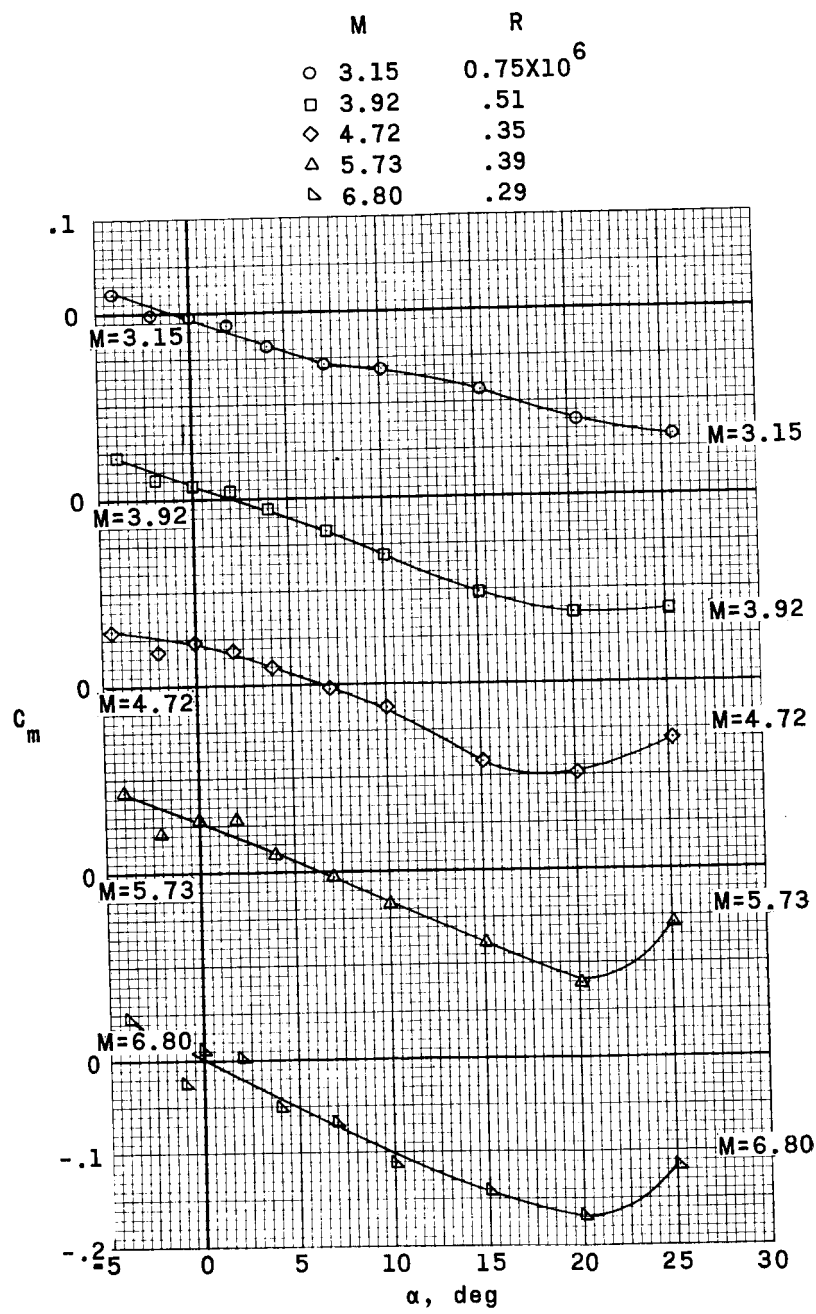
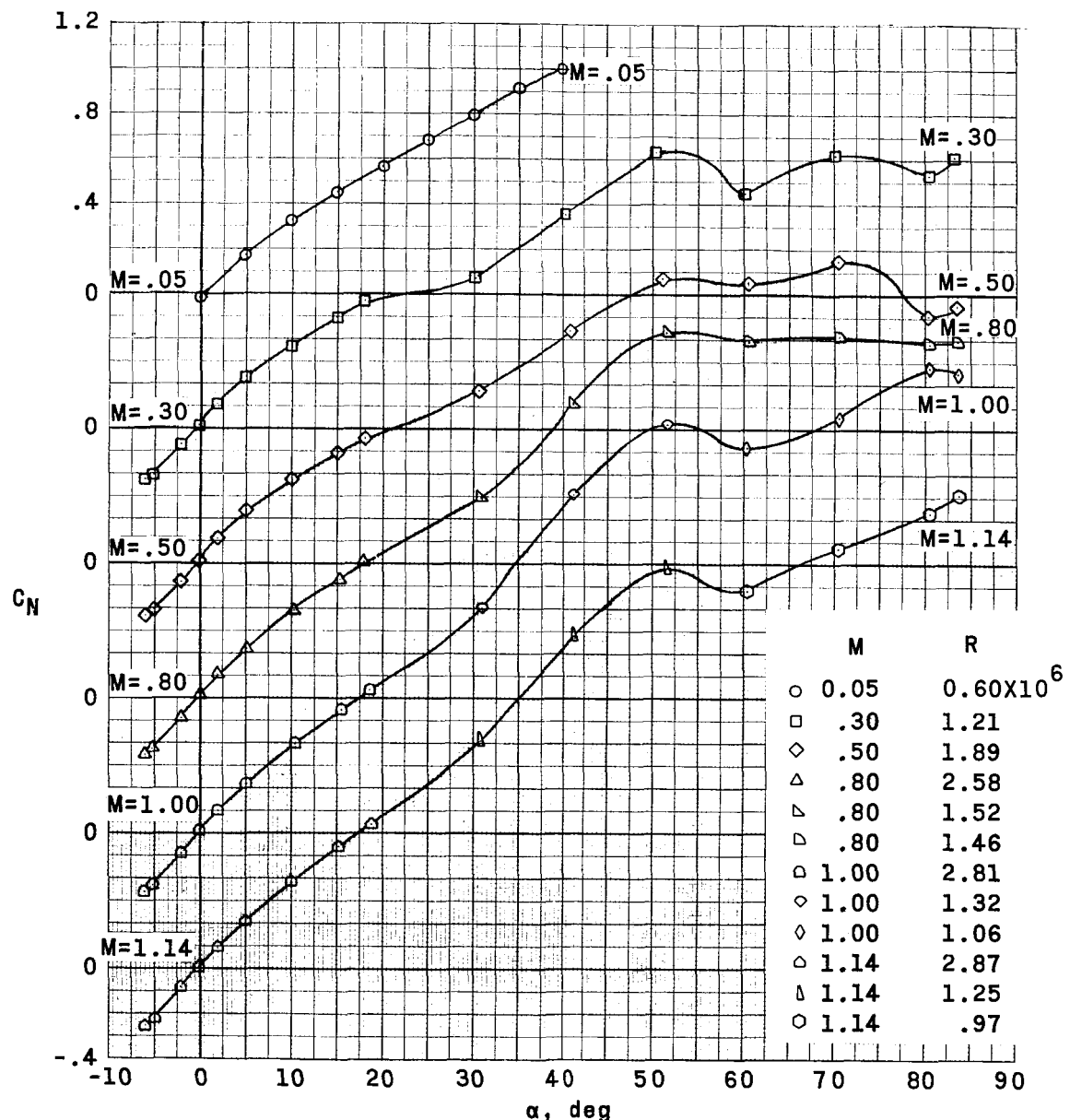
(e)  $M = 3.15$  to  $6.80$ .

Figure 4.- Concluded.

**41** CLASSIFIED

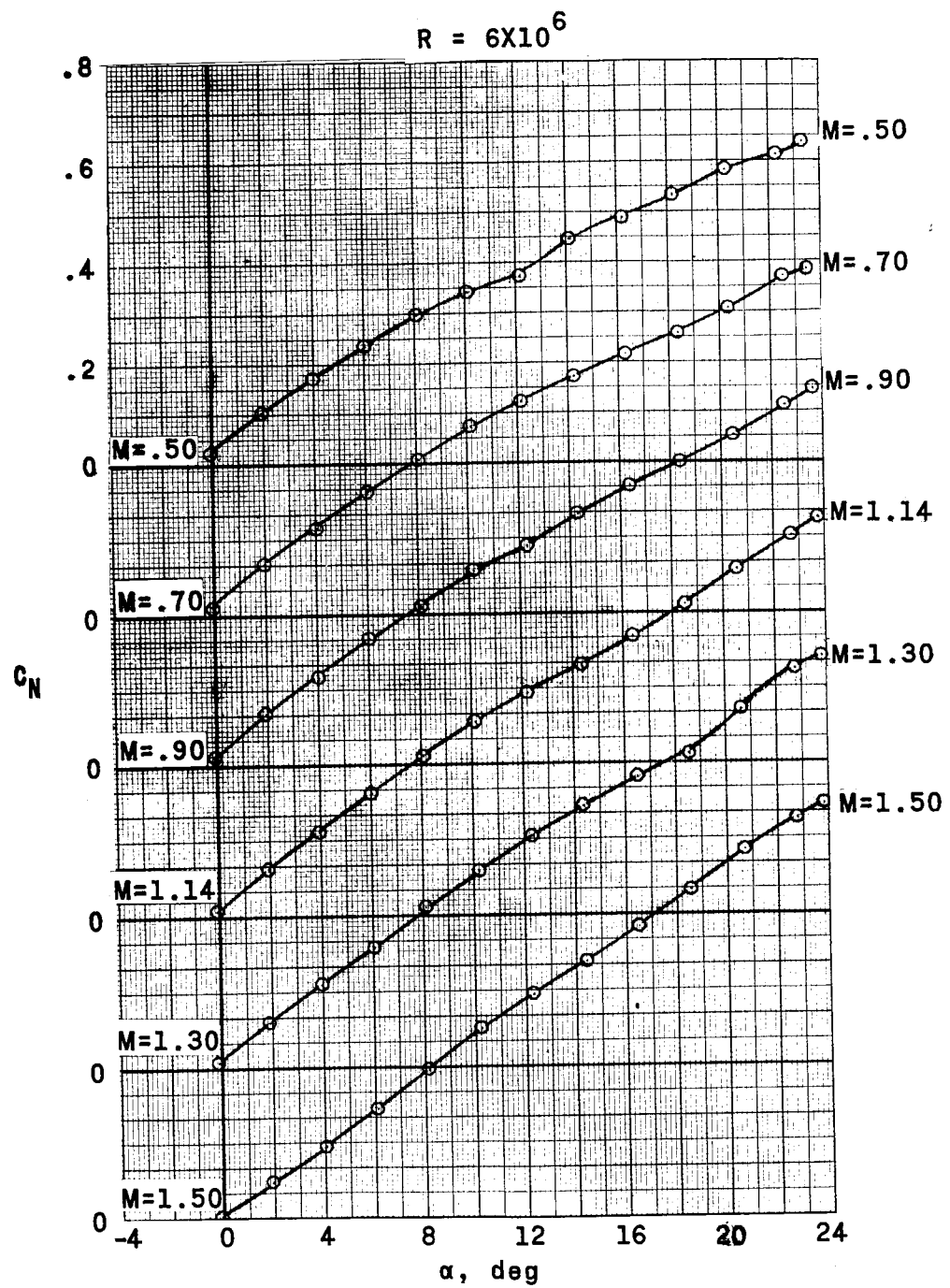


(a)  $M = 0.05$  to  $1.14$ .

Figure 5.- Variation of normal-force coefficient with angle of attack.  
Escape configuration.

03191320 11:53:00

42

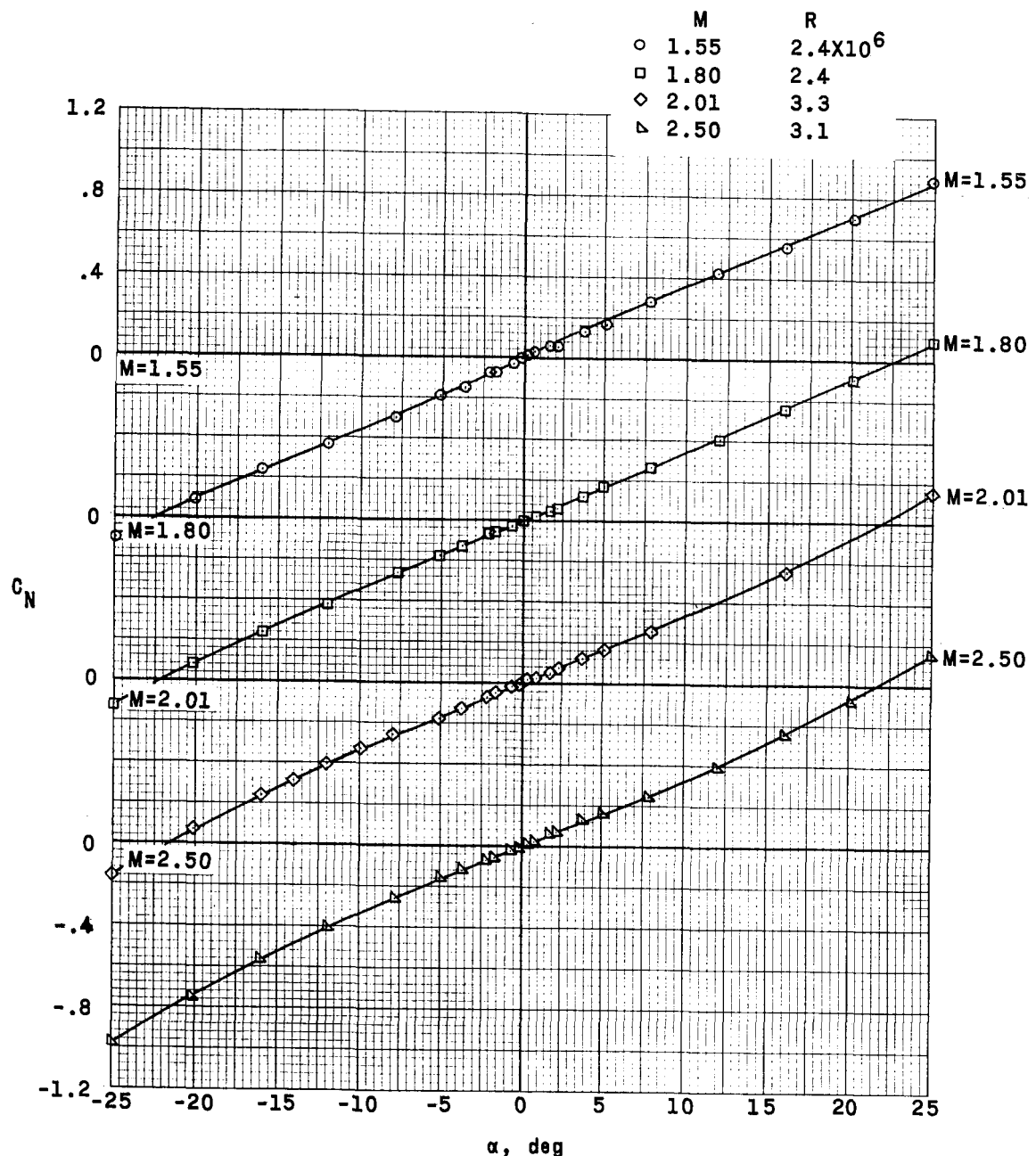


(b)  $M = 0.50$  to  $1.50$ .

Figure 5.- Continued.

DECLASSIFIED

43



(c)  $M = 1.55 \text{ to } 2.50.$

Figure 5.- Continued.

0319122A1000

44

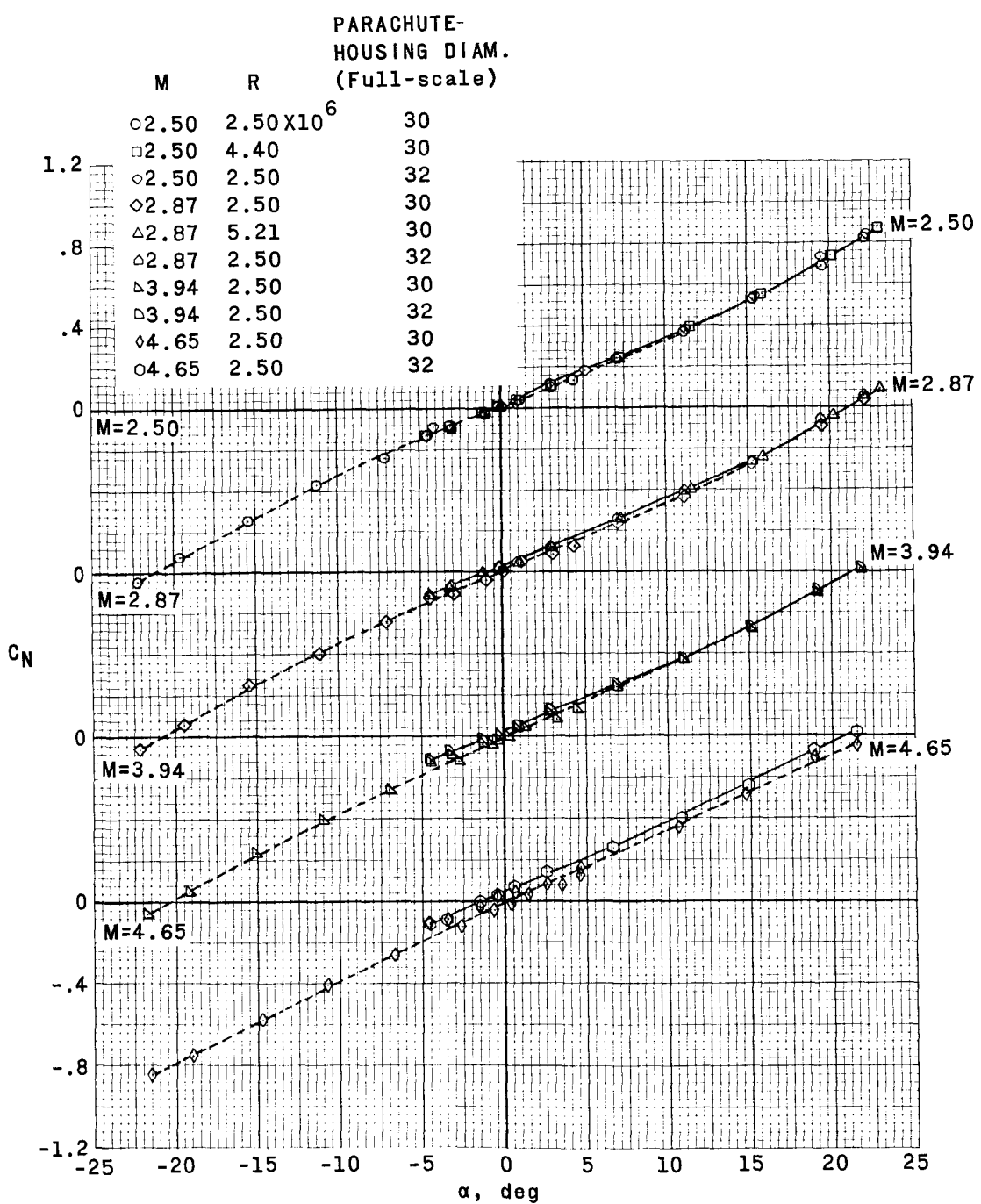
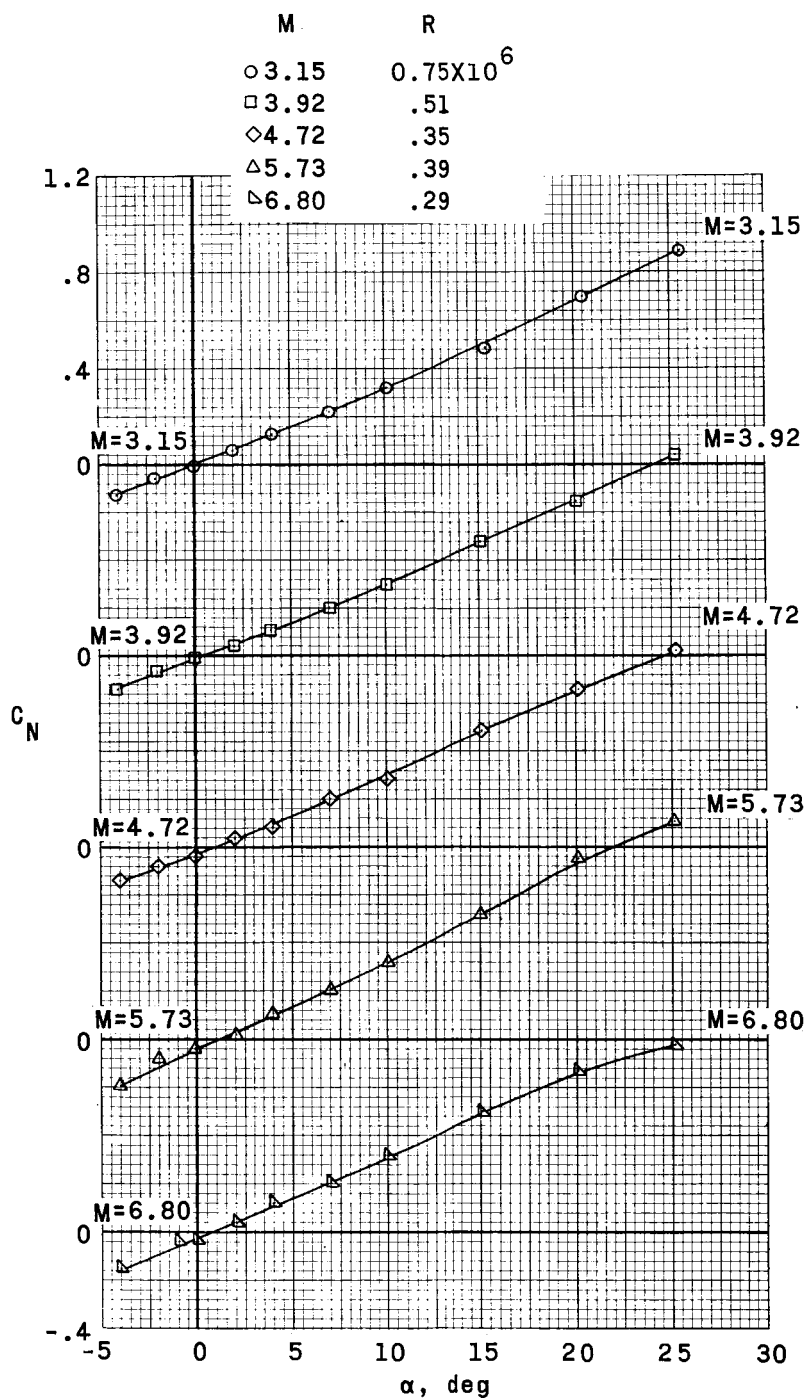
(d)  $M = 2.50$  to  $4.65$ .

Figure 5.- Continued.

DECLASSIFIED

45



(e)  $M = 3.15$  to  $6.80$ .

Figure 5.- Concluded.

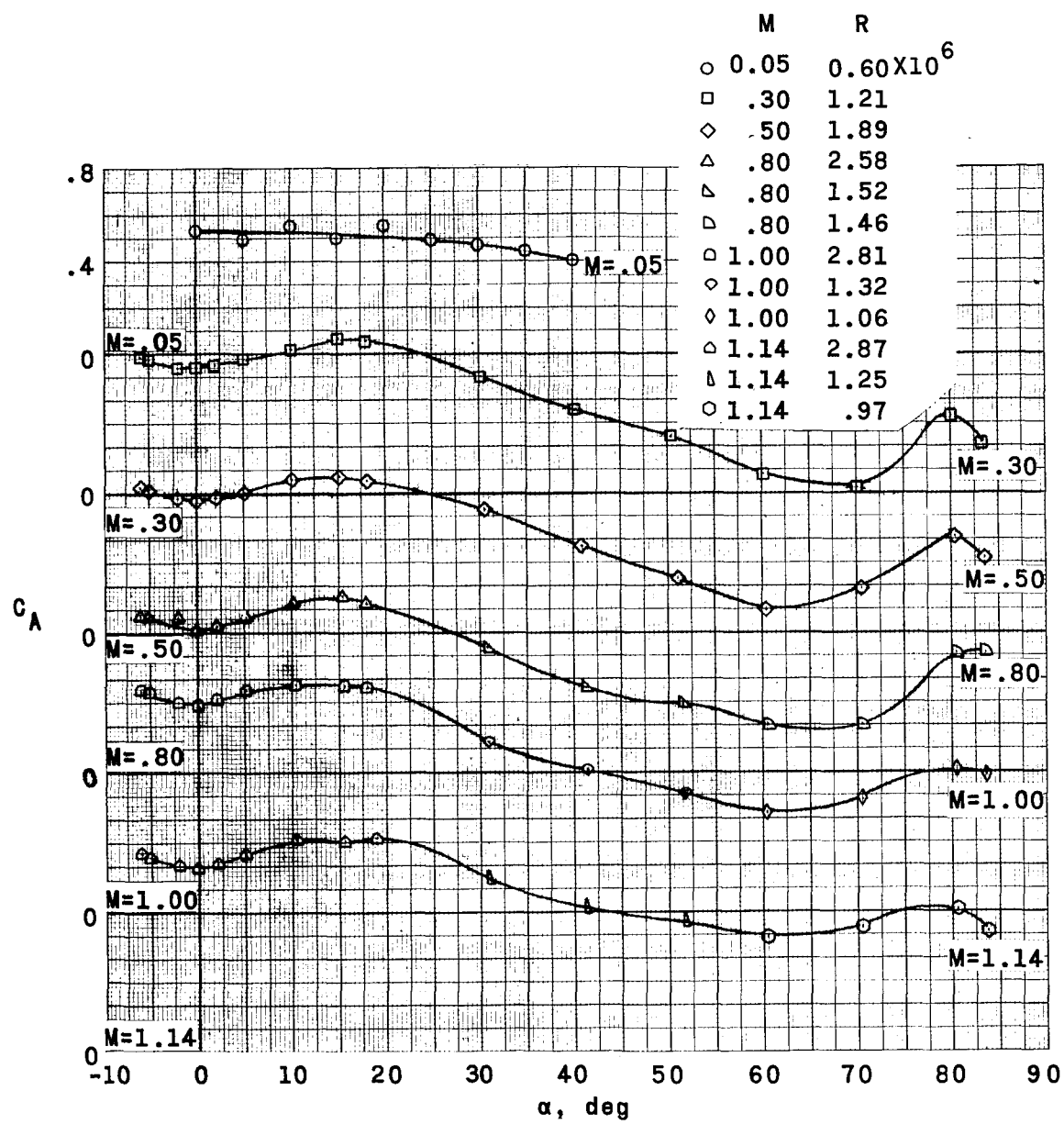
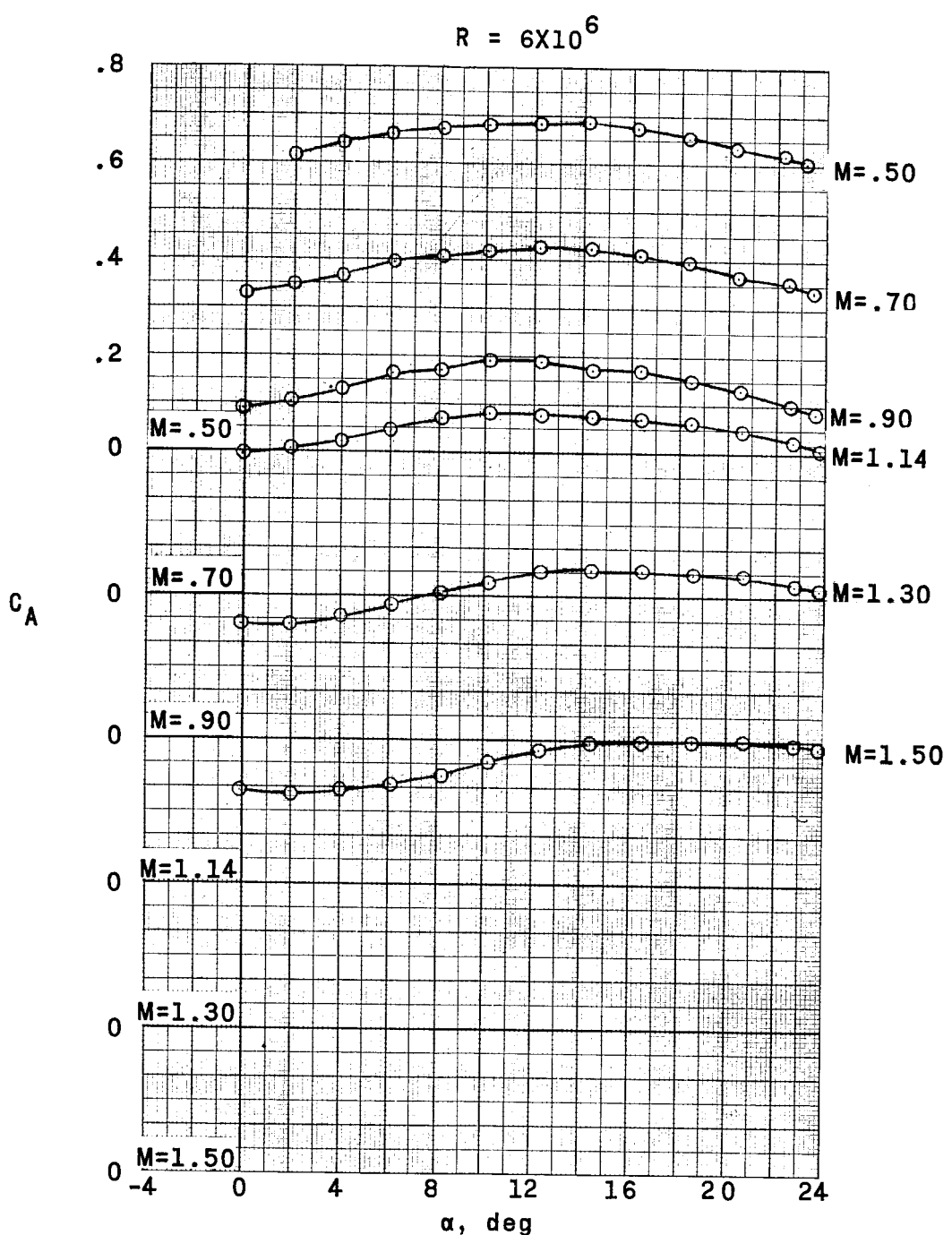
(a)  $M = 0.05$  to 1.50.

Figure 6.- Variation of axial-force coefficient with angle of attack.  
Escape configuration.

DECLASSIFIED

47



(b)  $M = 0.50$  to  $1.50$ .

Figure 6.- Continued.

0319122A1030

48

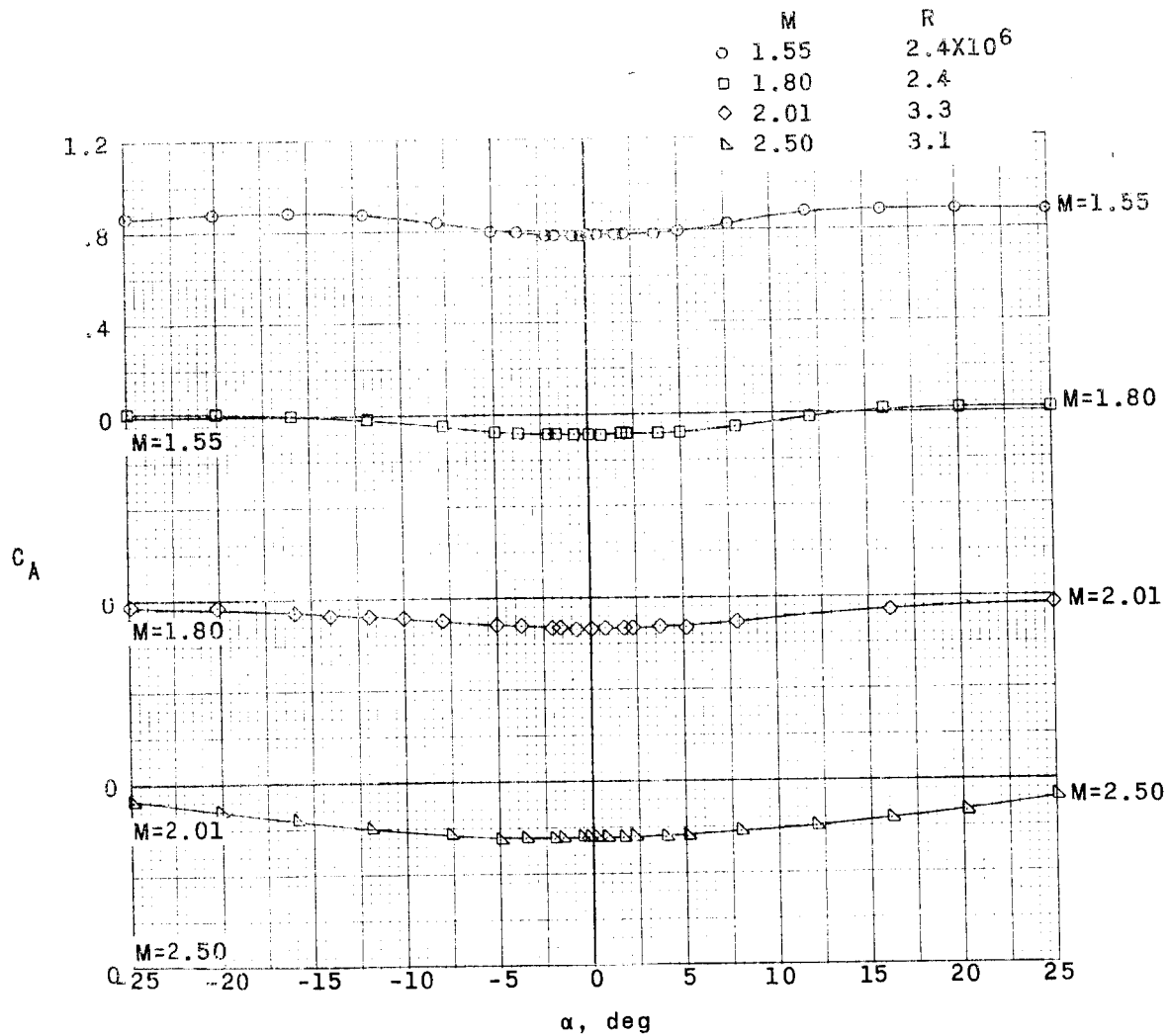
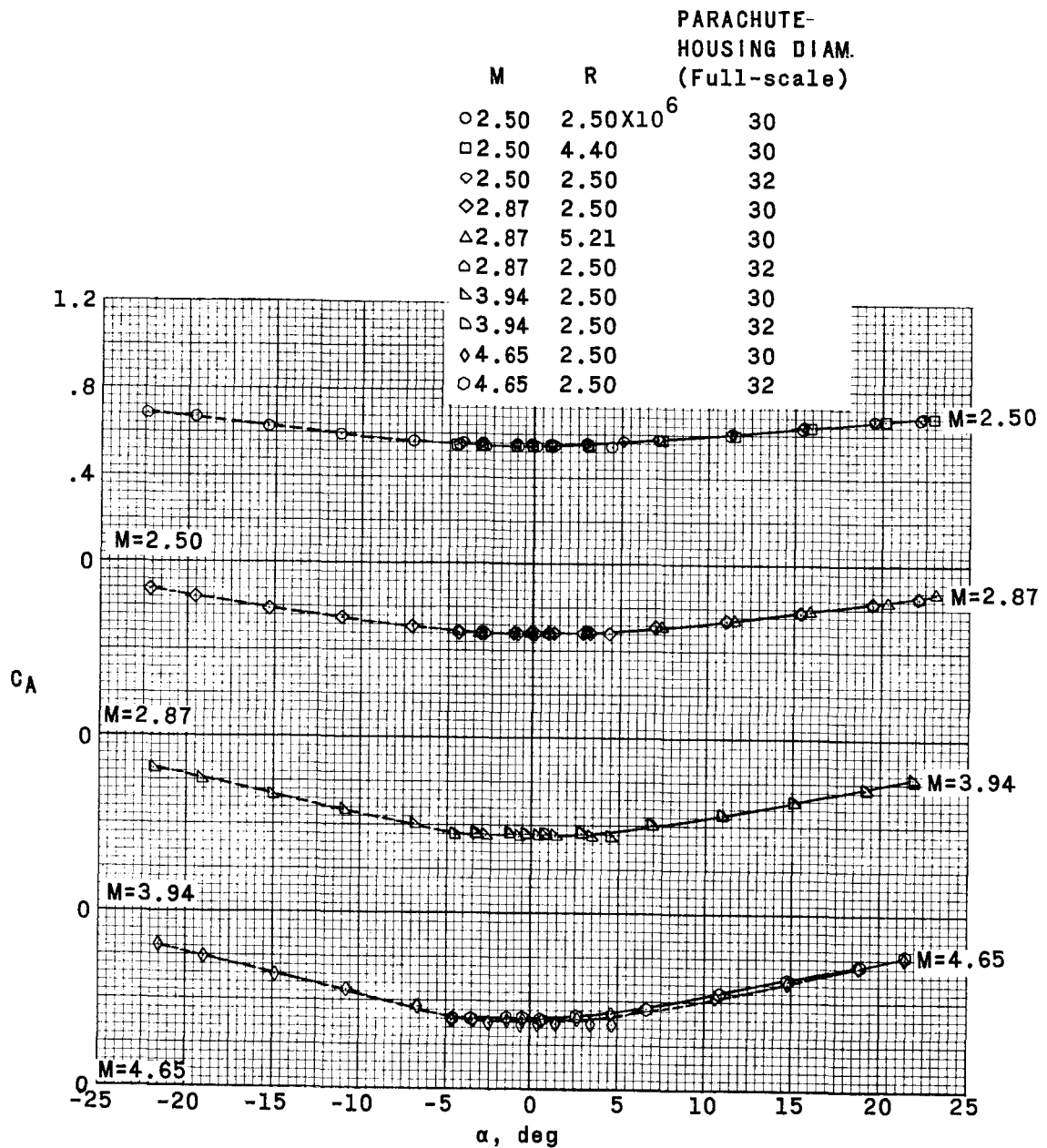
(c)  $M = 1.55$  to  $2.50$ .

Figure 6.- Continued.

DECLASSIFIED

49



(d)  $M = 2.50$  to  $4.65$ .

Figure 6.- Continued.

0317022A1030

50

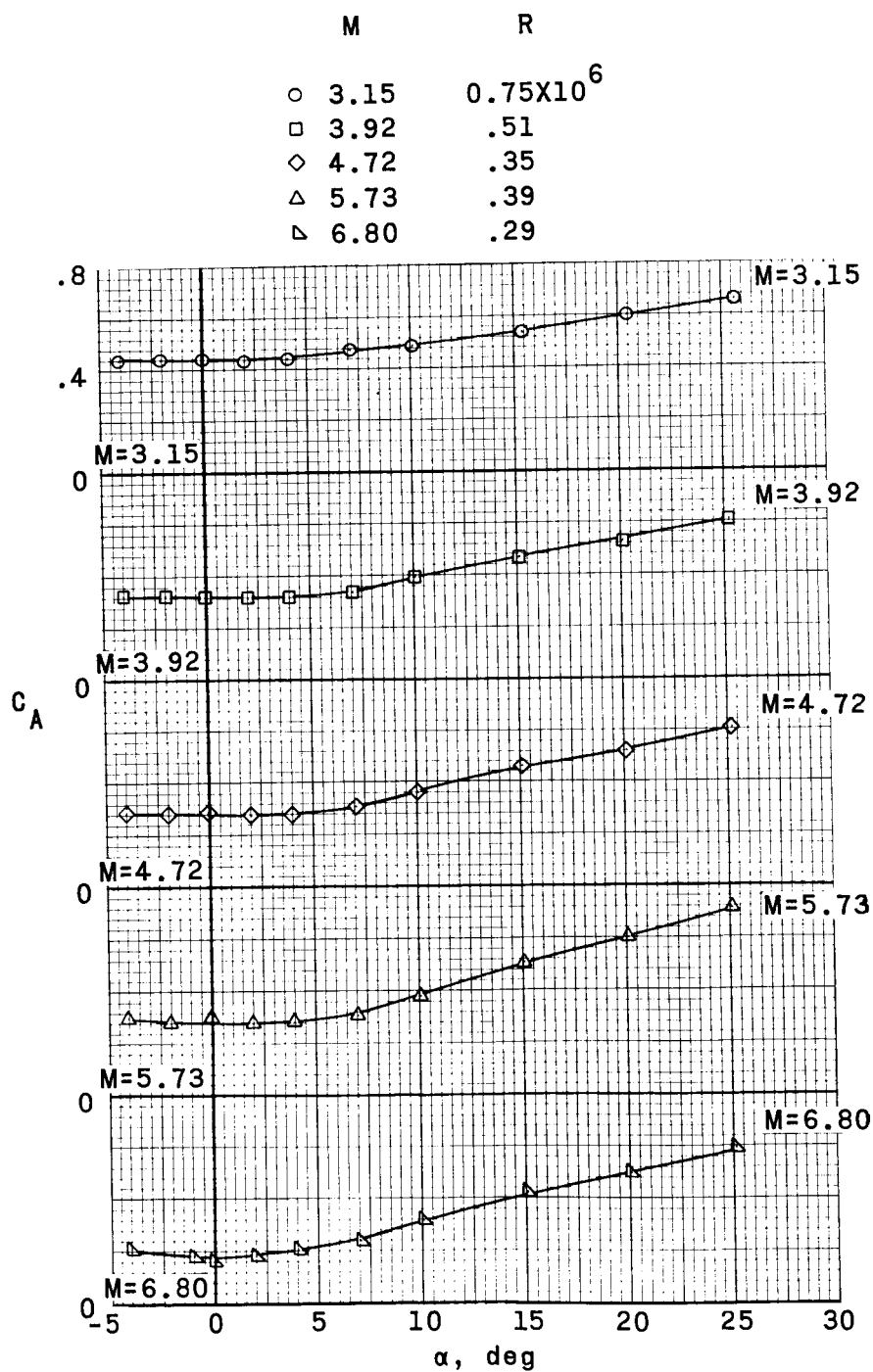
(e)  $M = 3.15$  to  $6.80$ .

Figure 6.- Concluded.

REF ID: A6572  
DECLASSIFIED

51

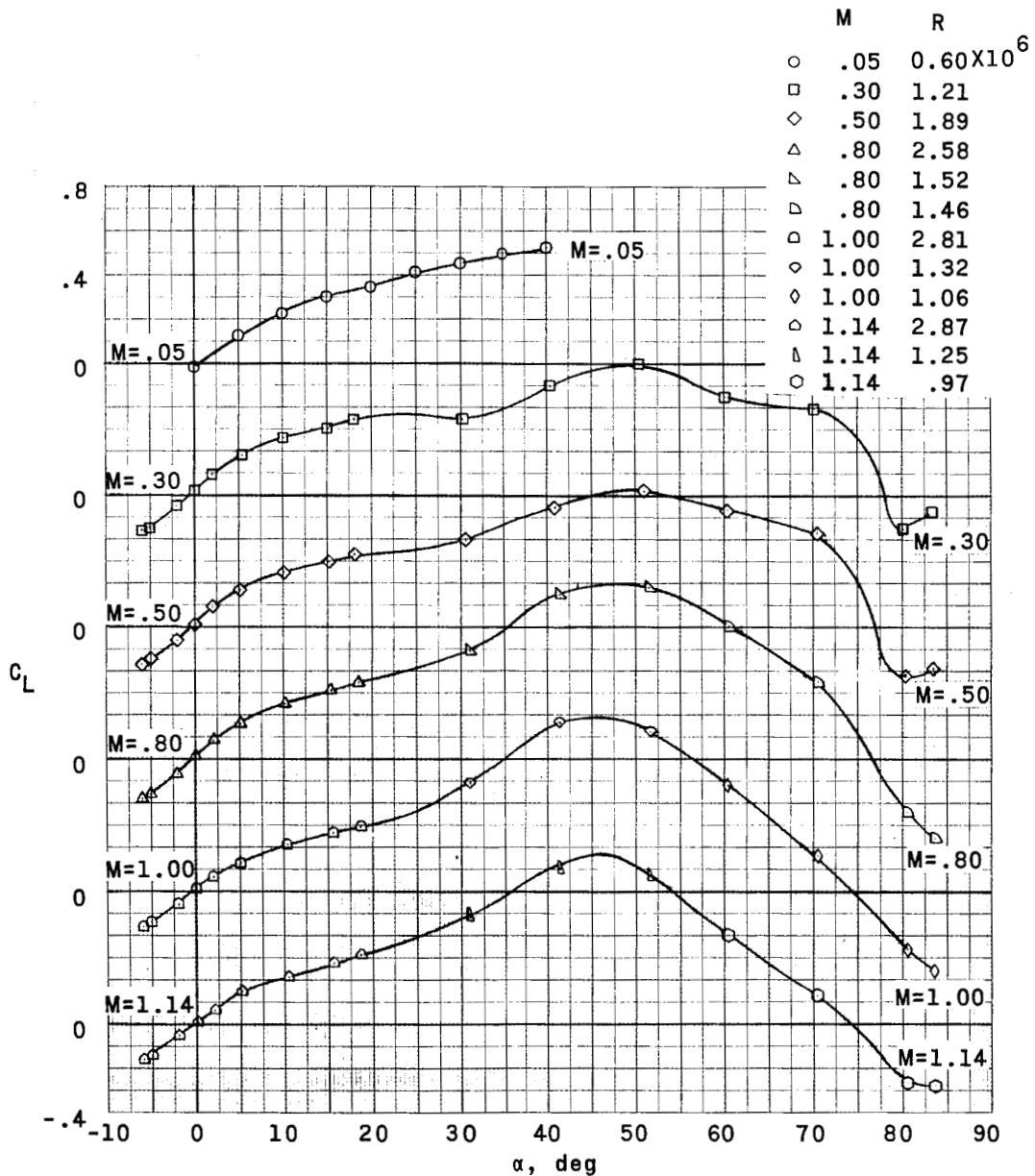
(a)  $M = 0.05$  to  $1.14$ .

Figure 7.- Variation of lift coefficient with angle of attack. Escape configuration.

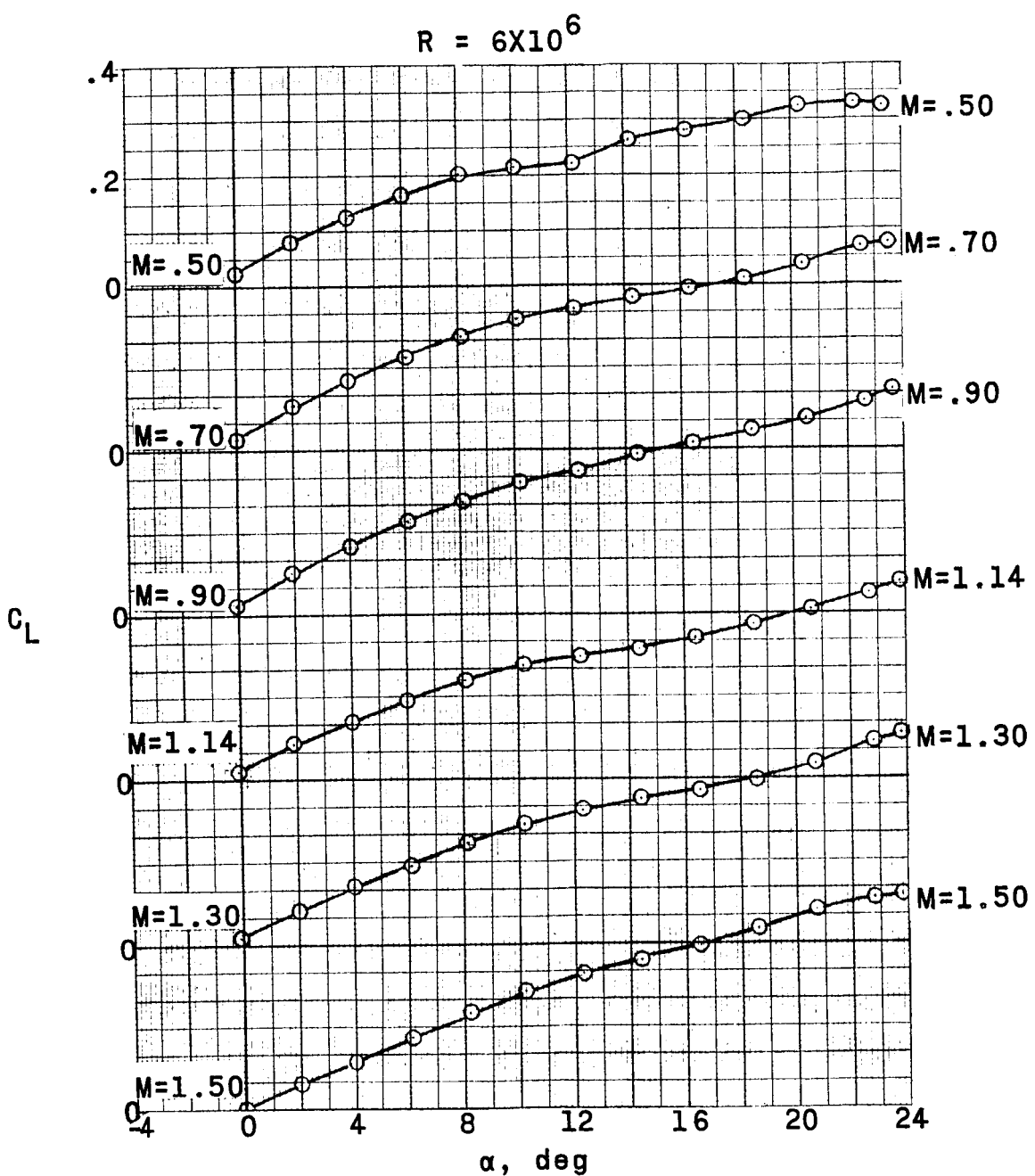
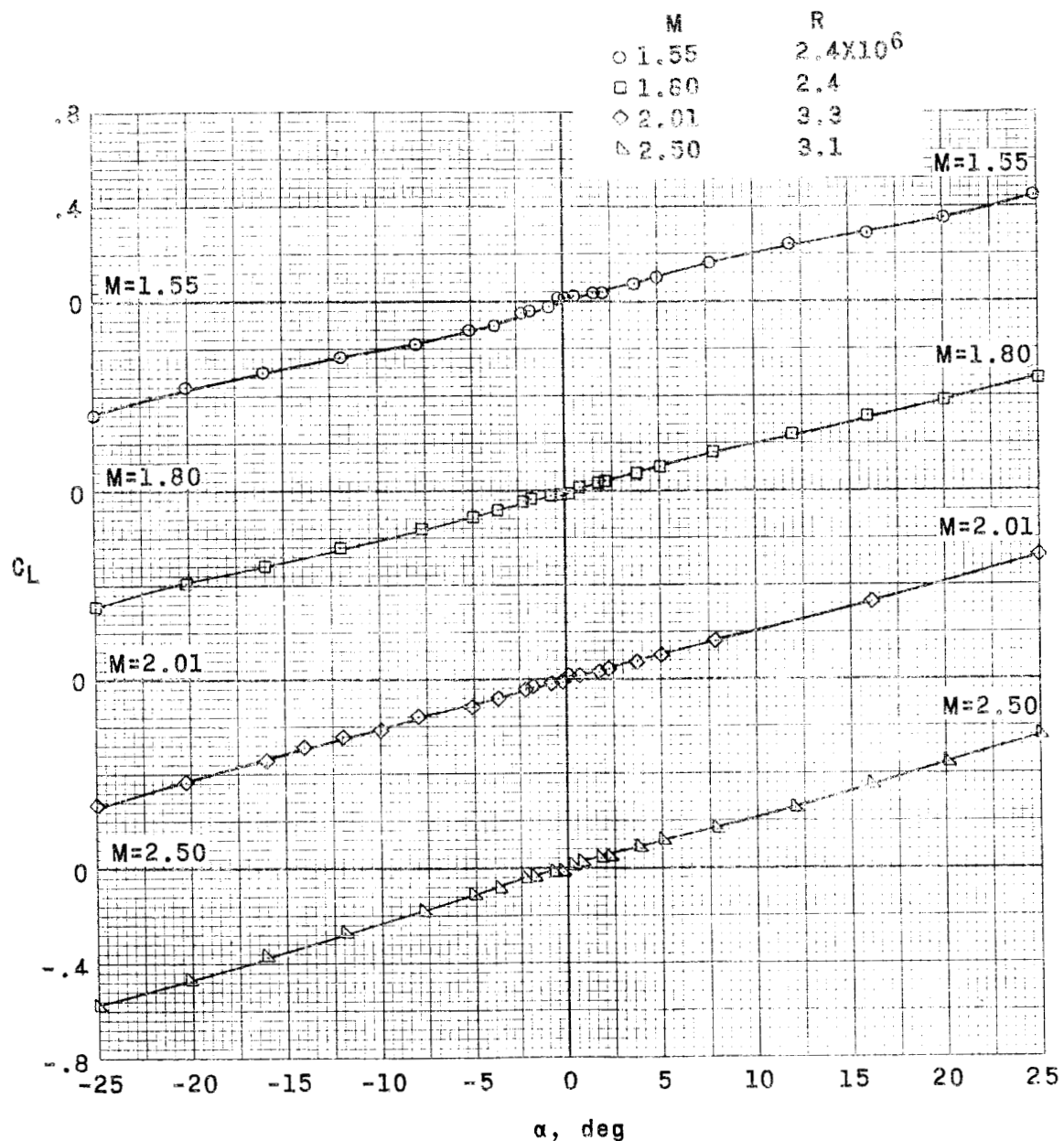
(b)  $M = 0.50$  to  $1.50$ .

Figure 7.- Continued.

10

REF CLASSIFIED

53



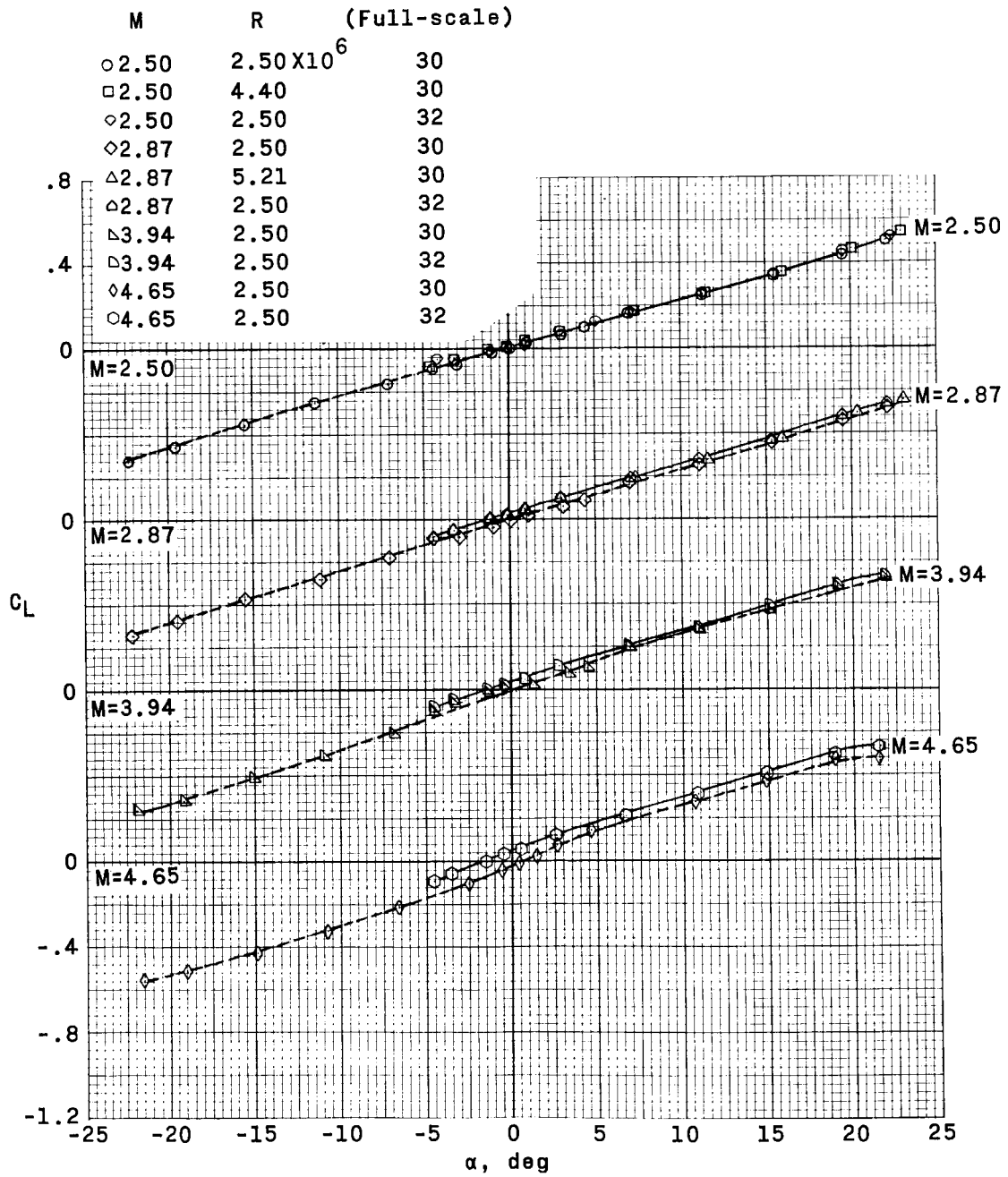
(c)  $M = 1.55$  to  $2.50$ .

Figure 7.- Continued.

031912201930



PARACHUTE-  
HOUSING DIAM.  
(Full-scale)



(a)  $M = 2.50$  to  $4.65$ .

Figure 7.- Continued.

REF ID: A6512  
DECLASSIFIED

55

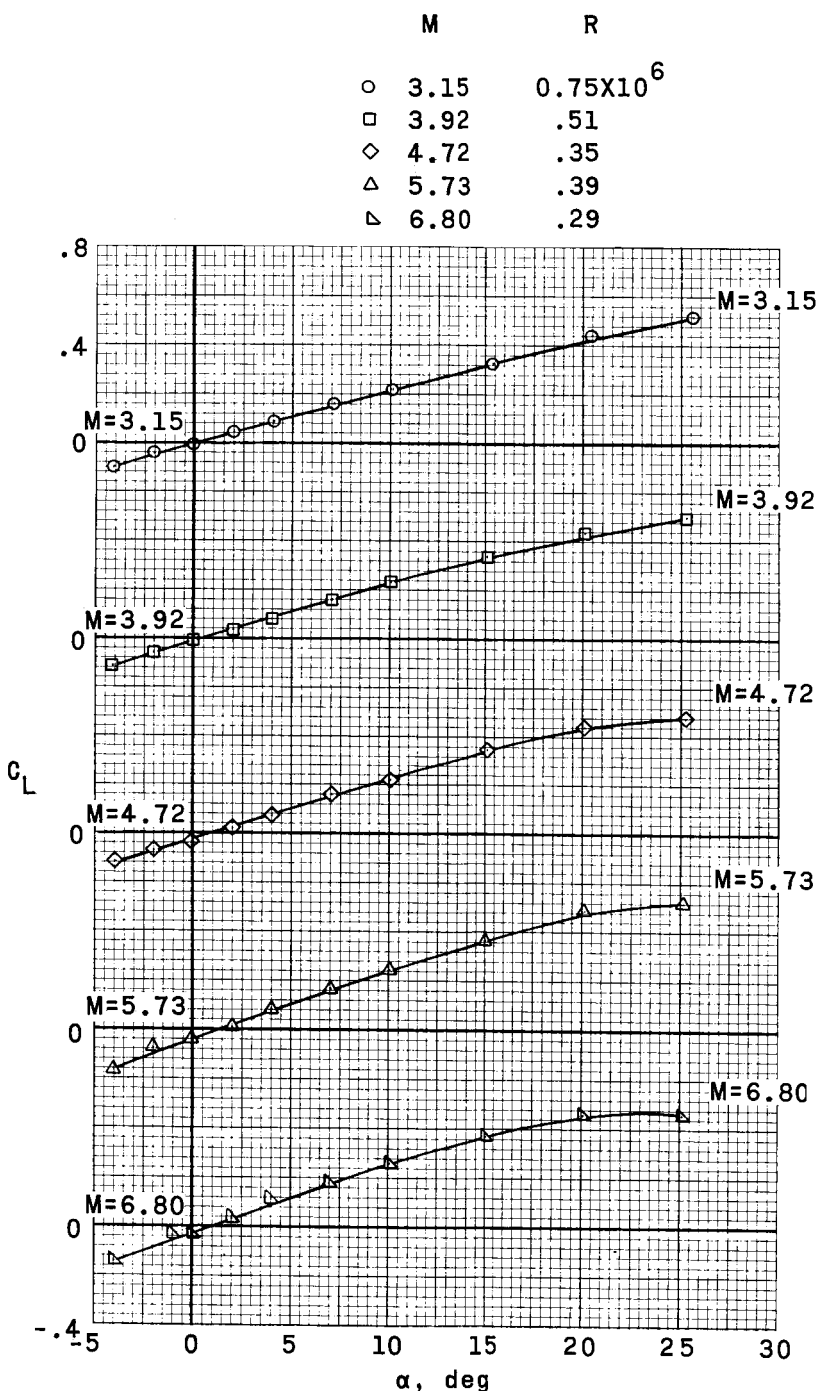
(e)  $M = 3.15$  to  $6.80$ .

Figure 7.- Concluded.

03191220.1030

56

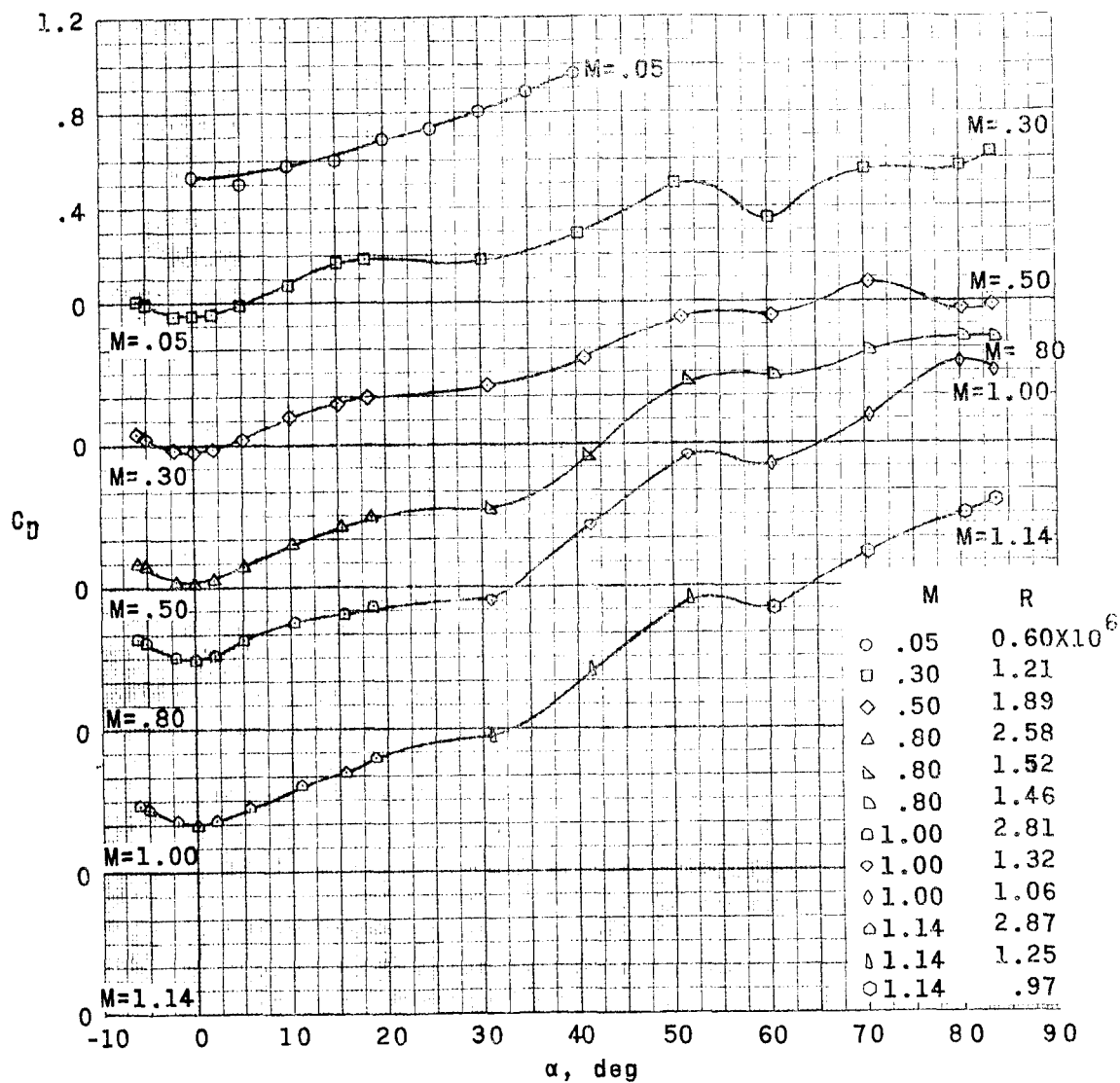
(a)  $M = 0.05$  to  $1.14$ .

Figure 8.- Variation of drag coefficient with angle of attack. Escape configuration.

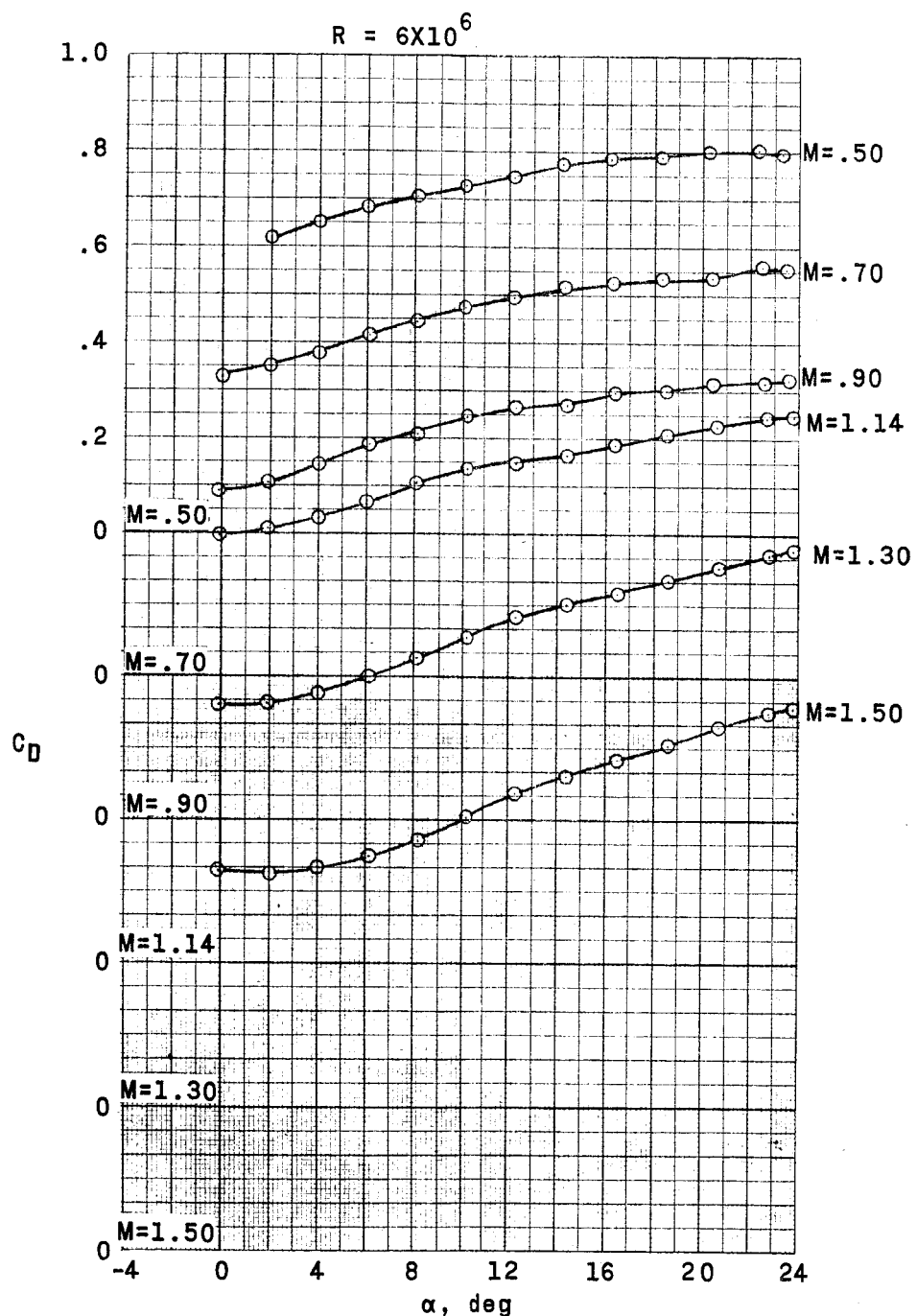
(b)  $M = 0.50$  to  $1.50$ .

Figure 8.- Continued.

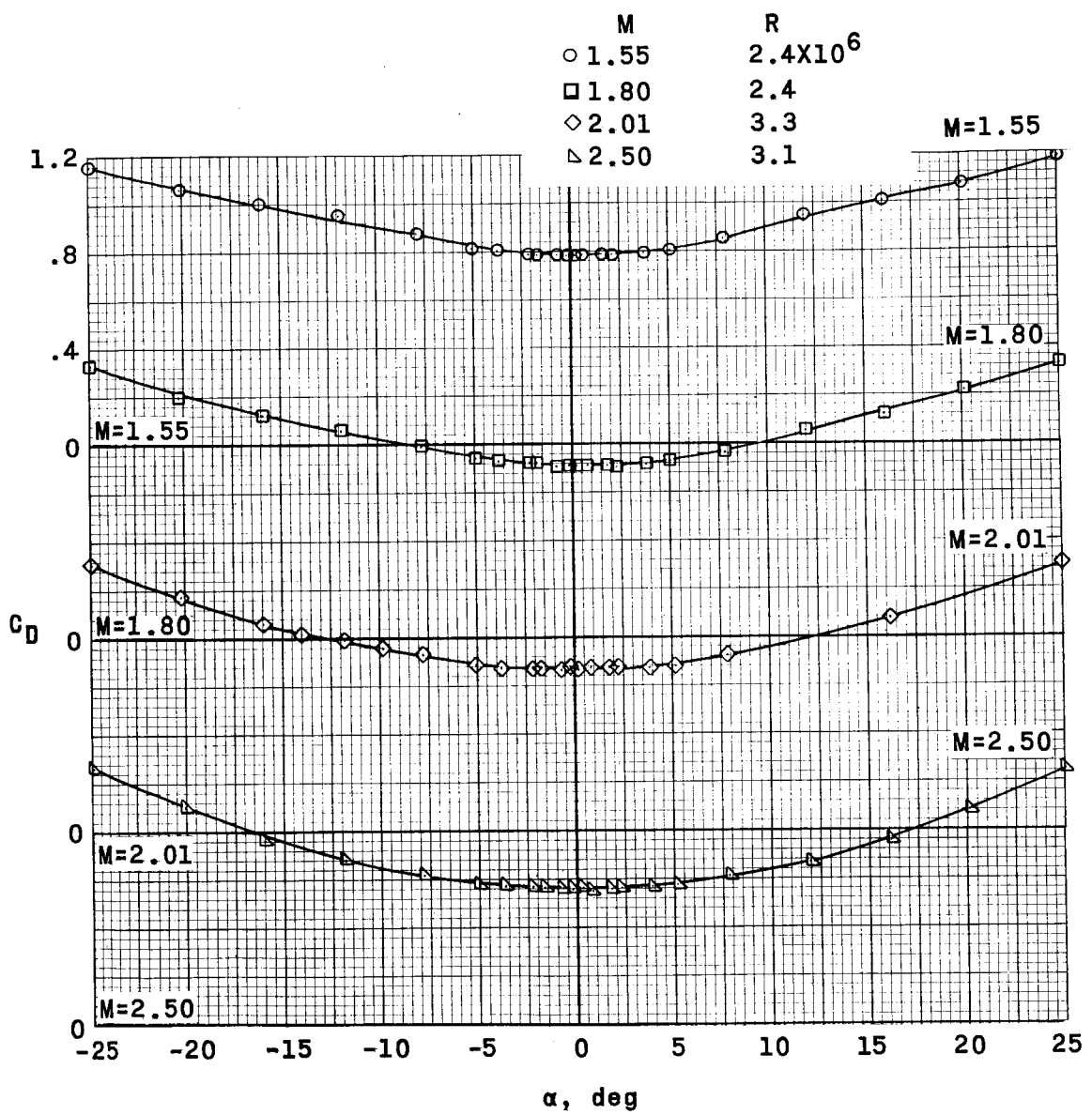
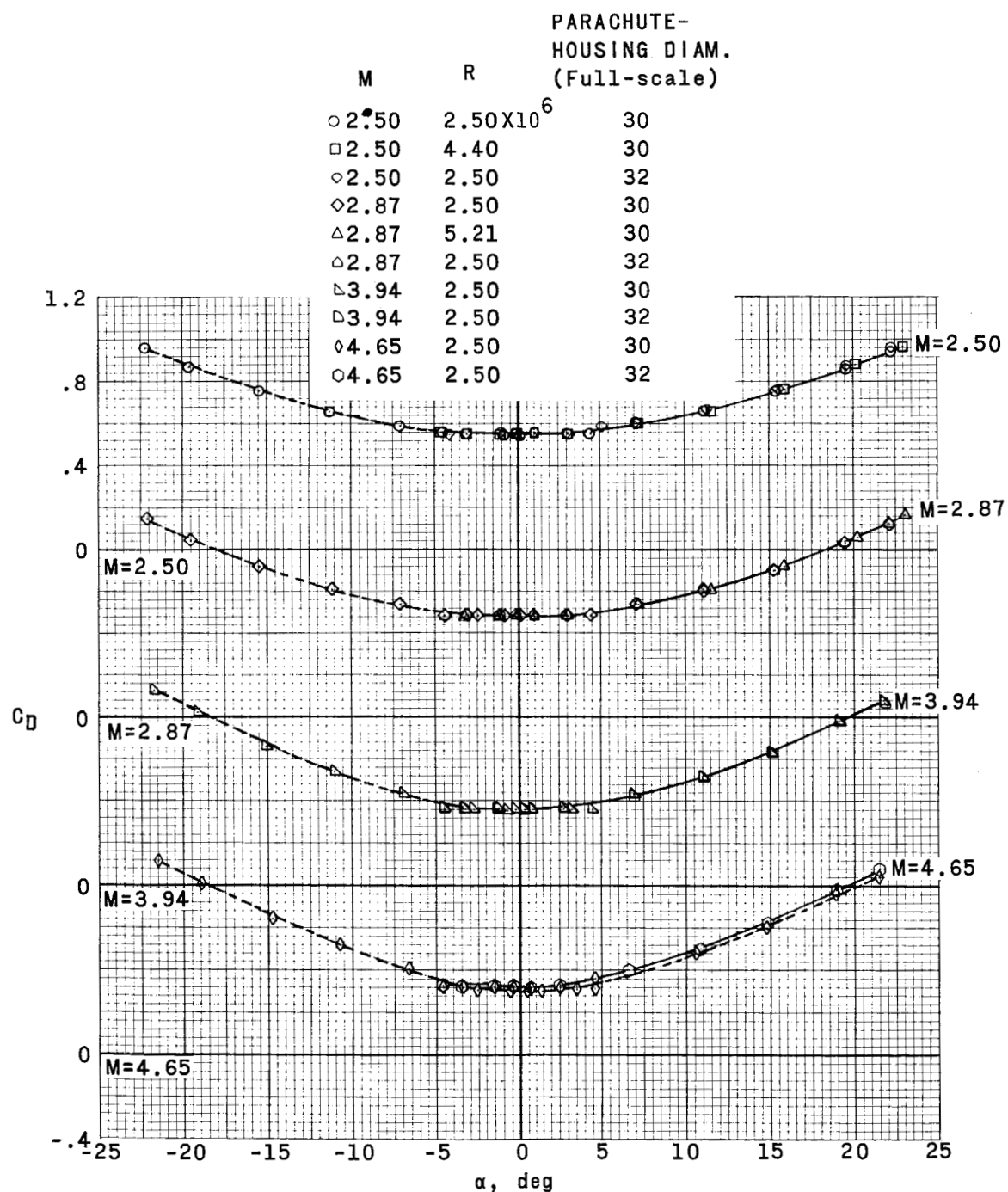
(c)  $M = 1.55$  to  $2.50$ .

Figure 8.- Continued.

DECLASSIFIED

59



(d)  $M = 2.50$  to  $4.65$ .

Figure 8.- Continued.

0313122A.J030

60

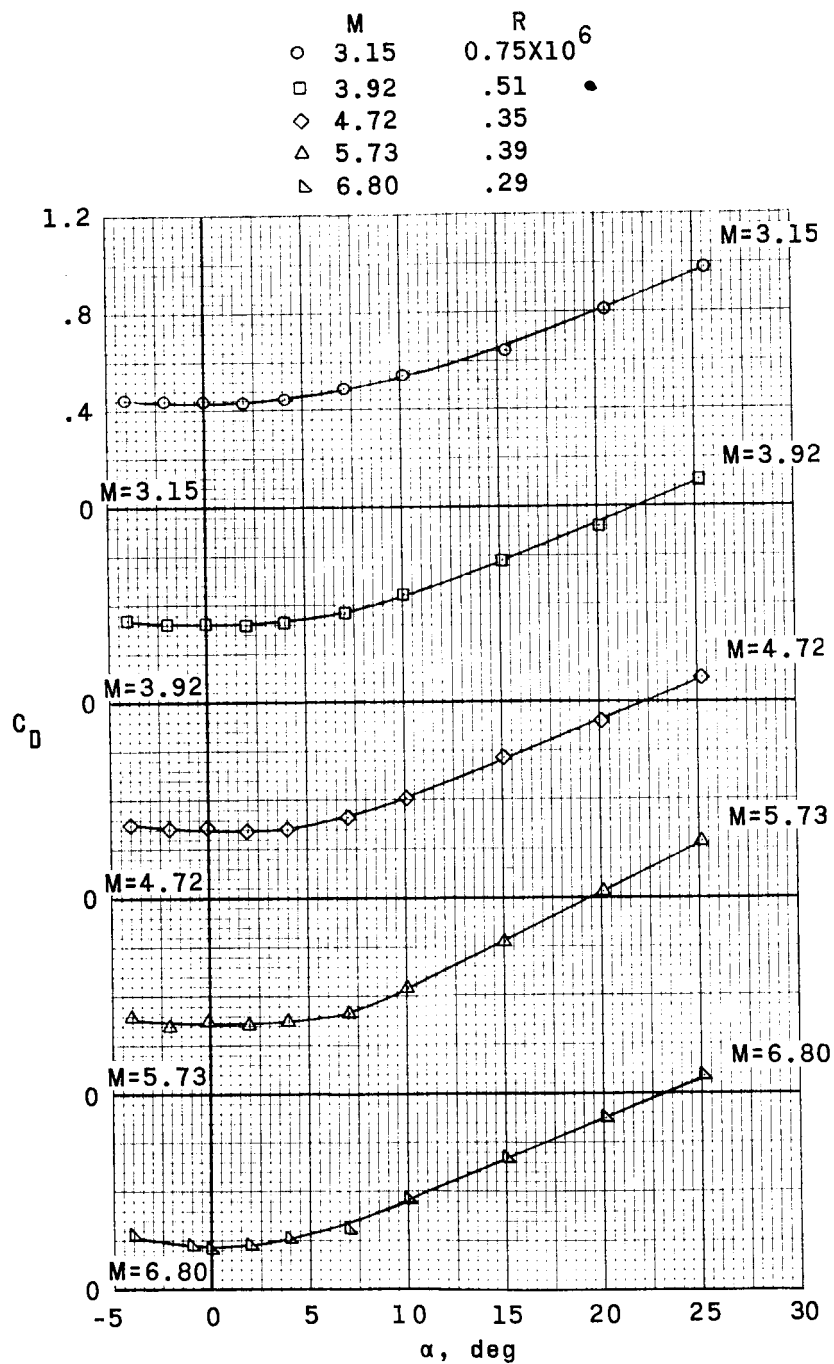
(e)  $M = 3.15$  to  $6.80$ .

Figure 8.- Concluded.

REF ID: A6972  
DECLASSIFIED

61

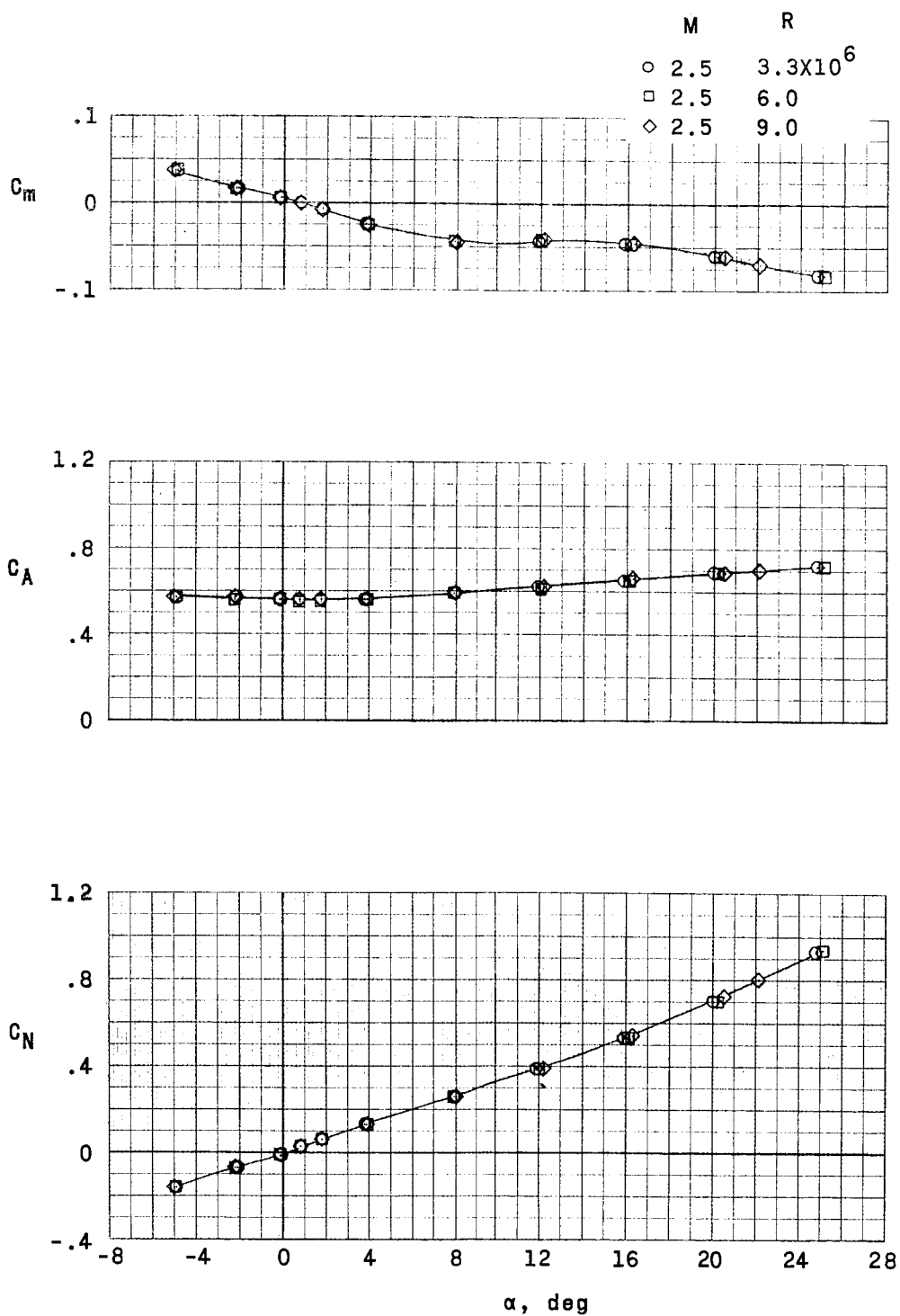


Figure 9.- Effect of Reynolds number on the longitudinal aerodynamic characteristics of the production escape configuration.  $M = 2.5$ .

031912 20.1030

8

62

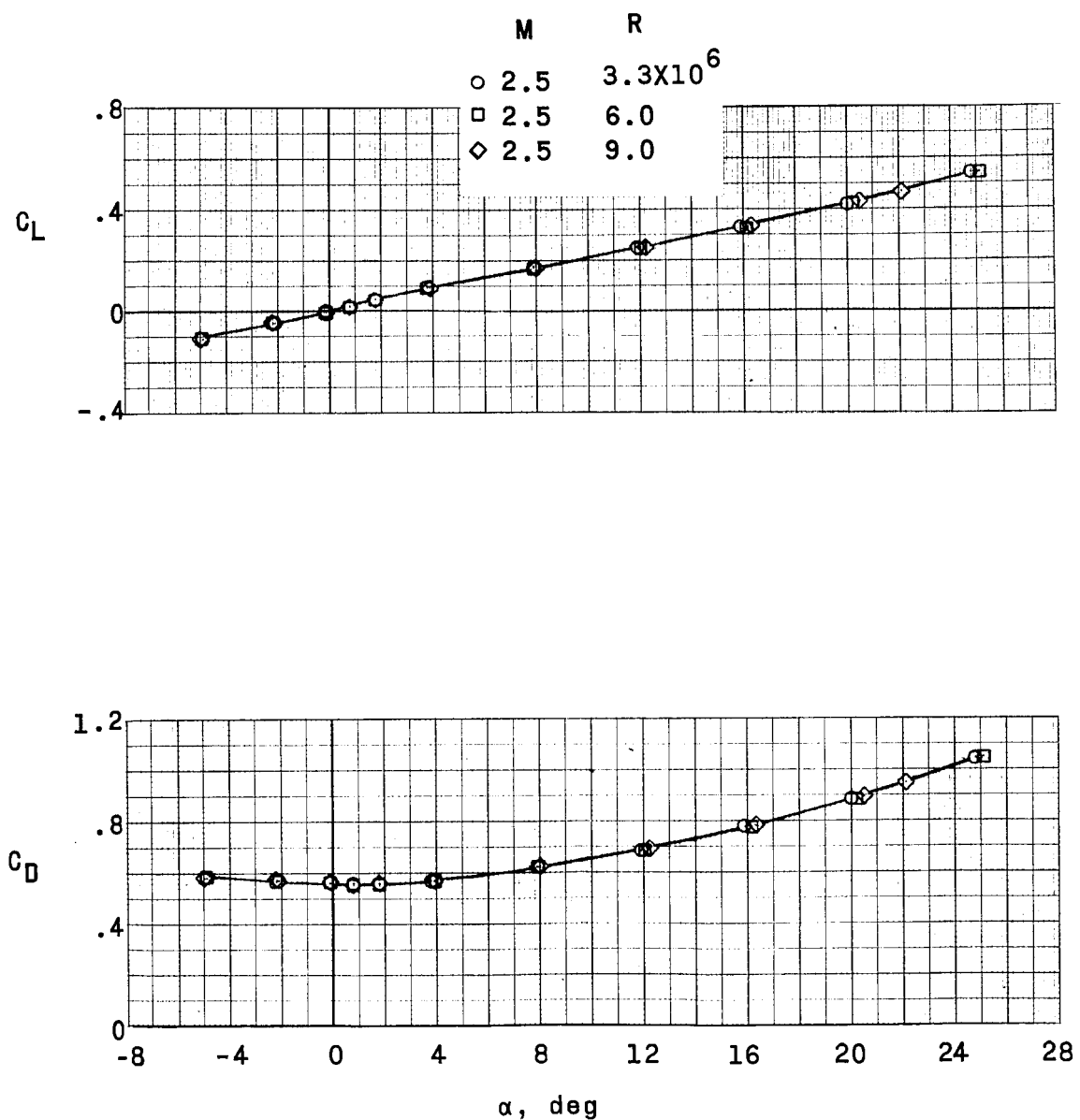


Figure 9.- Concluded.

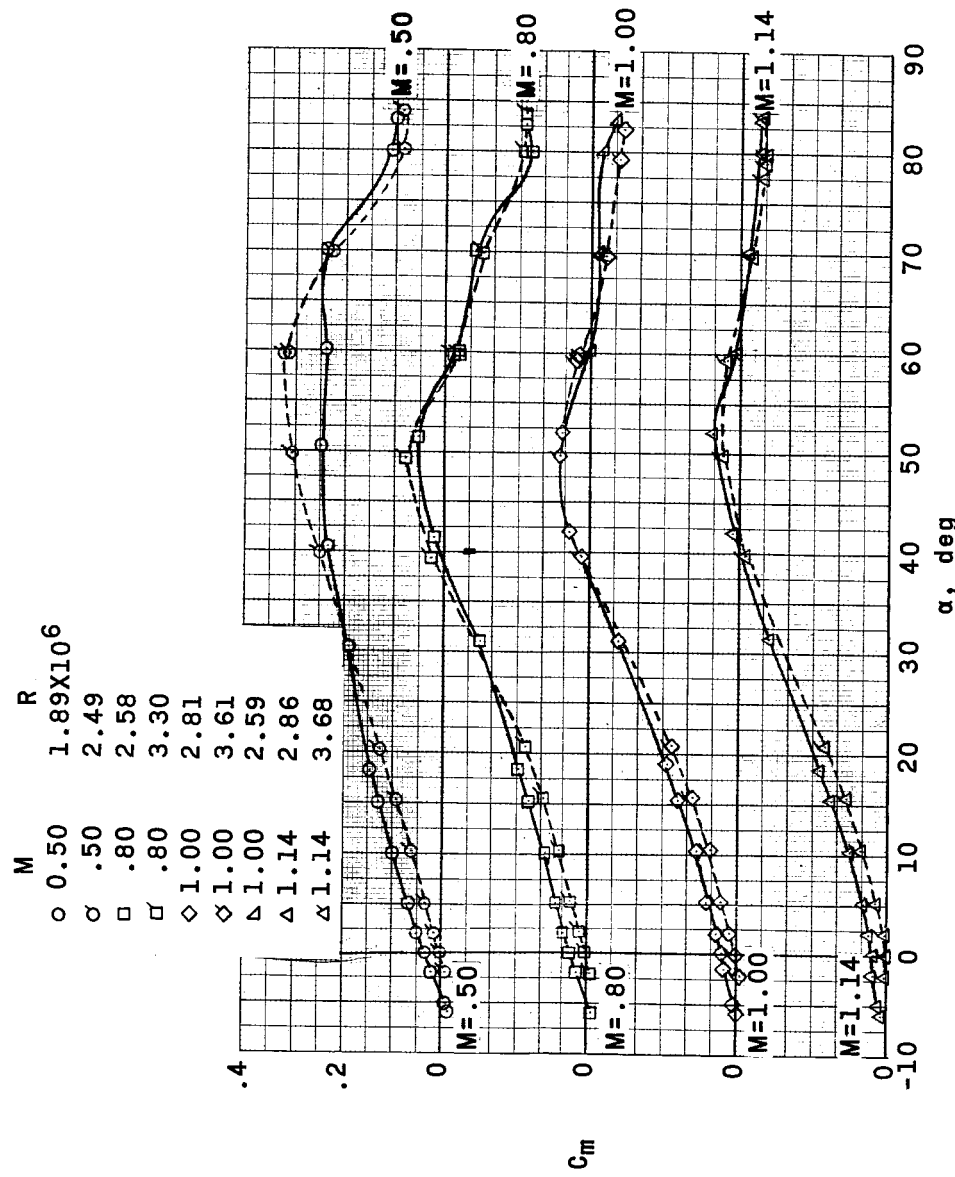
(a)  $M = 0.5$  to  $1.14$ .

Figure 10.- Variation of pitching-moment coefficient with angle of attack. Exit configuration; flagged symbols denote models without destabilizer flap.

0319122A.J030



64

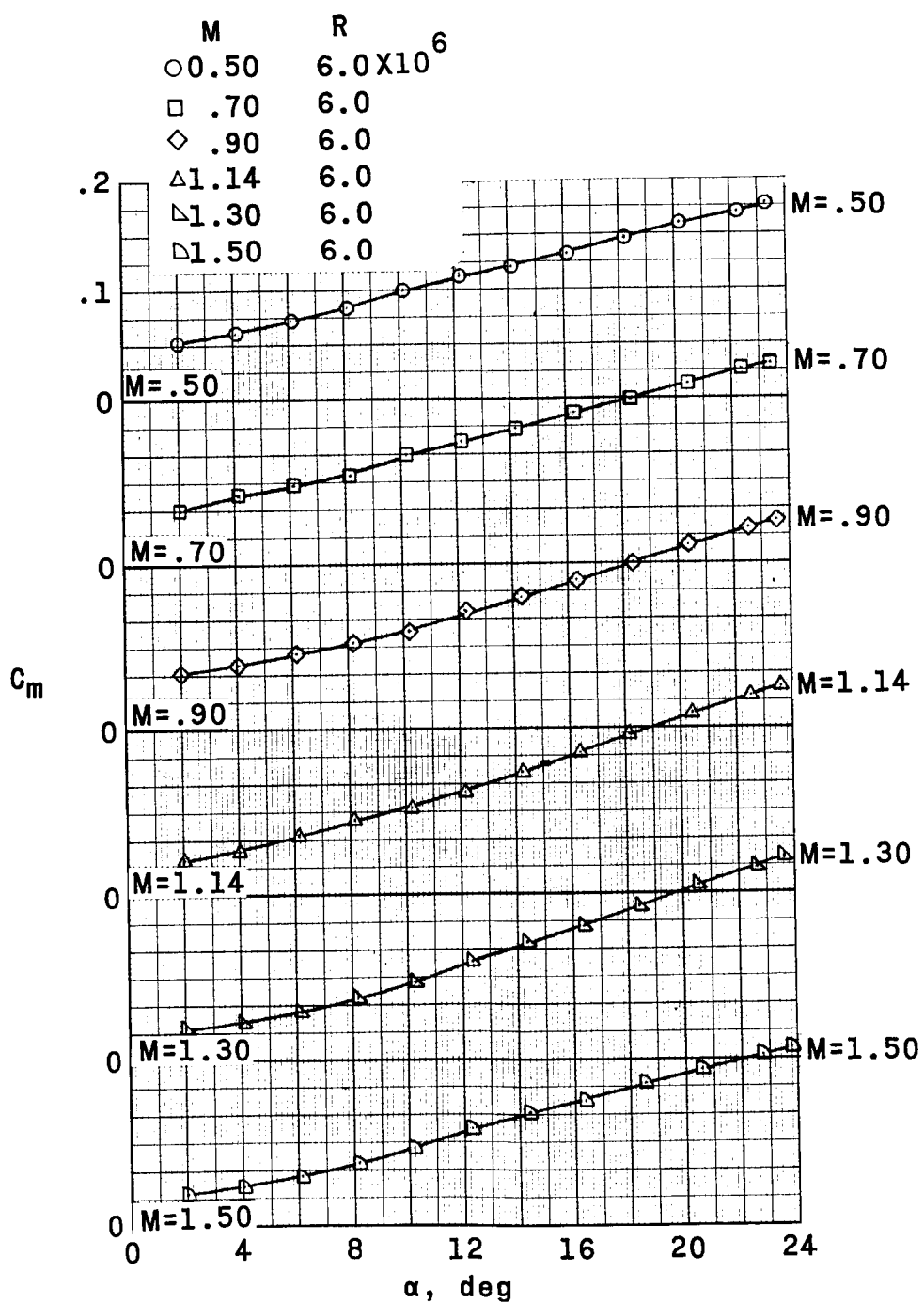
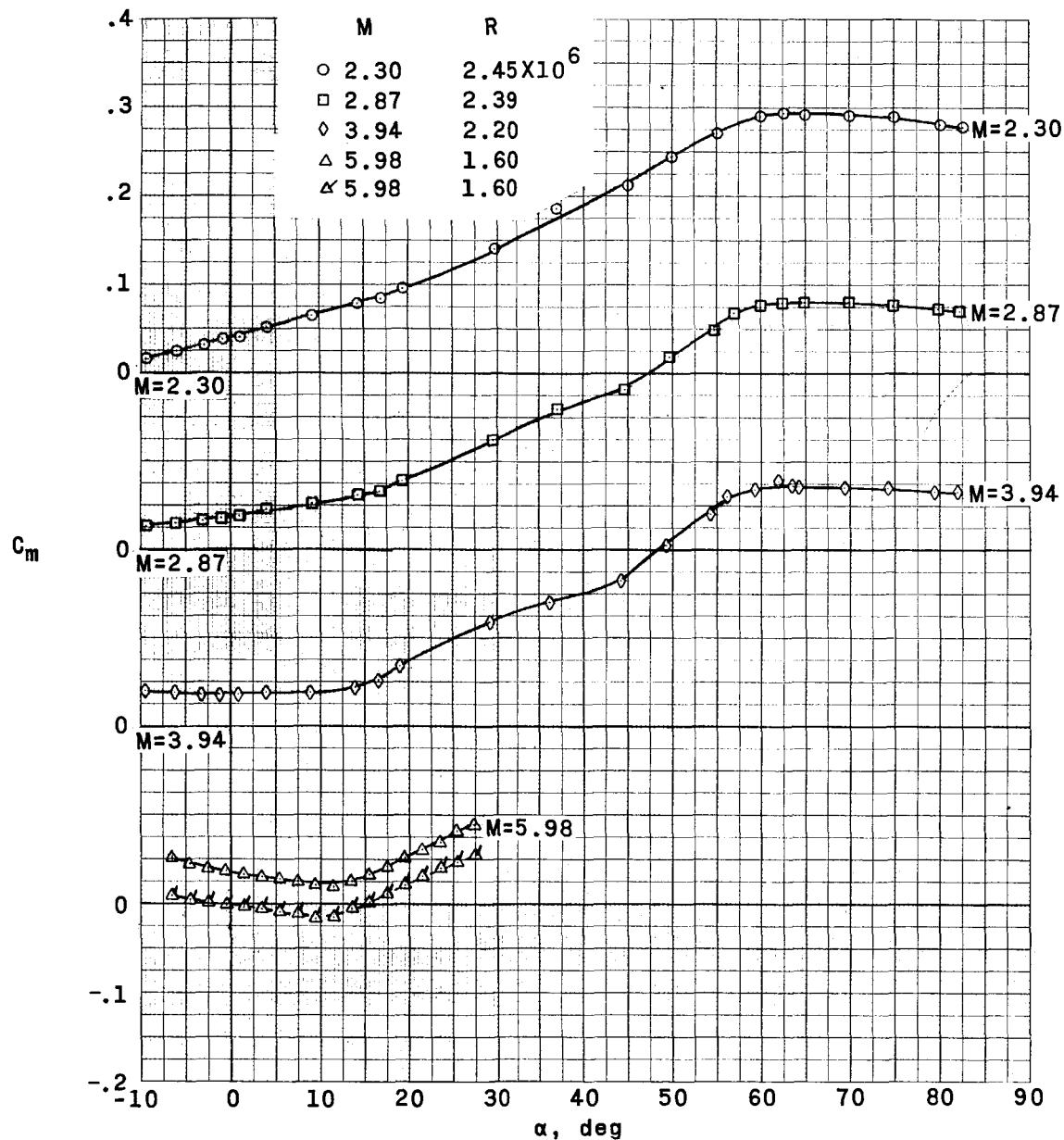
(b)  $M = 0.5$  to  $1.50$ .

Figure 10.- Continued.



DECLASSIFIED

65



(c)  $M = 2.30$  to  $5.98$ .

Figure 10.- Continued.

03171220 1030 8

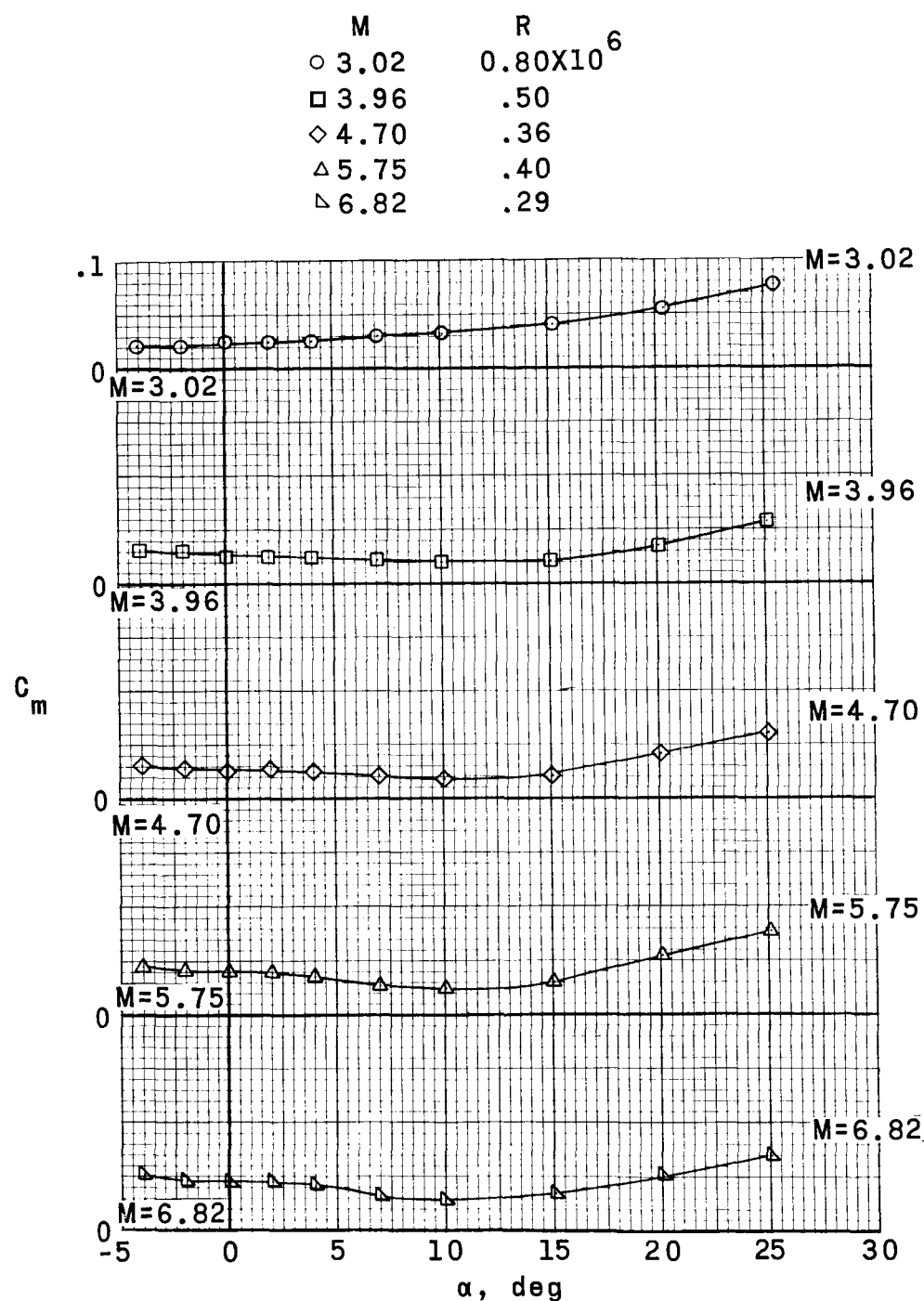
(d)  $M = 3.02$  to  $6.82$ .

Figure 10.- Concluded.

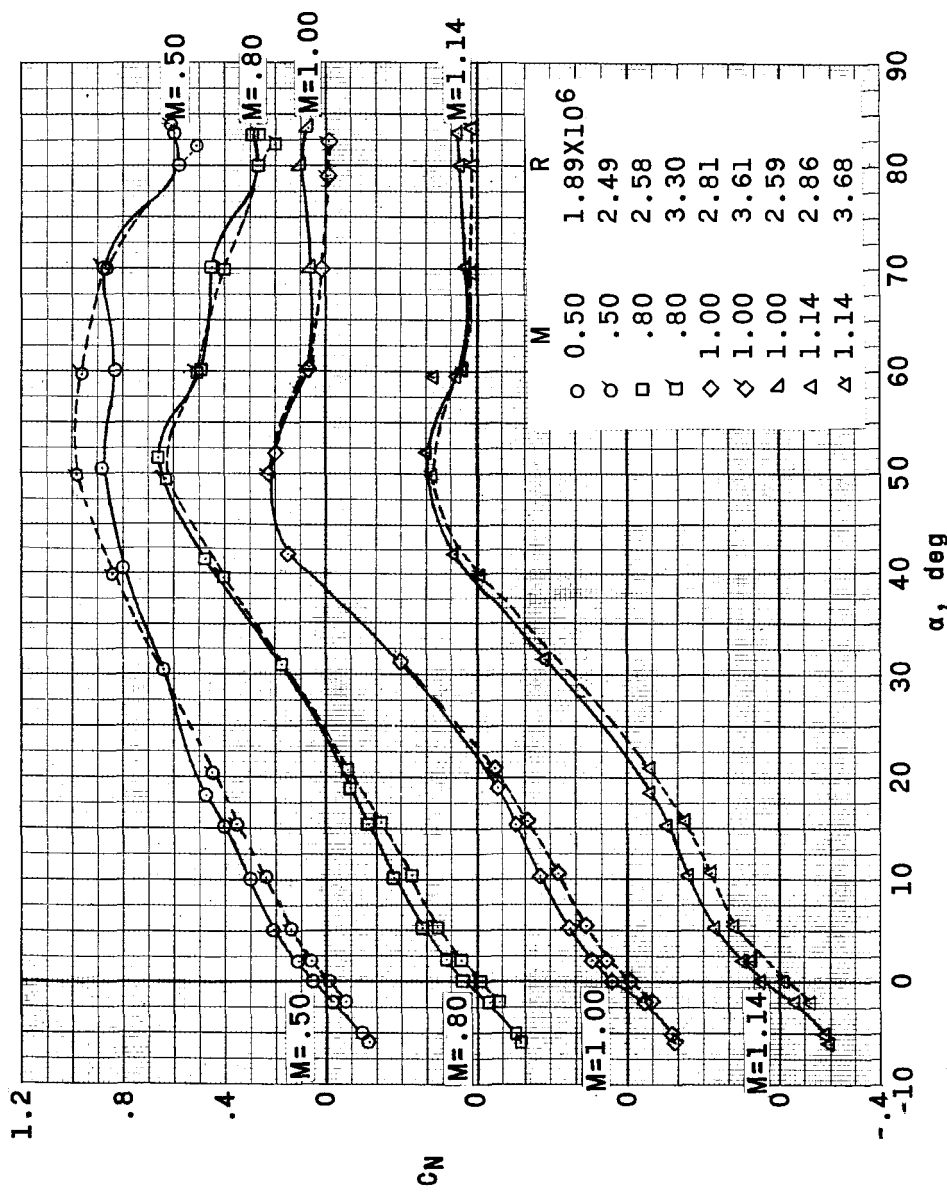
(a)  $M = 0.5$  to  $1.14$ .

Figure 11.- Variation of normal-force coefficient with angle of attack. Exit configuration; flagged symbols denote models without destabilizer flap.

03191020 1530

8

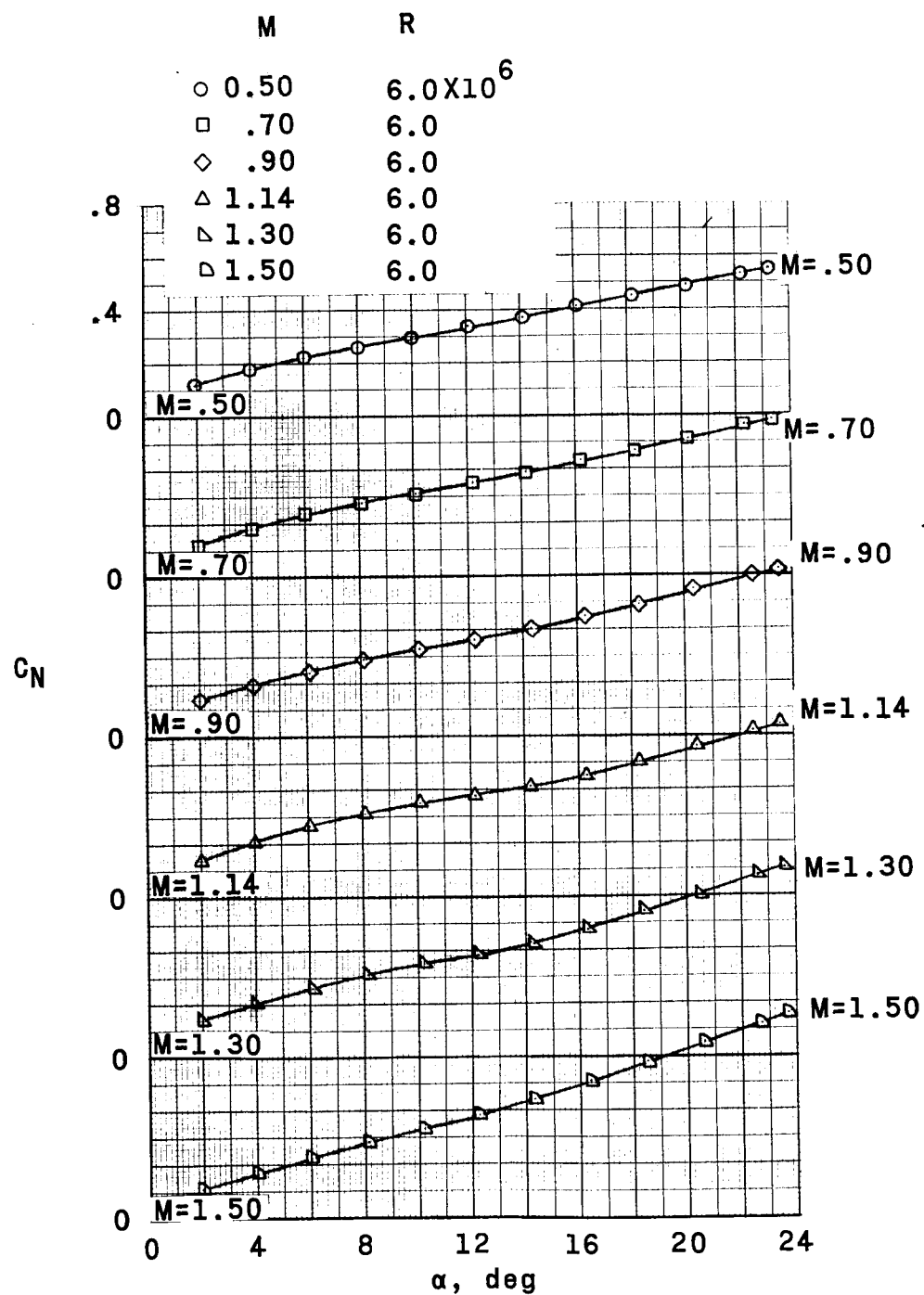
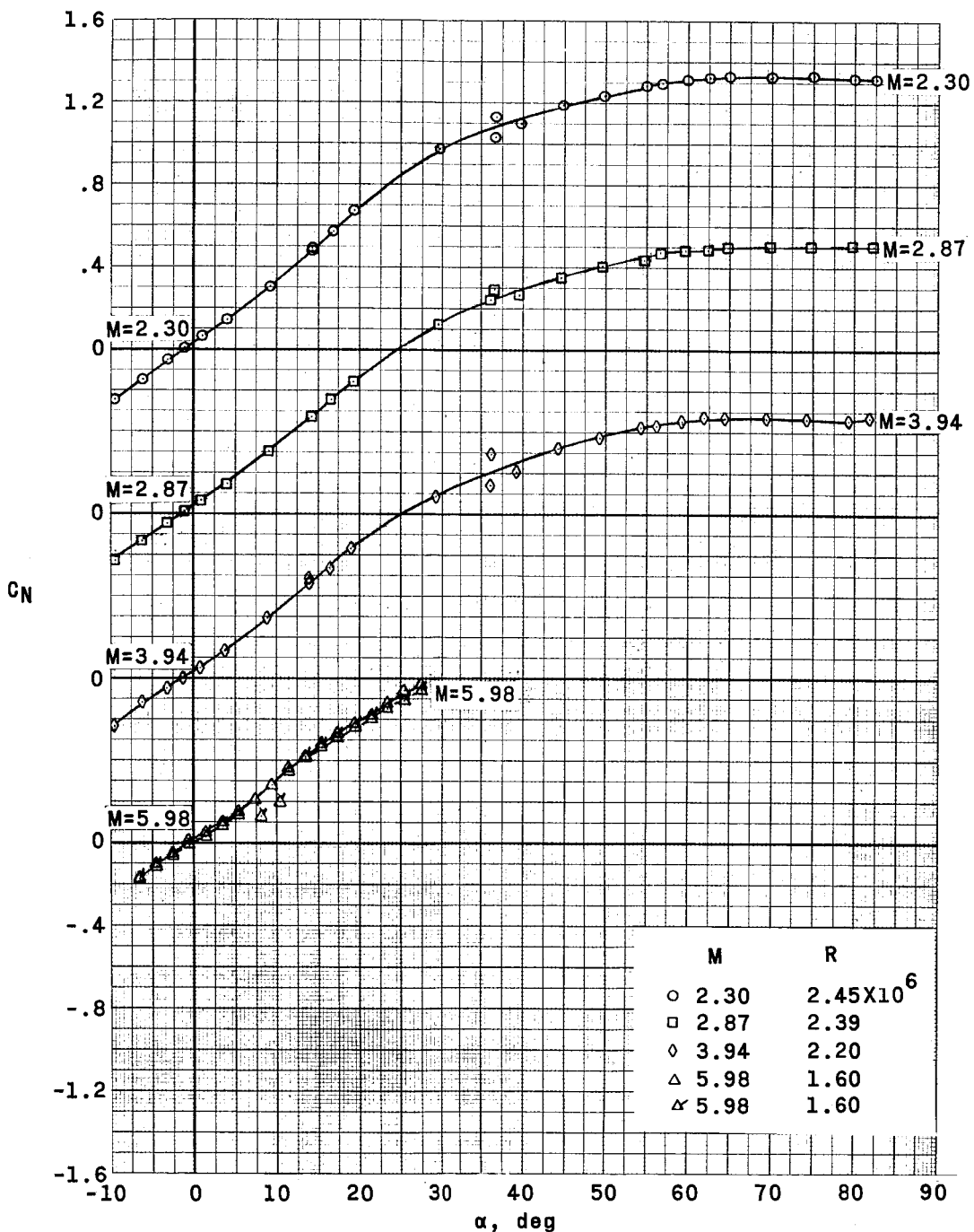
(b)  $M = 0.50$  to  $1.50$ .

Figure 11.- Continued.

REF ID: A6542

69



(c)  $M = 2.30$  to  $5.98$ .

Figure 11.- Continued.

03191230 10000

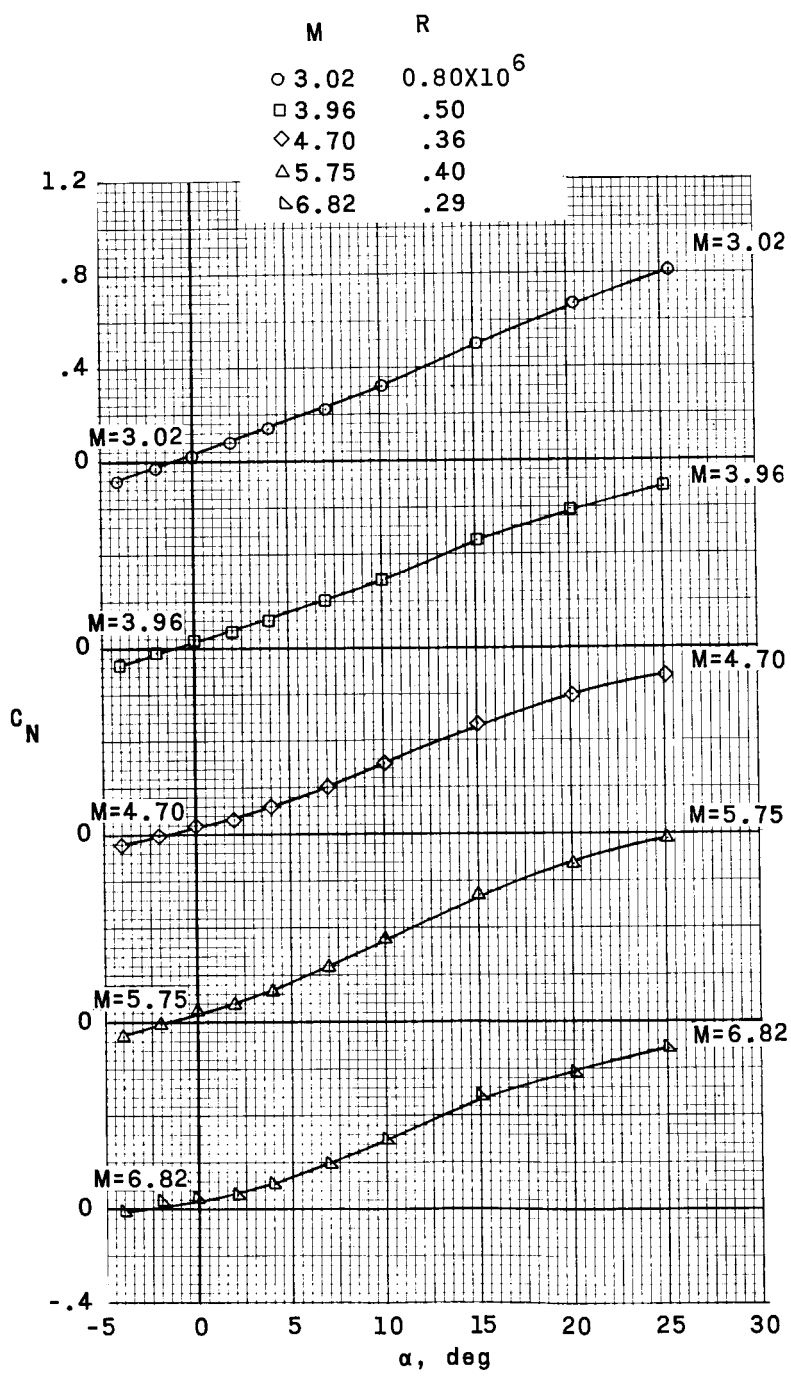
(d)  $M = 3.02 \text{ to } 6.82.$ 

Figure 11.- Concluded.

REFLOGGED

71

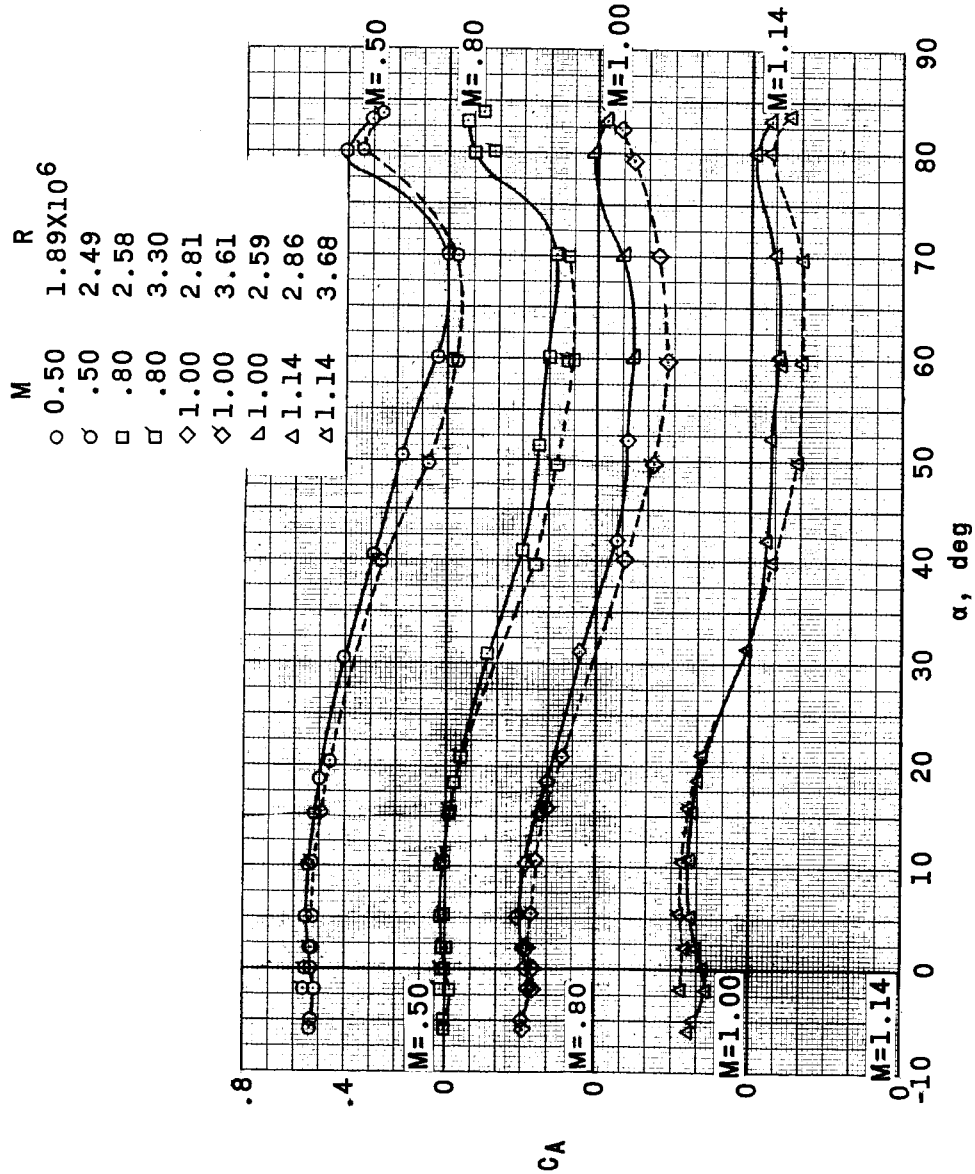


Figure 12.- Variation of axial-force coefficient with angle of attack. Exit configuration; flagged symbols denote models without destabilizer flap.

03171220110300

8

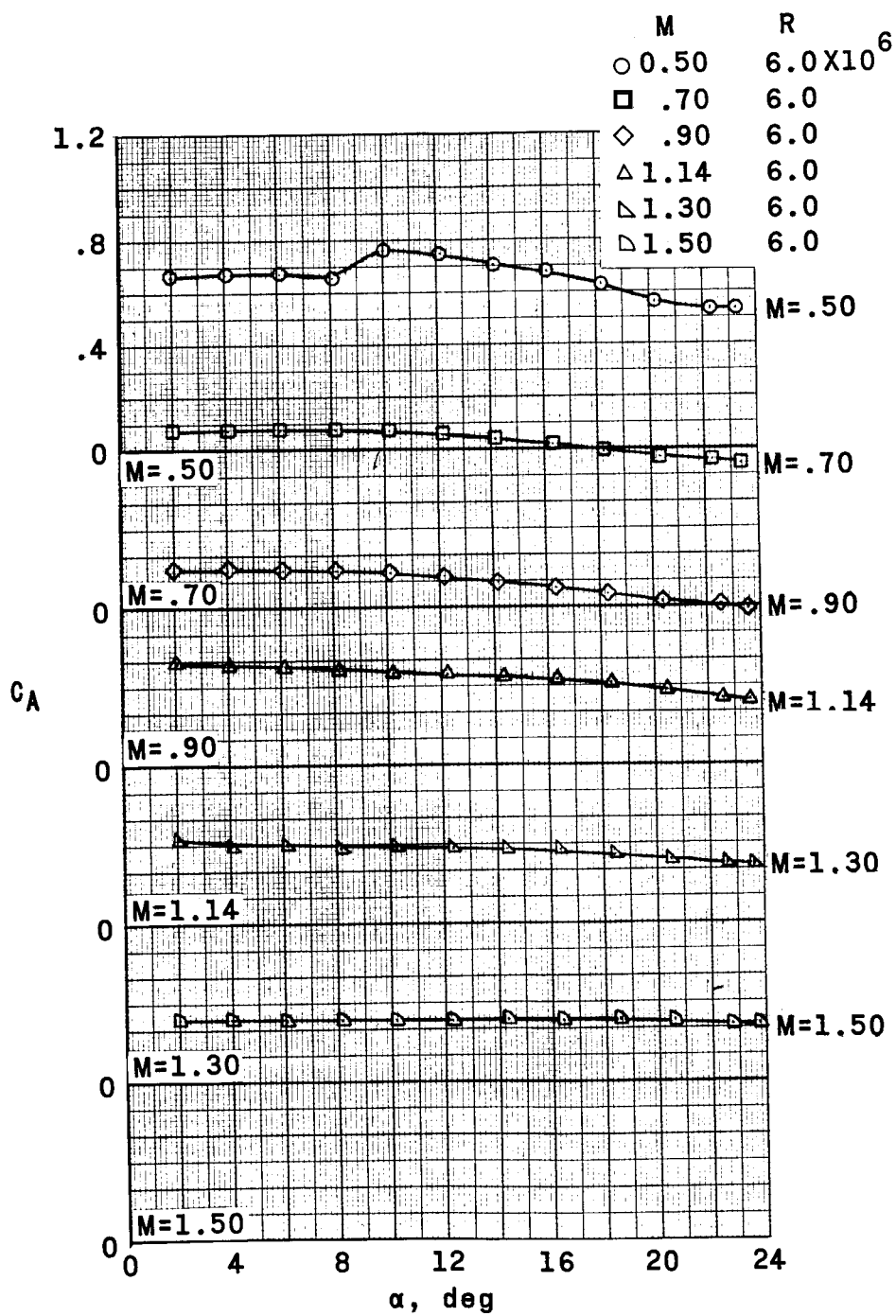
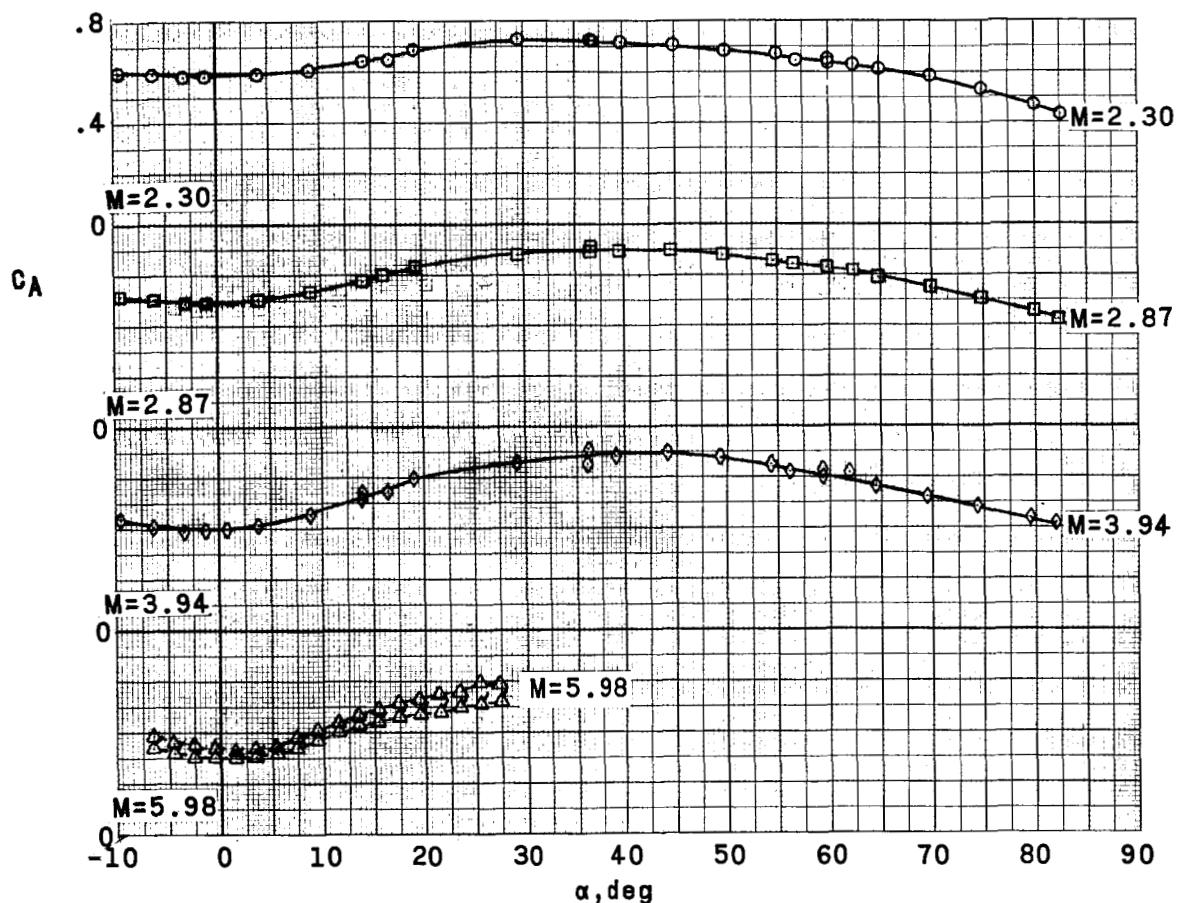
(b)  $M = 0.50$  to  $1.50$ .

Figure 12.- Continued.

REF ID: A65792  
DECLASSIFIED

73

M	R
○ 2.30	$2.45 \times 10^6$
□ 2.87	2.39
◊ 3.94	2.20
△ 5.98	1.60
△ 5.98	1.60



(c)  $M = 2.30$  to  $5.98$ .

Figure 12.- Continued.

0319122A1030 8

M	R
○ 3.02	$0.80 \times 10^6$
□ 3.96	.50
◇ 4.70	.36
△ 5.75	.40
▽ 6.82	.29

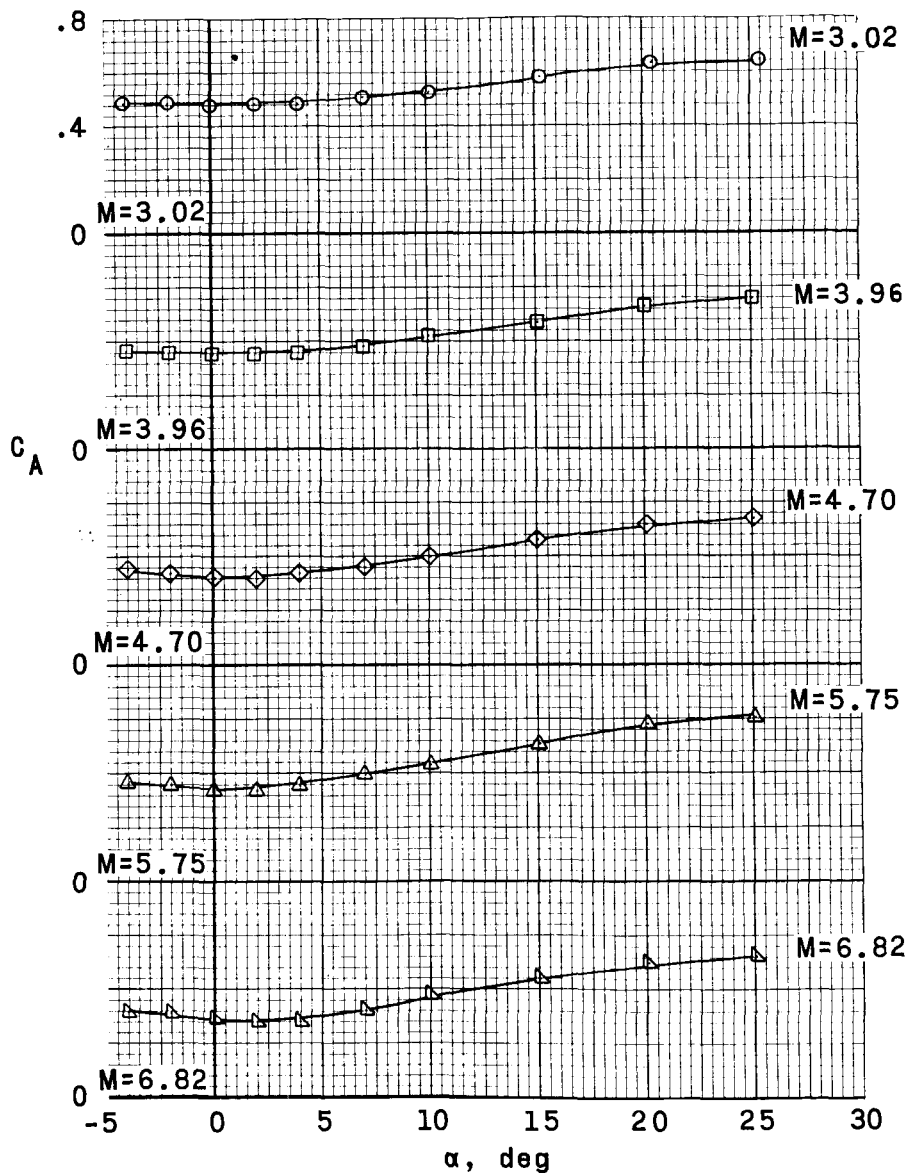
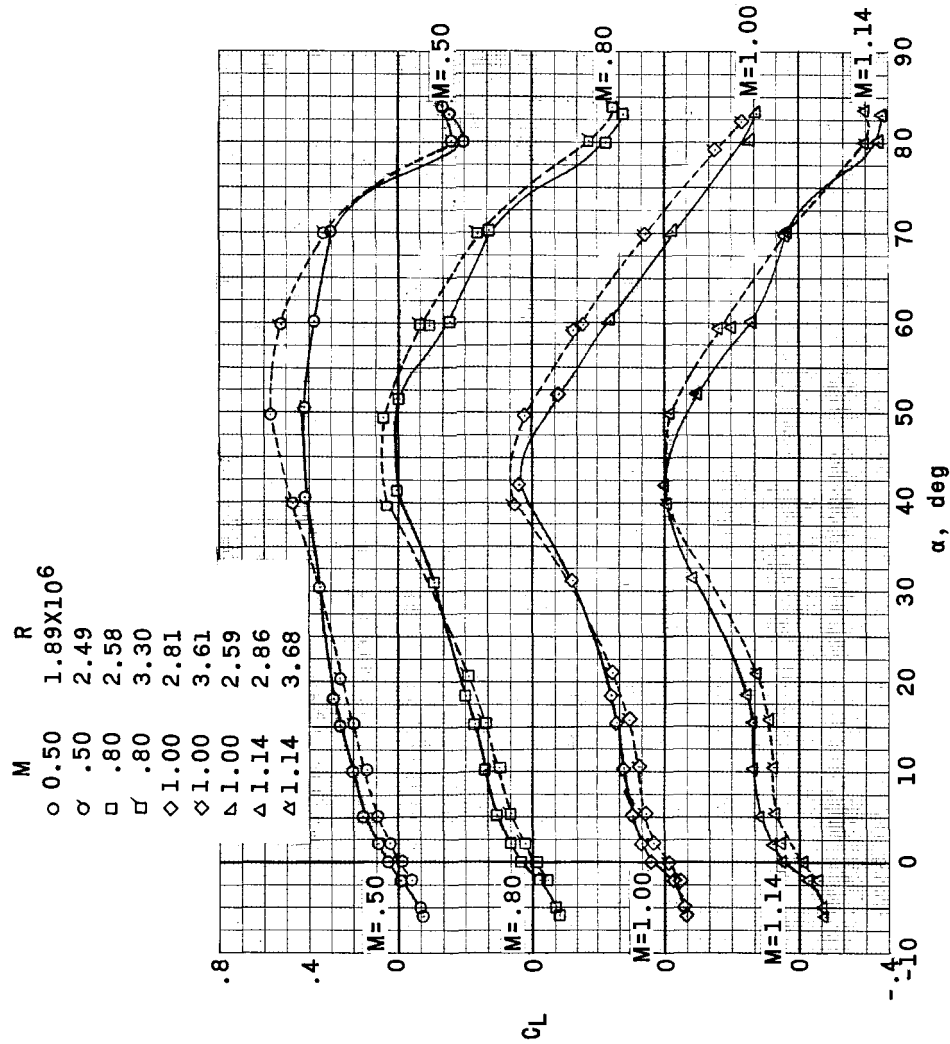
(d)  $M = 3.02$  to  $6.82$ .

Figure 12.- Concluded.

REF ID: A6520

75



(a)  $M = 0.5$  to  $1.14$ .

Figure 13.- Variation of lift coefficient with angle of attack. Exit configuration; flagged symbols denote models without destabilizer flap.

03171220 1030

76

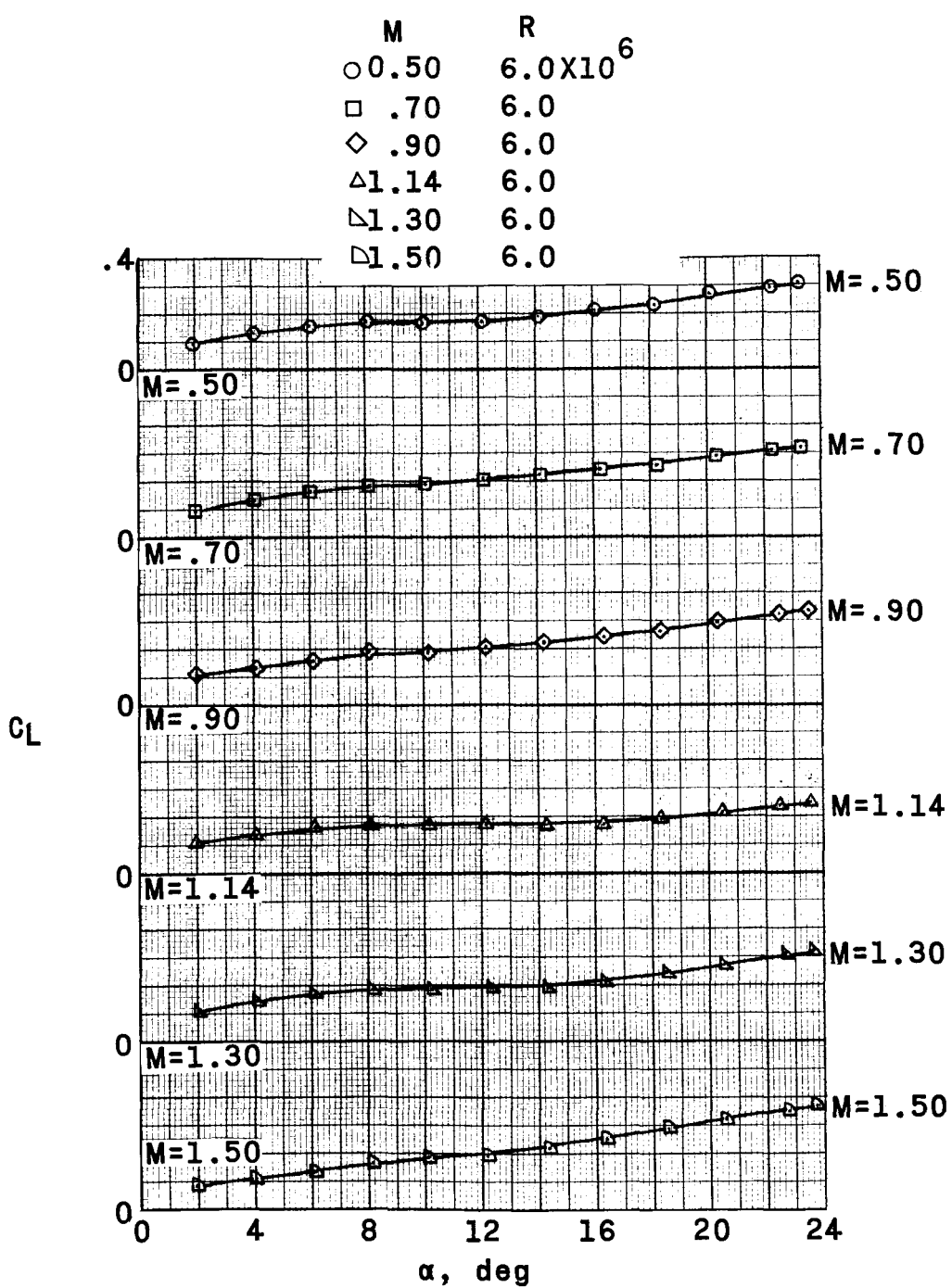
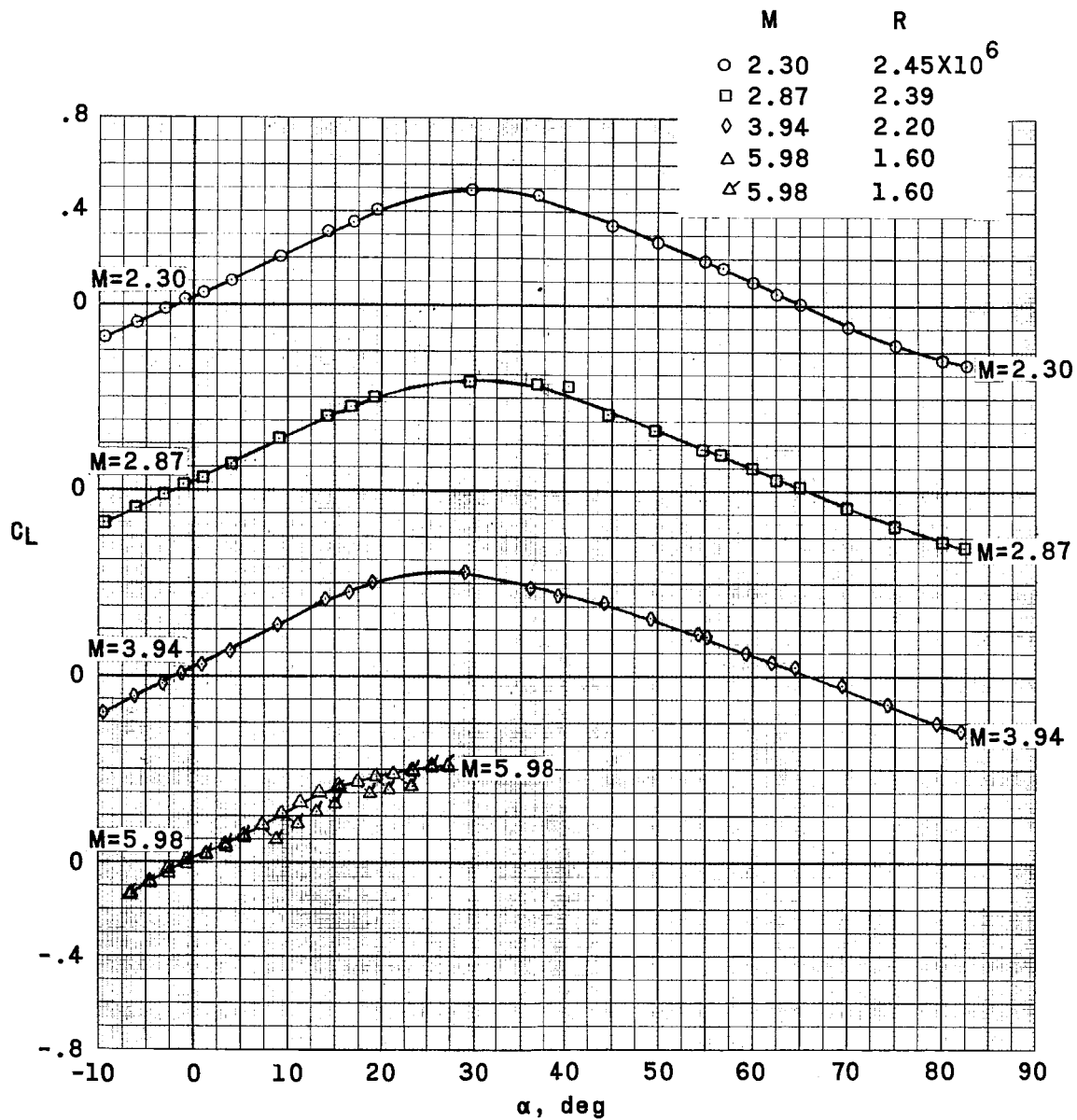
(b)  $M = 0.50$  to  $1.50$ .

Figure 13.- Continued.

DECLASSIFIED

77



(c)  $M = 2.30$  to  $5.98$ .

Figure 13.- Continued.

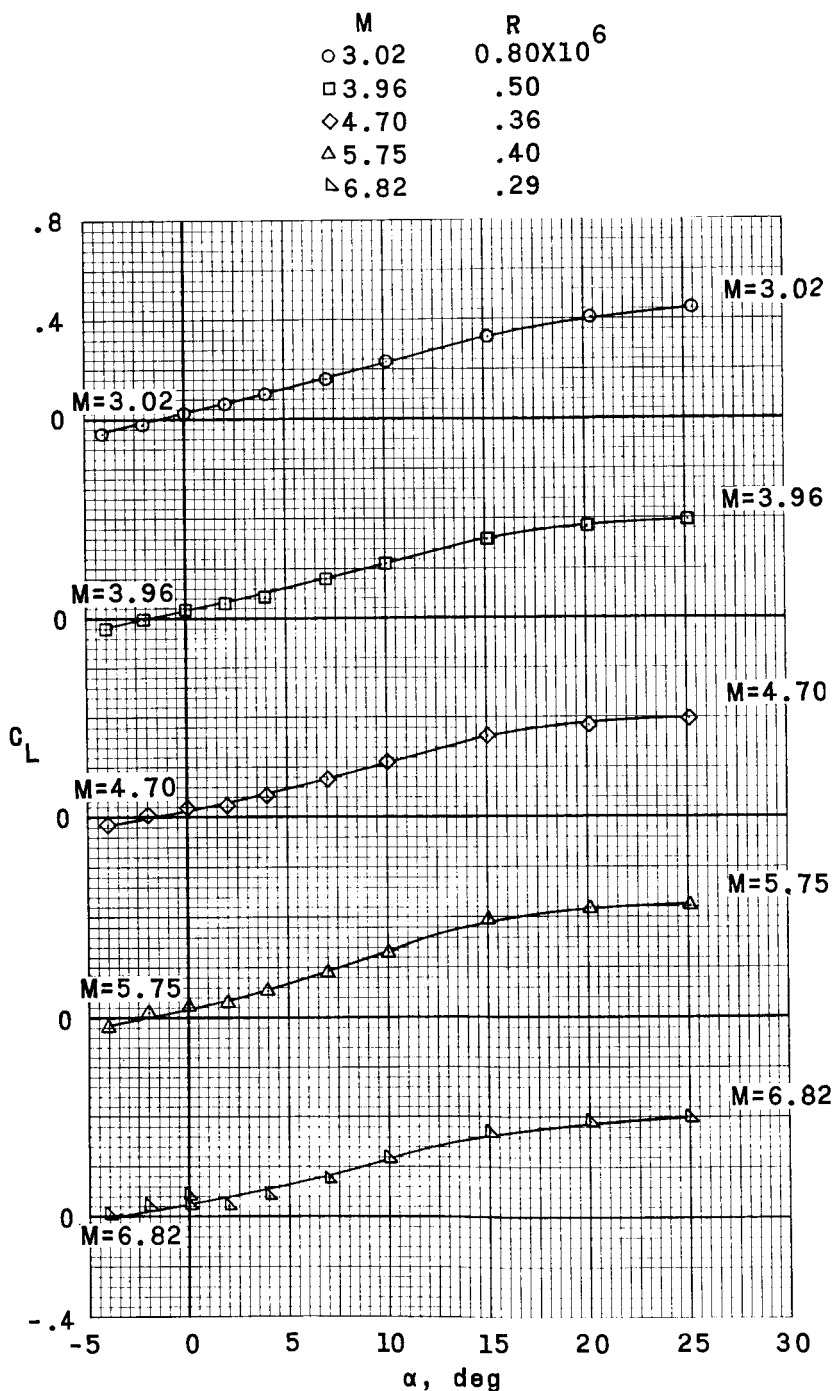
(d)  $M = 3.02$  to  $6.82$ .

Figure 13.- Concluded.

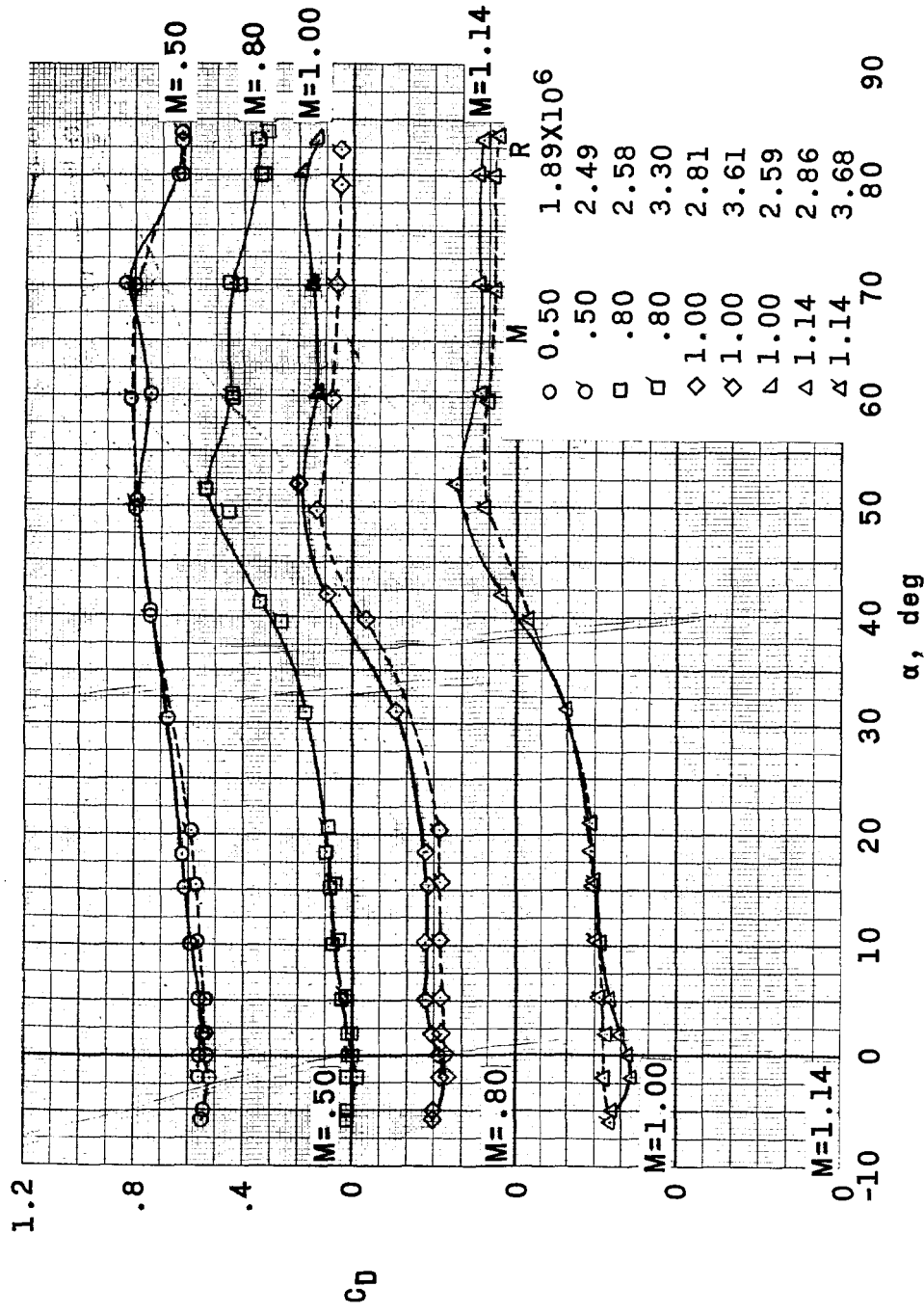
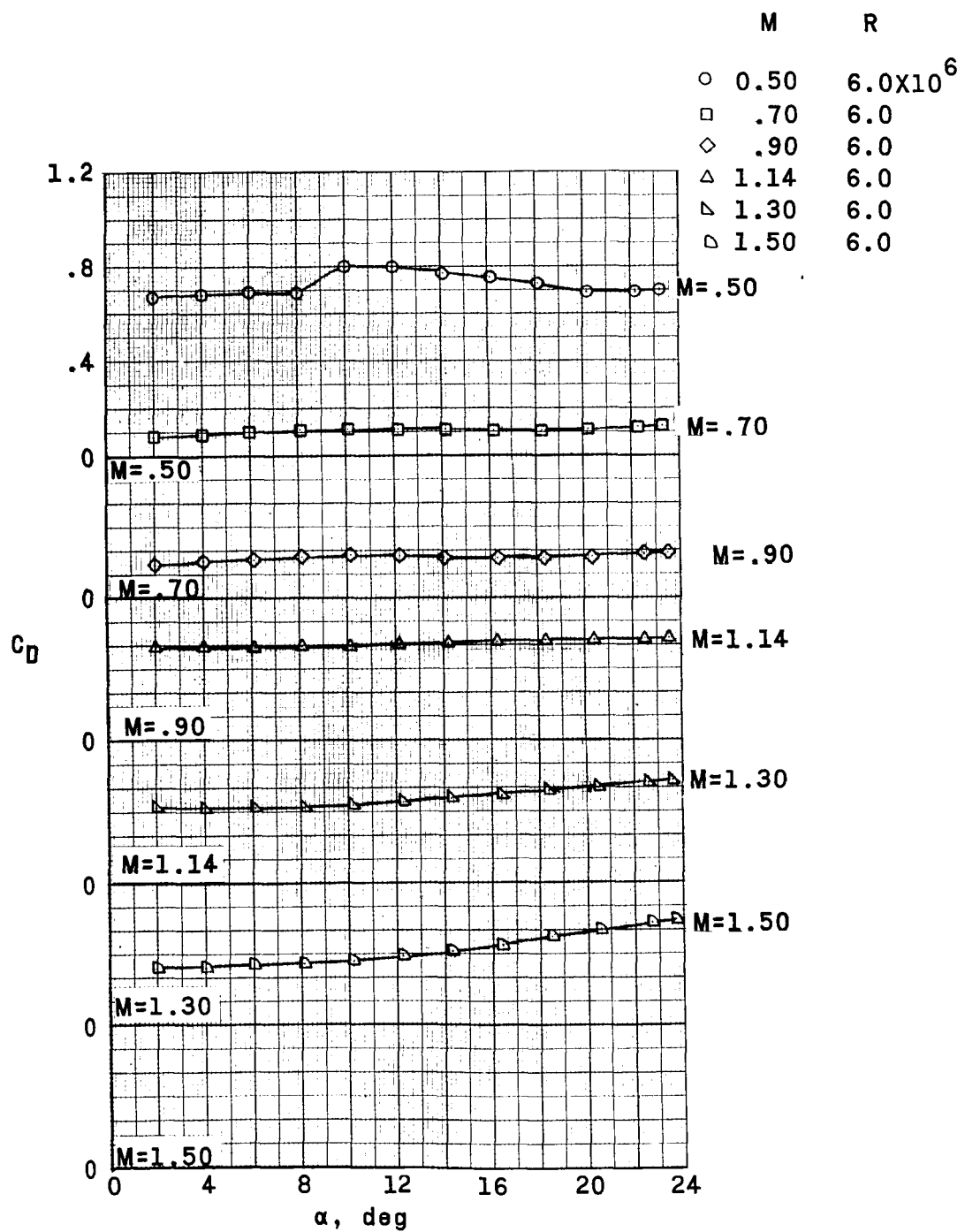
(a)  $M = 0.5$  to  $1.14$ .

Figure 14.- Variation of drag coefficient with angle of attack. Exit configuration; flagged symbols denote models without destabilizer flap.

03191020A1030 8

80



(b)  $M = 0.50$  to  $1.50$ .

Figure 14.- Continued.

REF ID: A6579

DECLASSIFIED

81

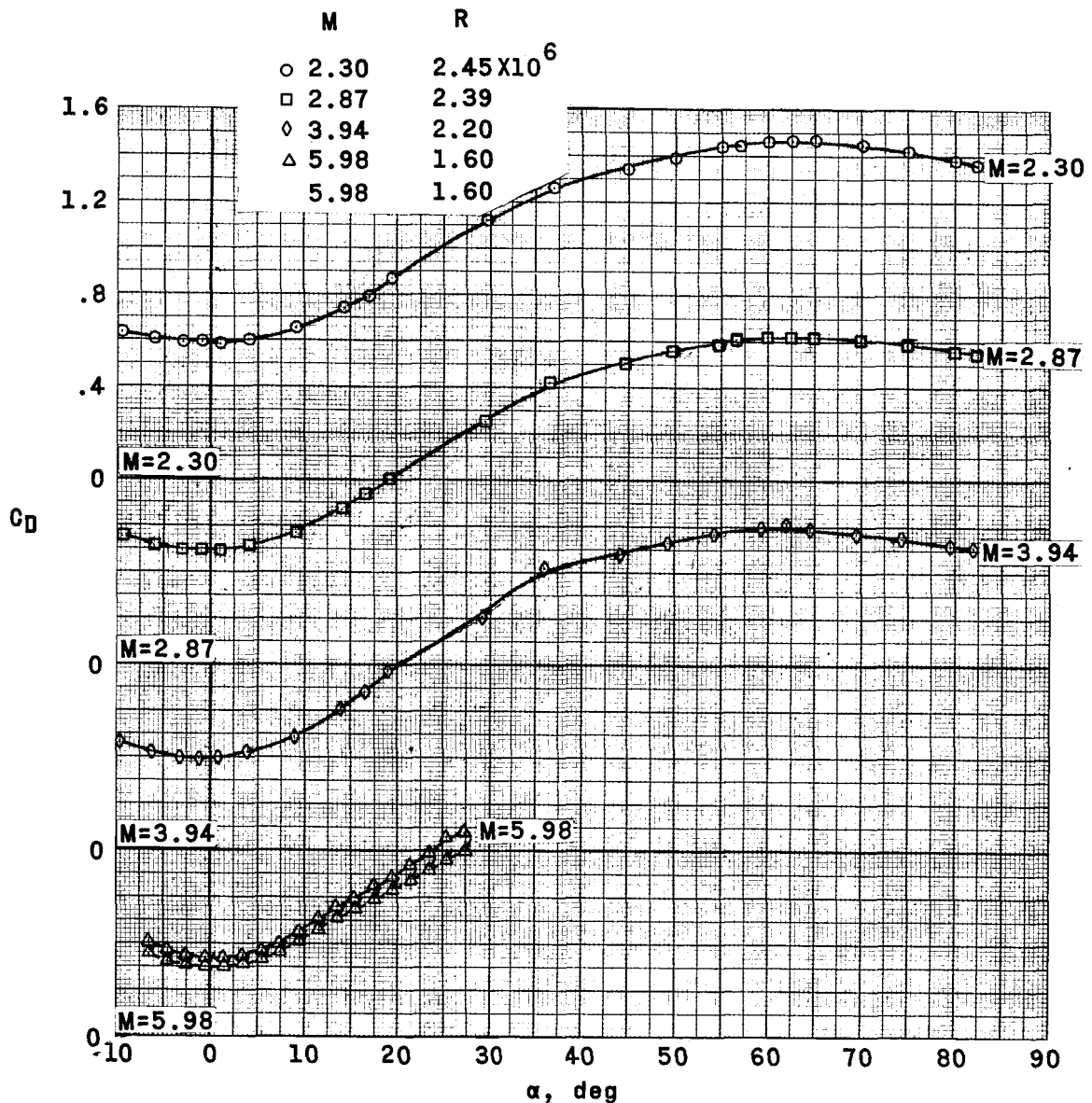
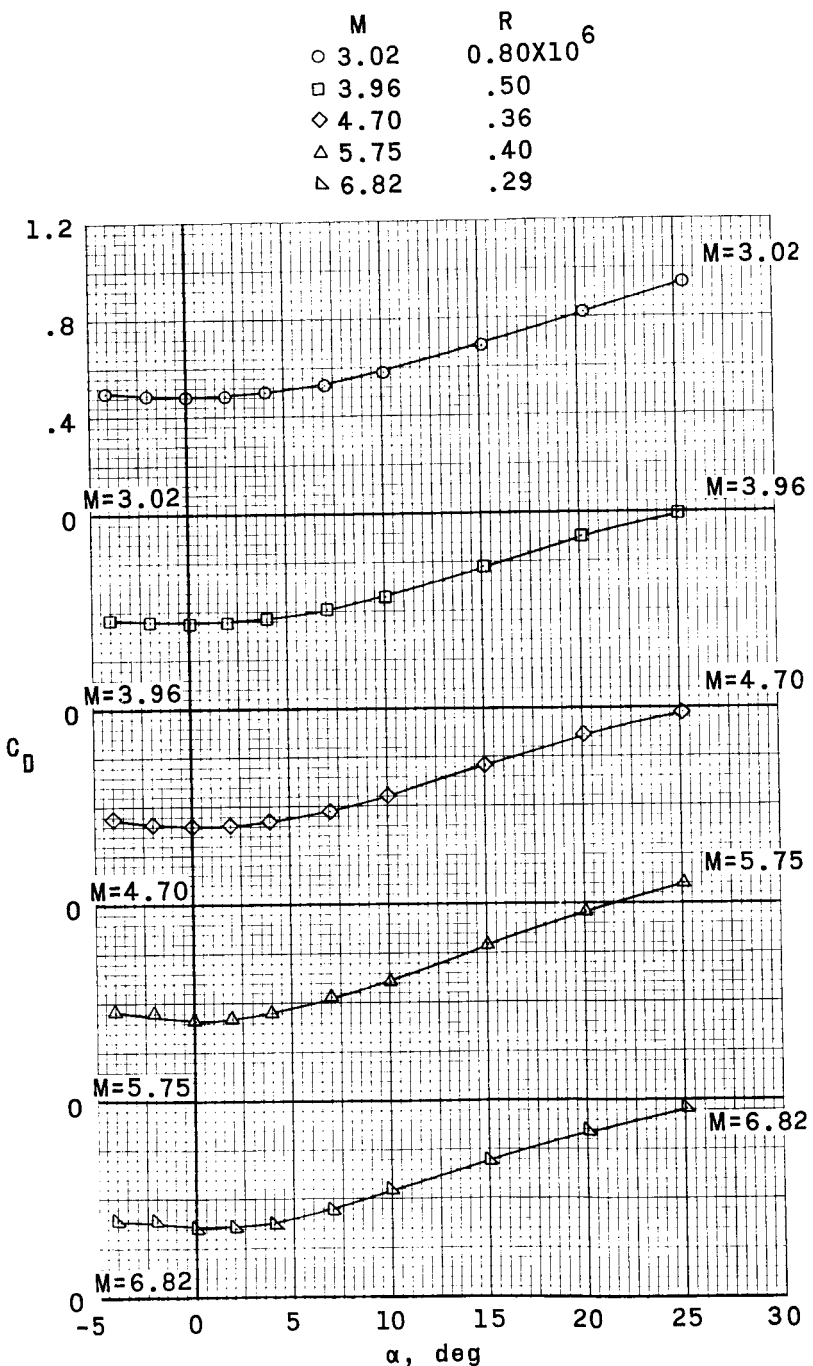


Figure 14.- Continued.

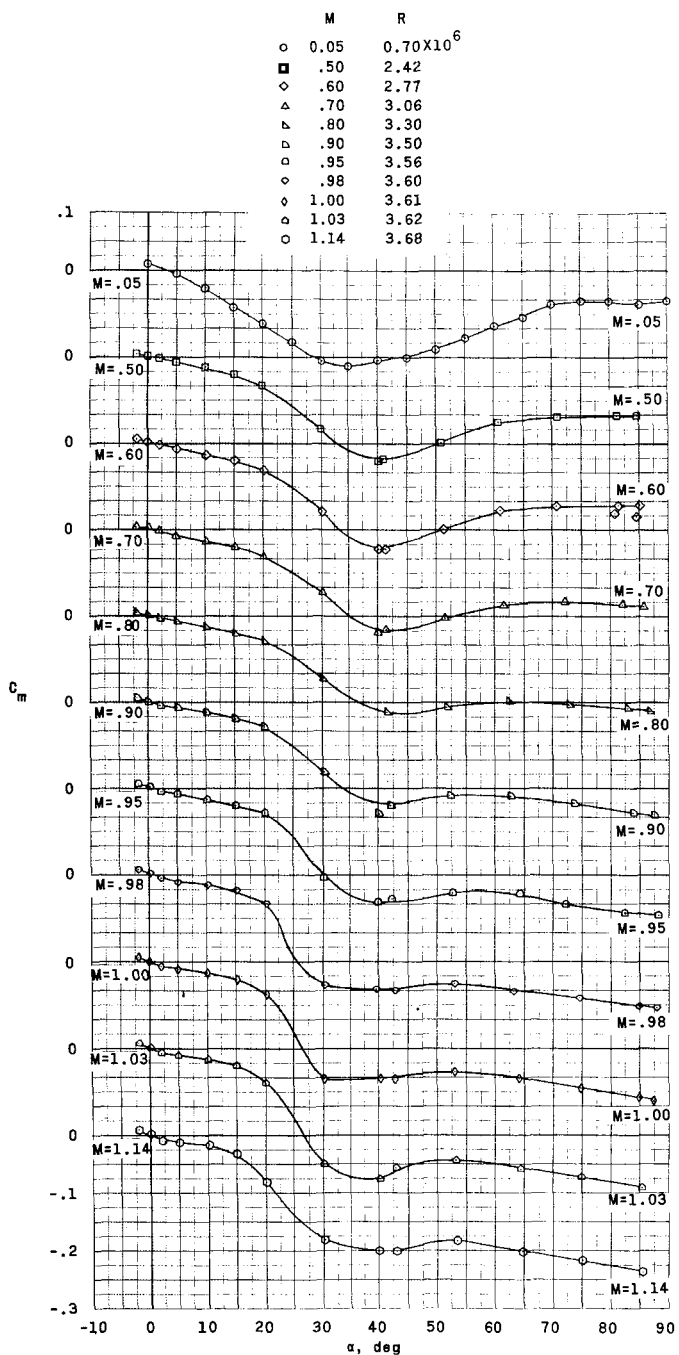


(d)  $M = 3.02$  to  $6.82$ .

Figure 14.- Concluded.

RECORDED & INDEXED

83



(a)  $M = 0.05$  to  $1.14$ .

Figure 15.- Variation of pitching-moment coefficient with angle of attack. Reentry configuration.

031712201030

8

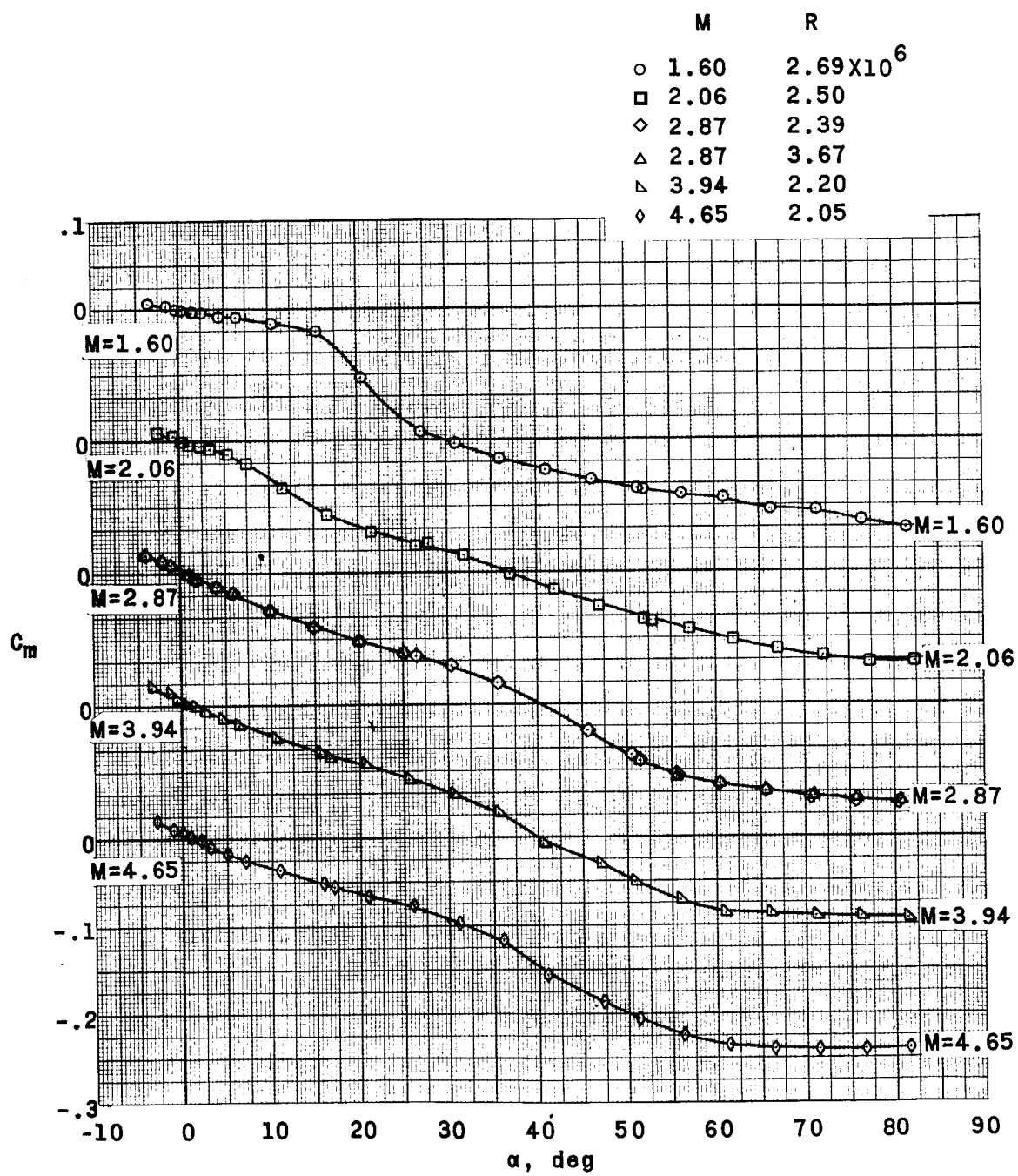
(b)  $M = 1.60$  to  $4.65$ .

Figure 15.- Continued.

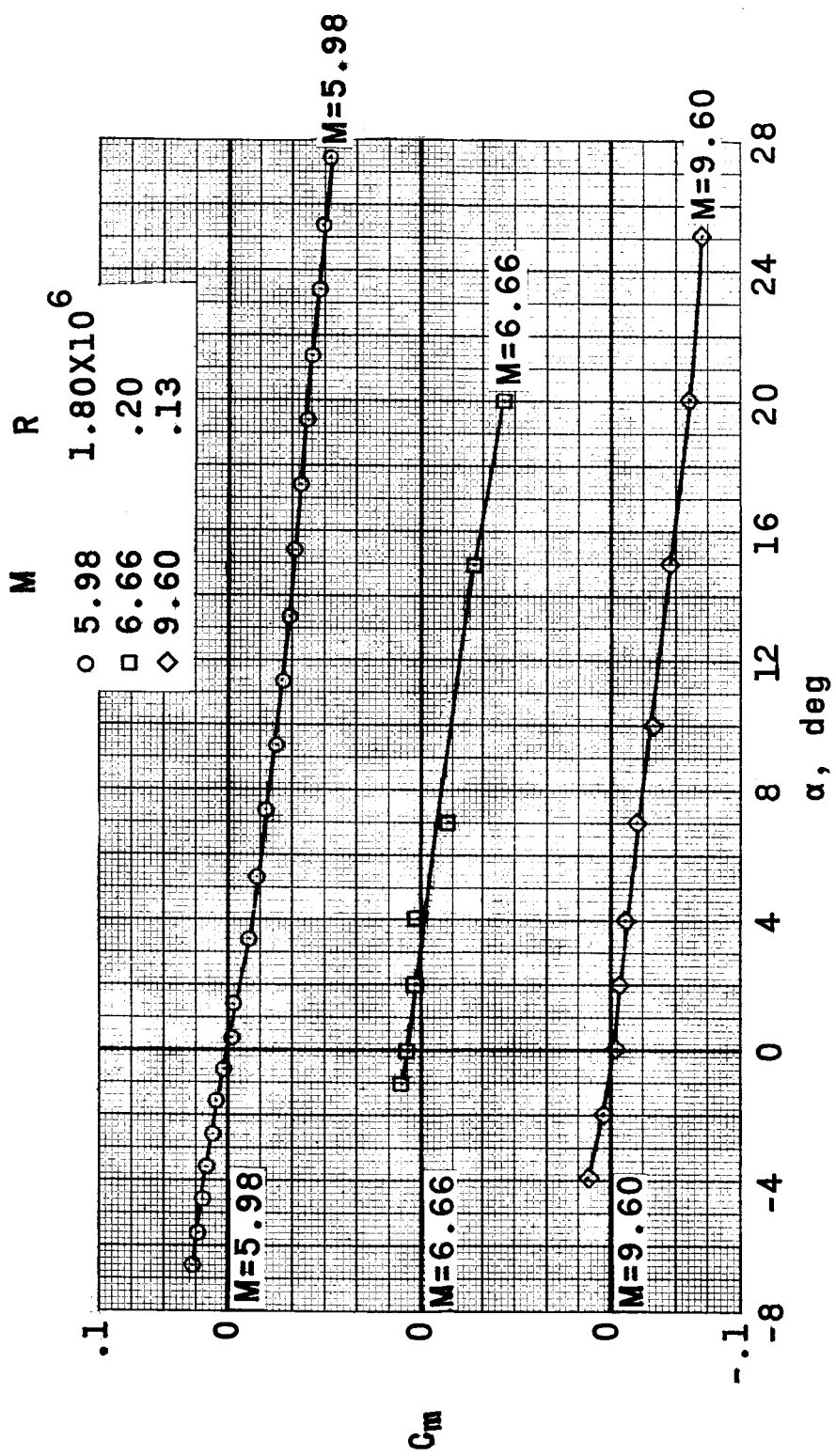
(c)  $M = 5.98$  to  $9.60$ .

Figure 15.- Concluded.

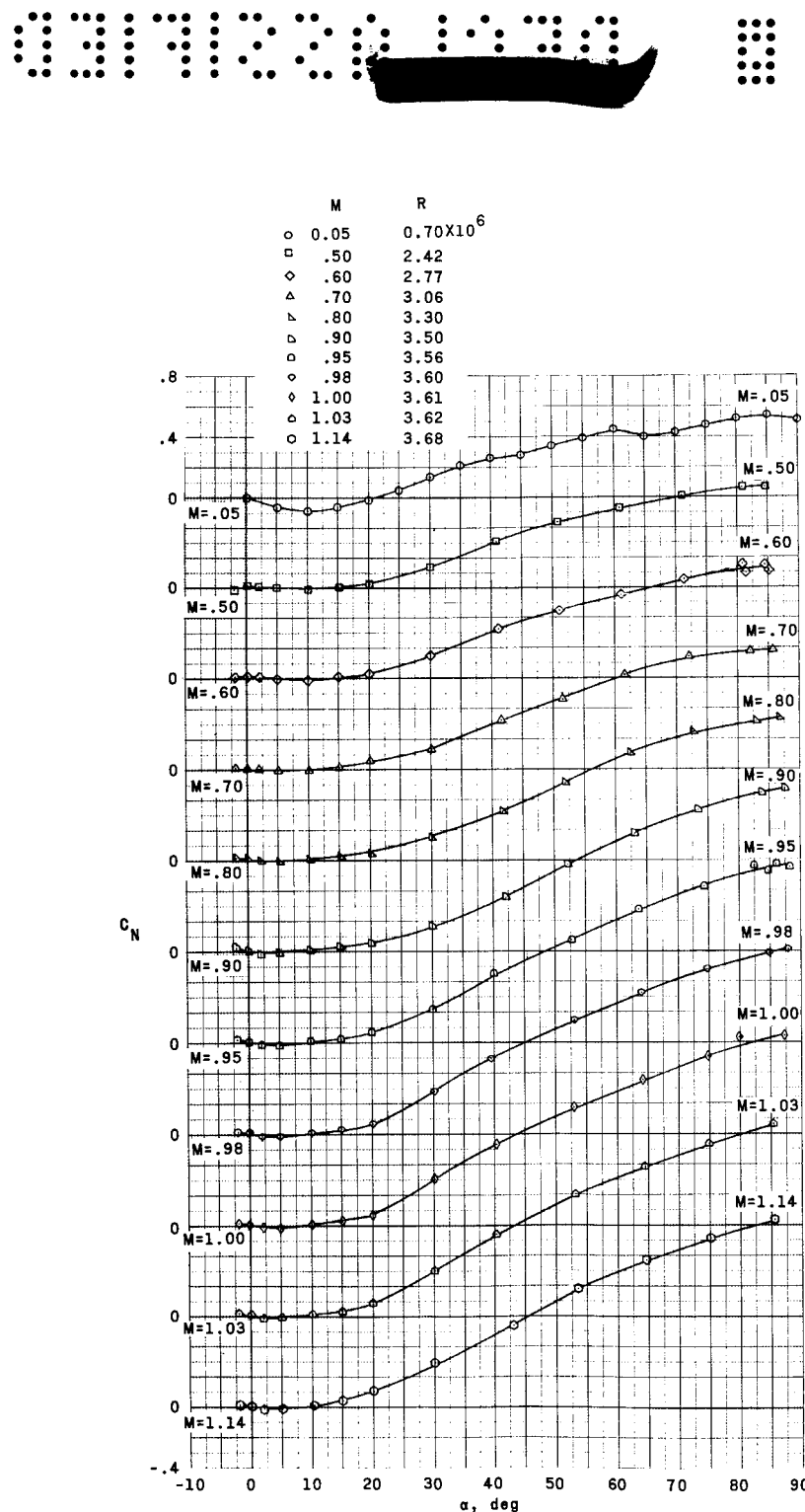
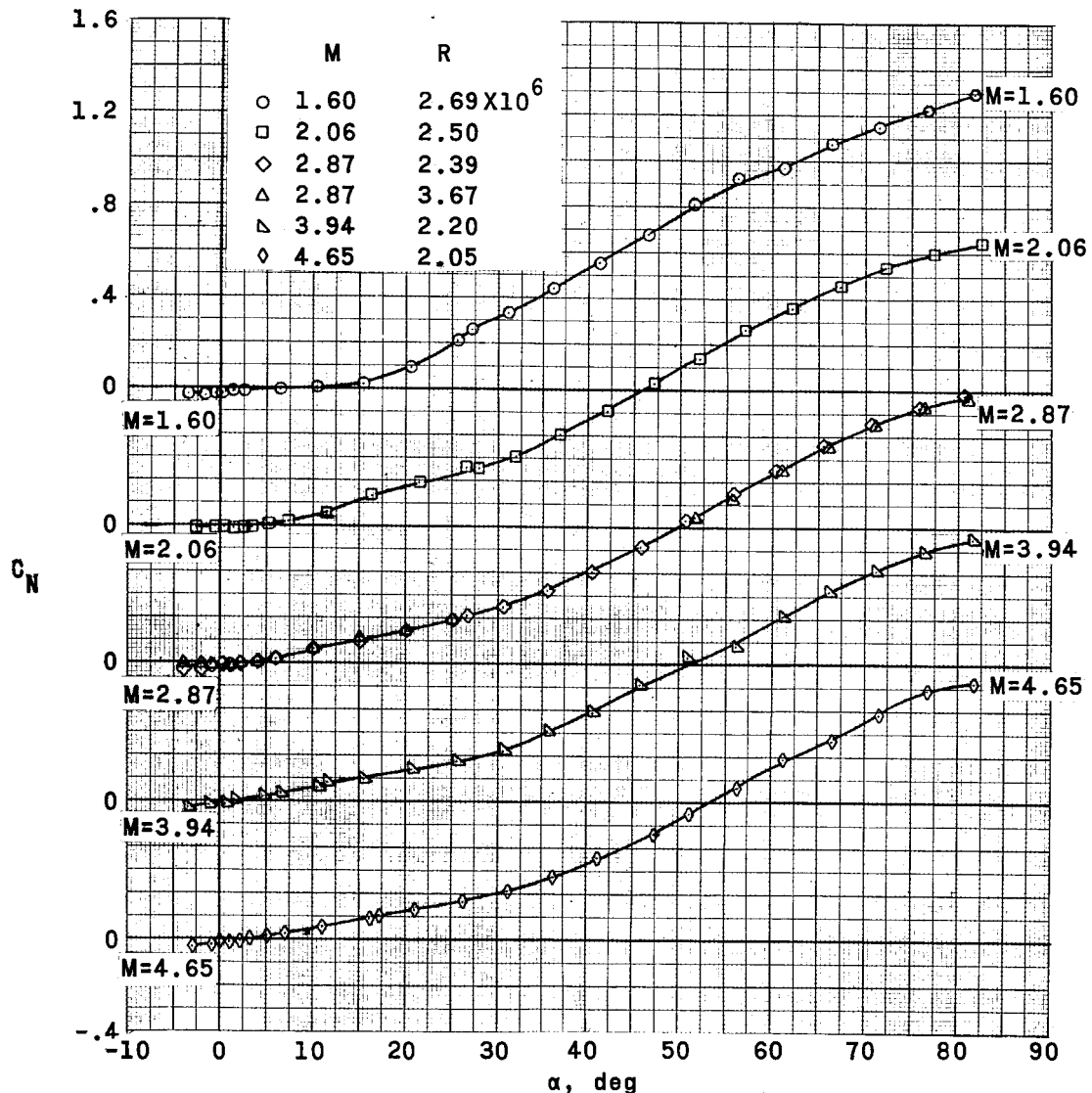
(a)  $M = 0.05$  to  $1.14$ .

Figure 16.- Variation of normal-force coefficient with angle of attack.  
Reentry configuration.

REF ID: A62742  
DECLASSIFIED

87



(b)  $M = 1.60$  to  $4.65$ .

Figure 16.- Continued.

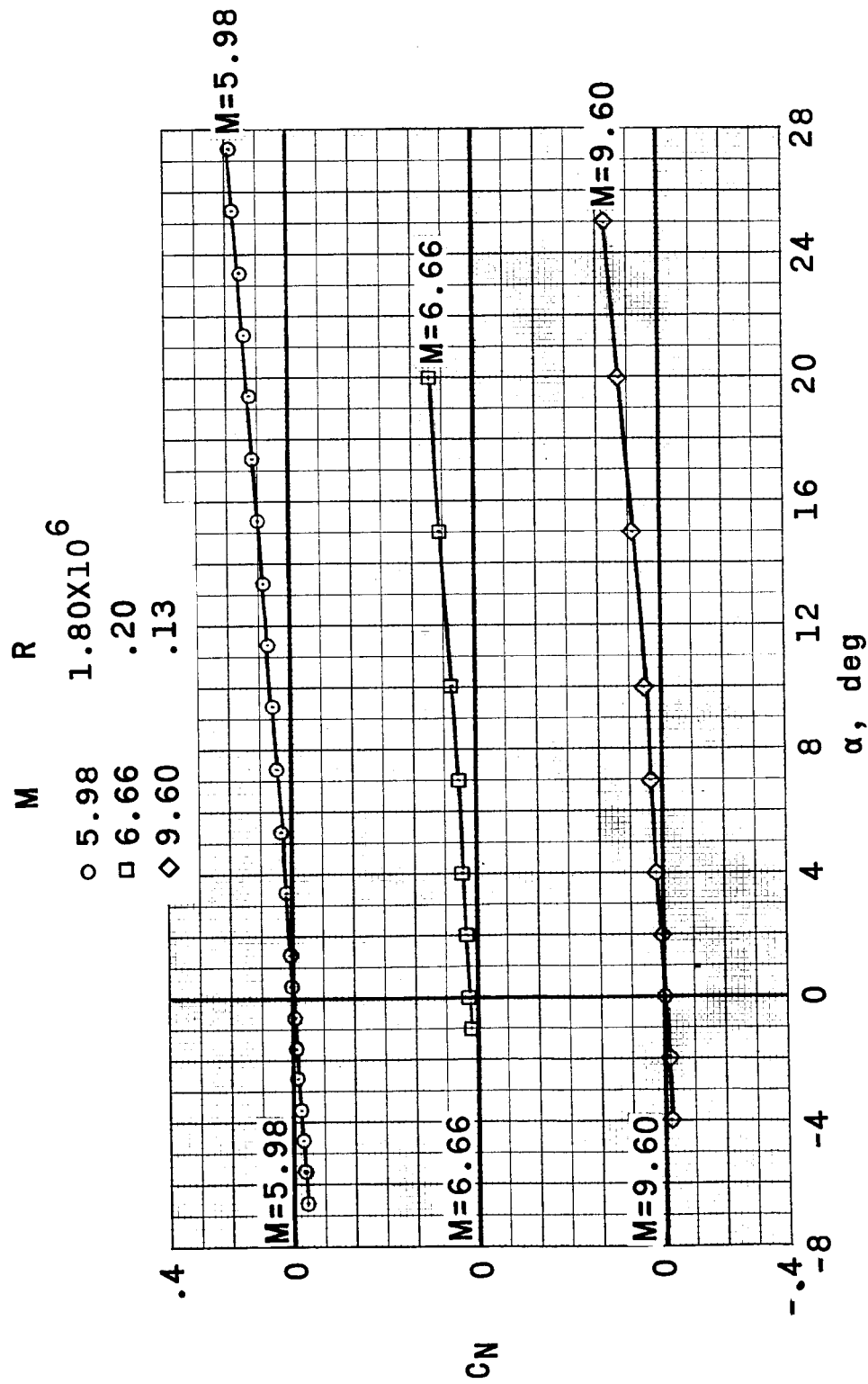
(c)  $M = 5.98$  to  $9.60$ .

Figure 16.- Concluded.

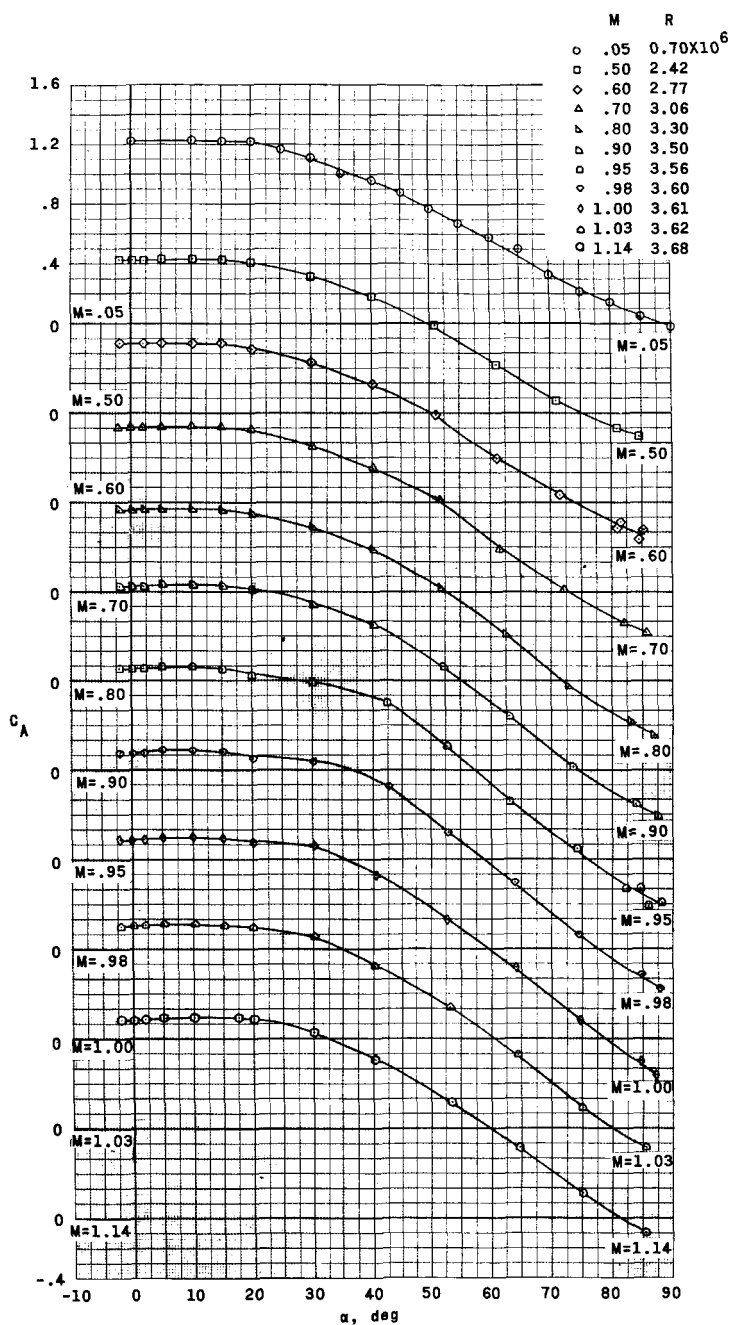
(a)  $M = 0.05$  to  $1.14$ .

Figure 17.- Variation of axial-force coefficient with angle of attack.  
Reentry configuration.

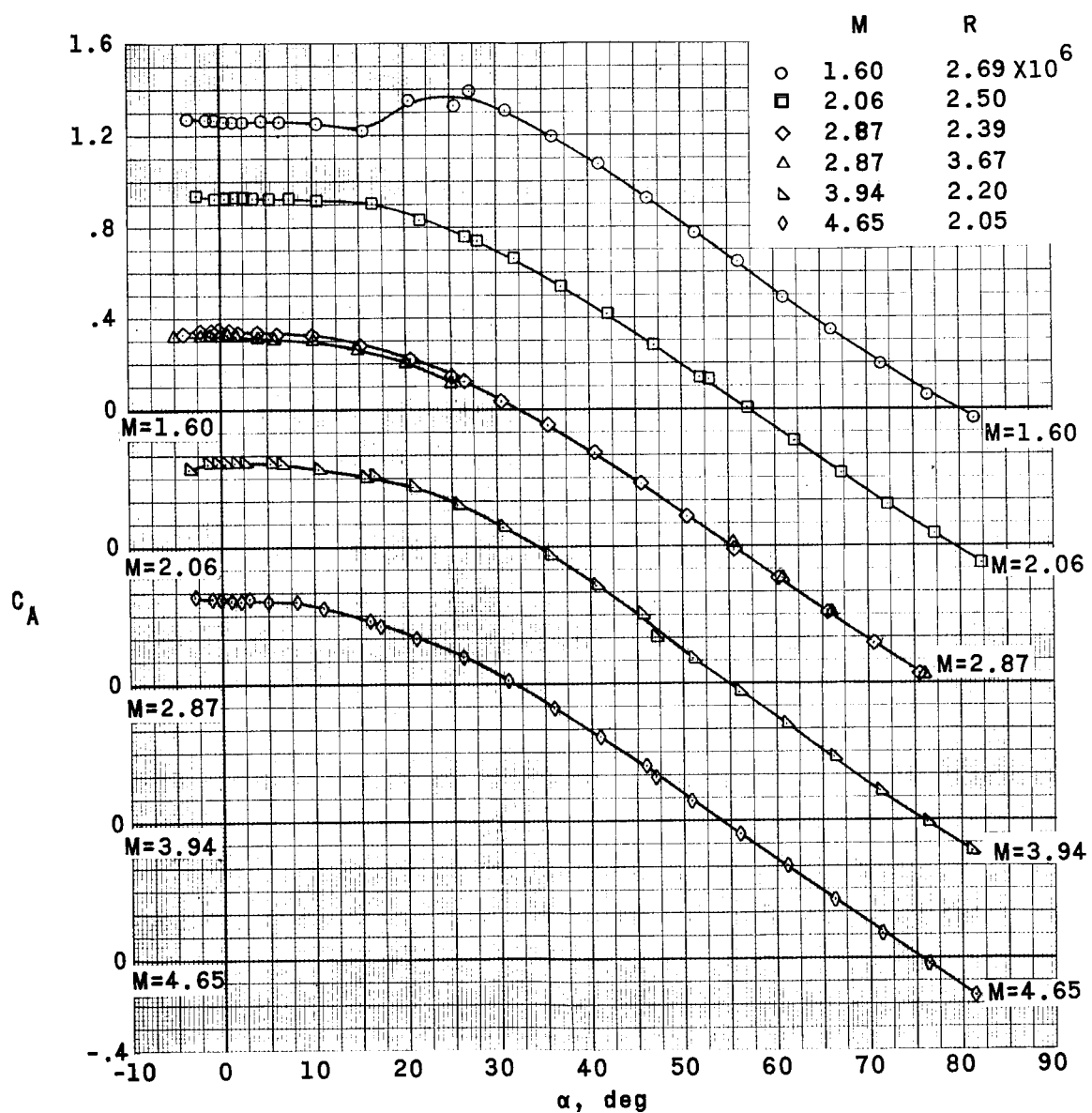
(b)  $M = 1.60$  to  $4.65$ .

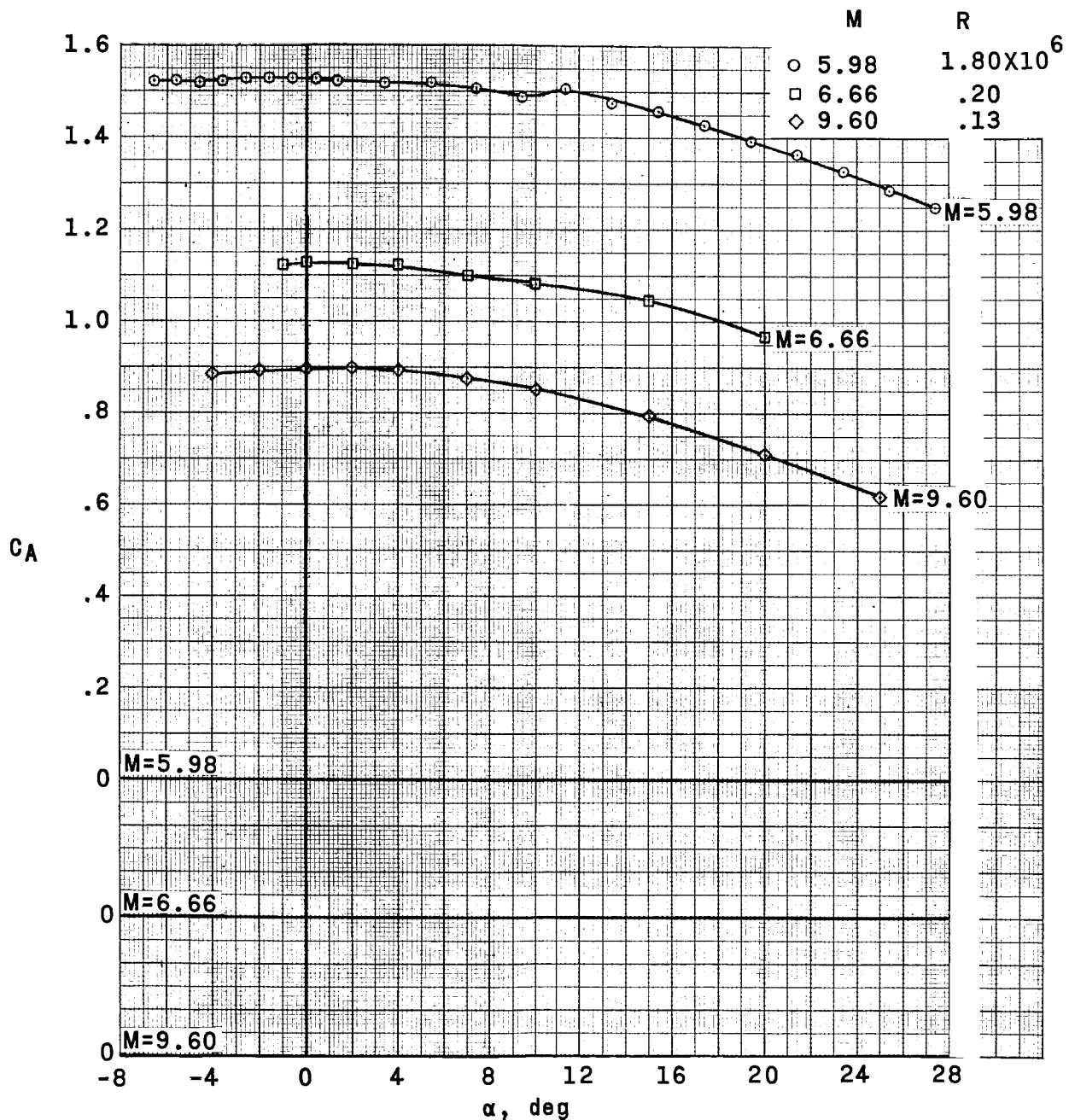
Figure 17.- Continued.

10

REF ID: A6512

REF ID: A6512

91



(c)  $M = 5.98$  to  $9.60$ .

Figure 17.- Concluded.

031712201000

92

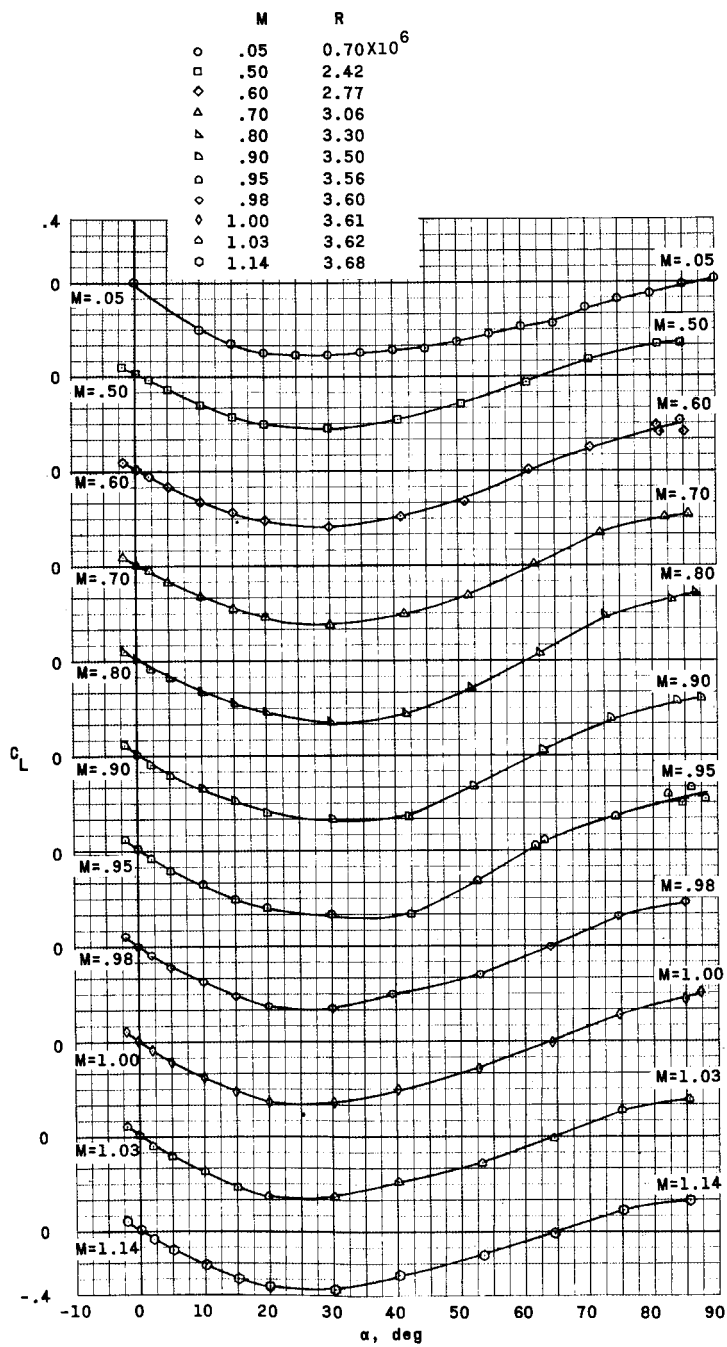
(a)  $M = 0.05$  to  $1.14$ .

Figure 18.- Variation of lift coefficient with angle of attack.  
 Reentry configuration.

DECLASSIFIED

DECLASSIFIED

93

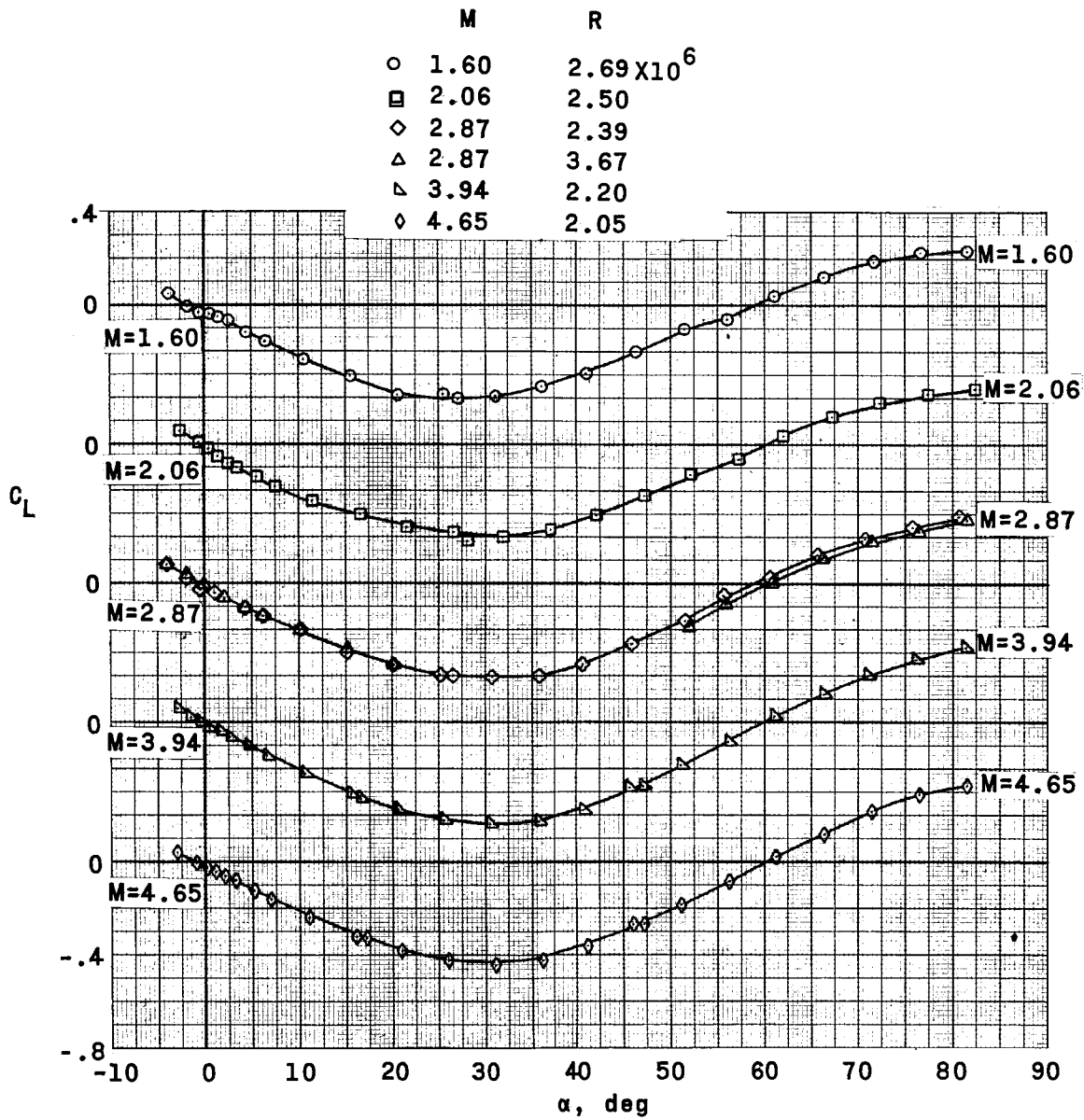
(b)  $M = 1.60$  to  $4.65$ .

Figure 18.- Continued.

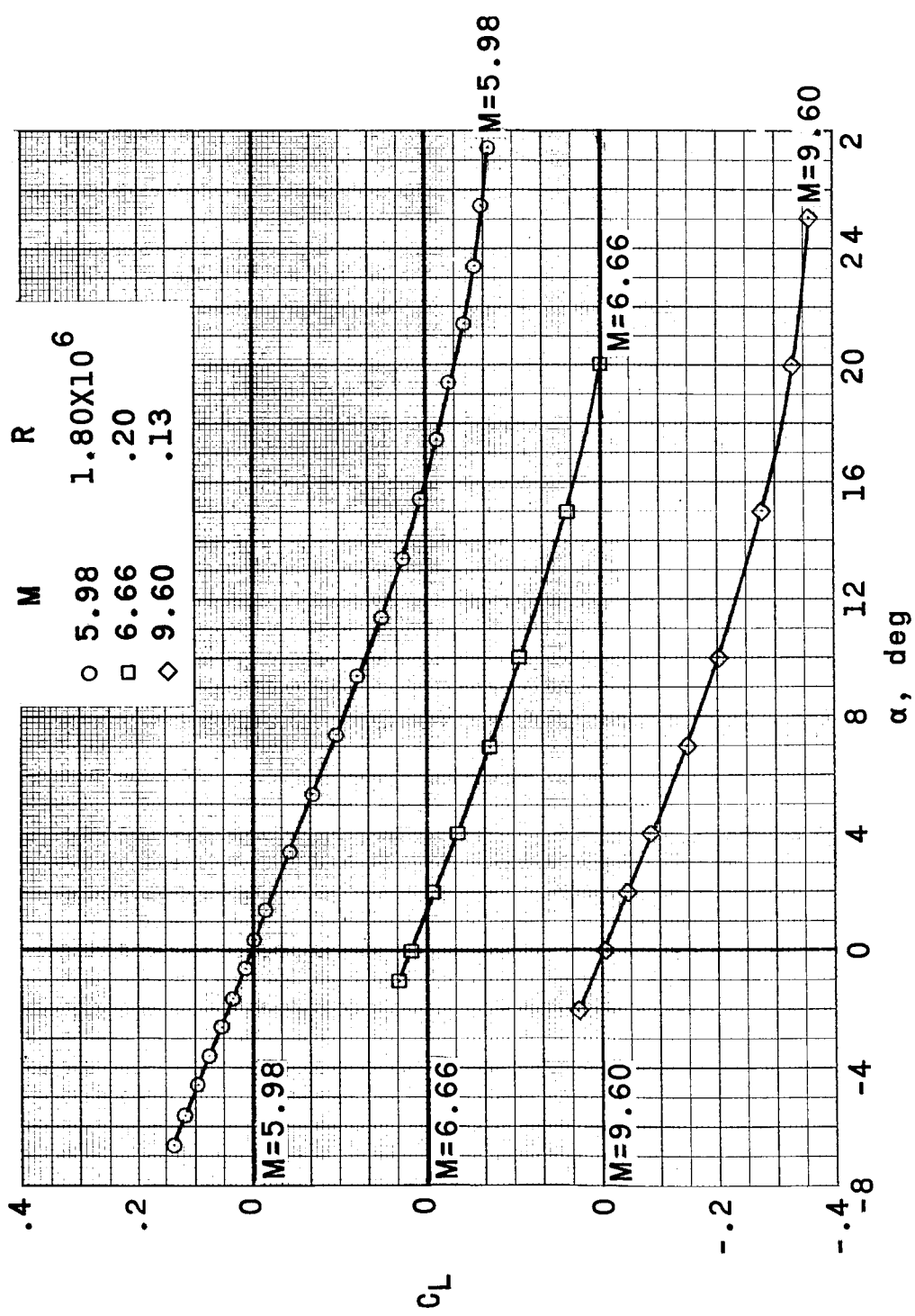
(c)  $M = 5.98$  to  $9.60$ .

Figure 18.- Concluded.

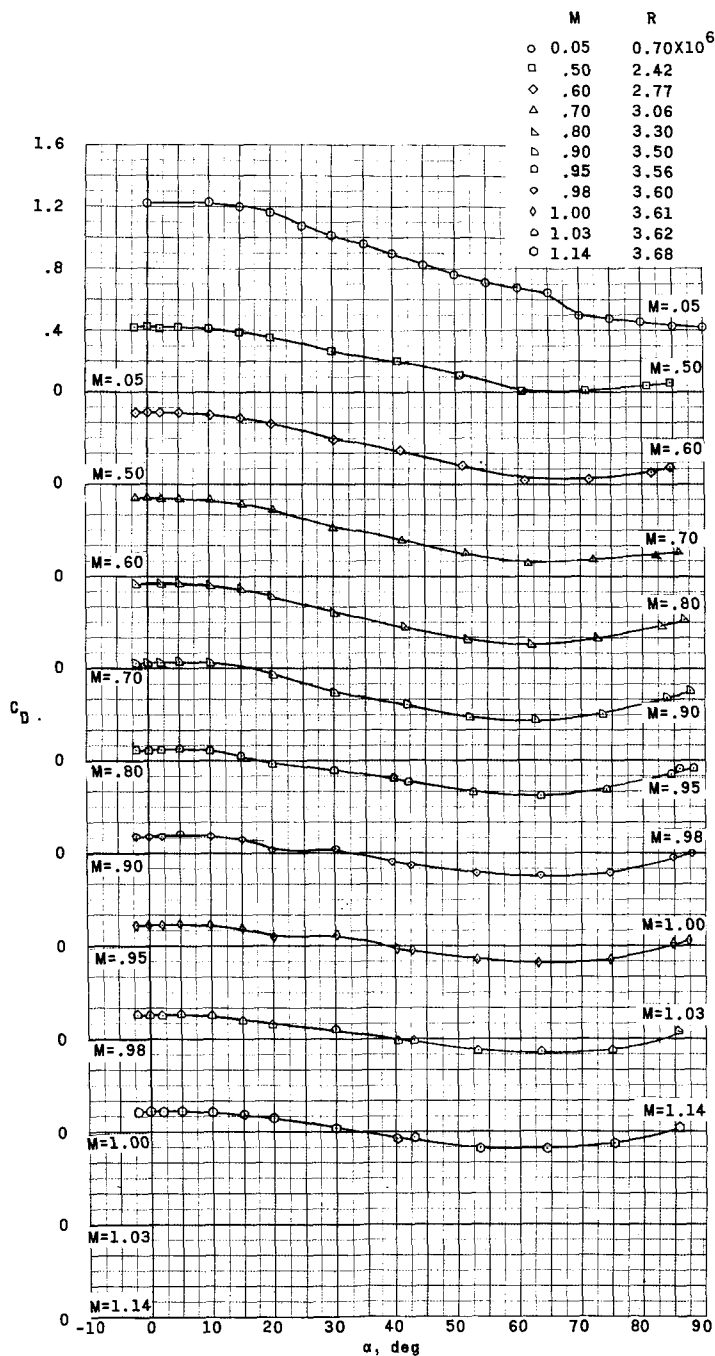
REF ID: A6212  
DECLASSIFIED(a)  $M = 0.05$  to  $1.14$ .

Figure 19.- Variation of drag coefficient with angle of attack.  
Reentry configuration.

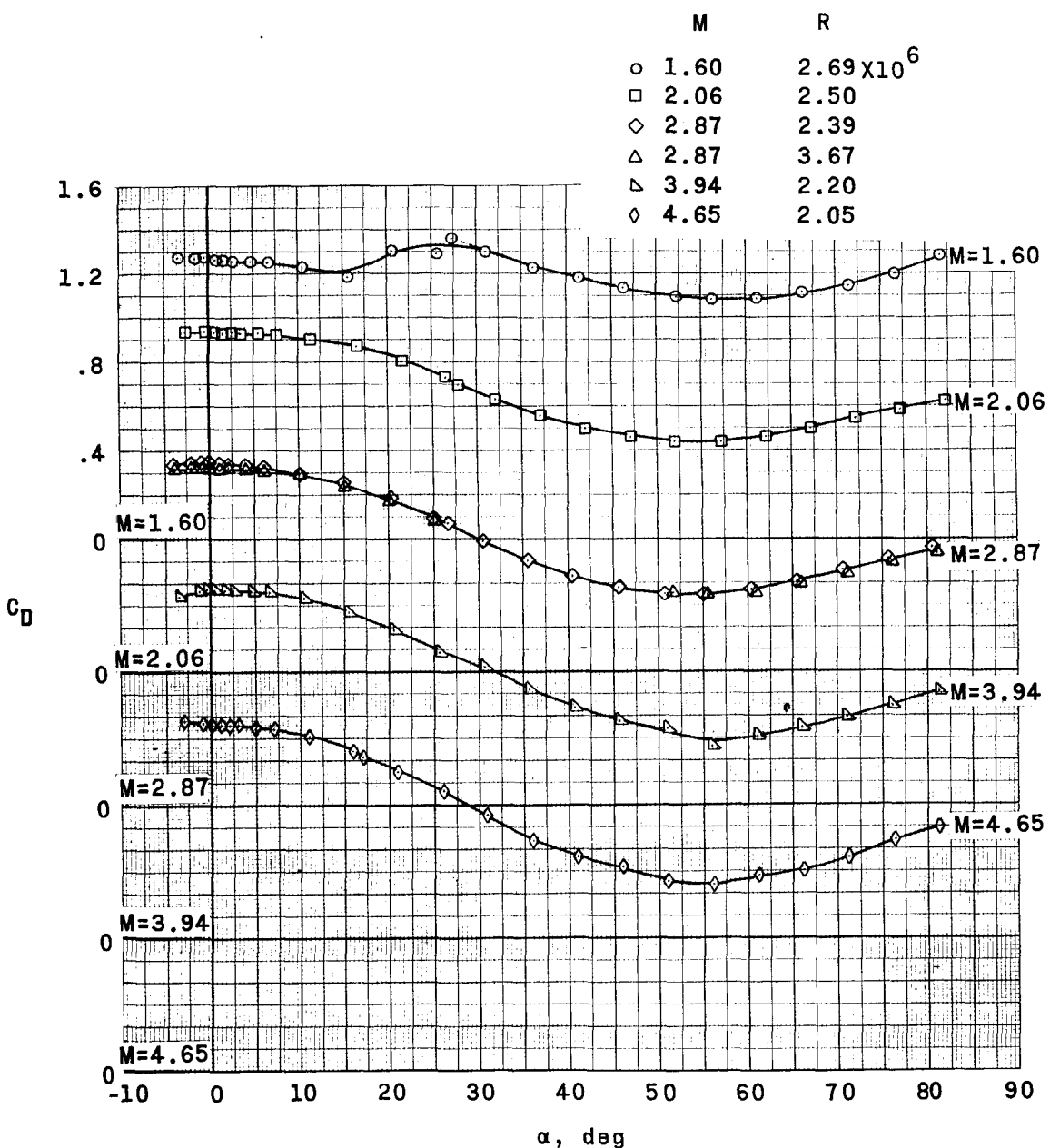
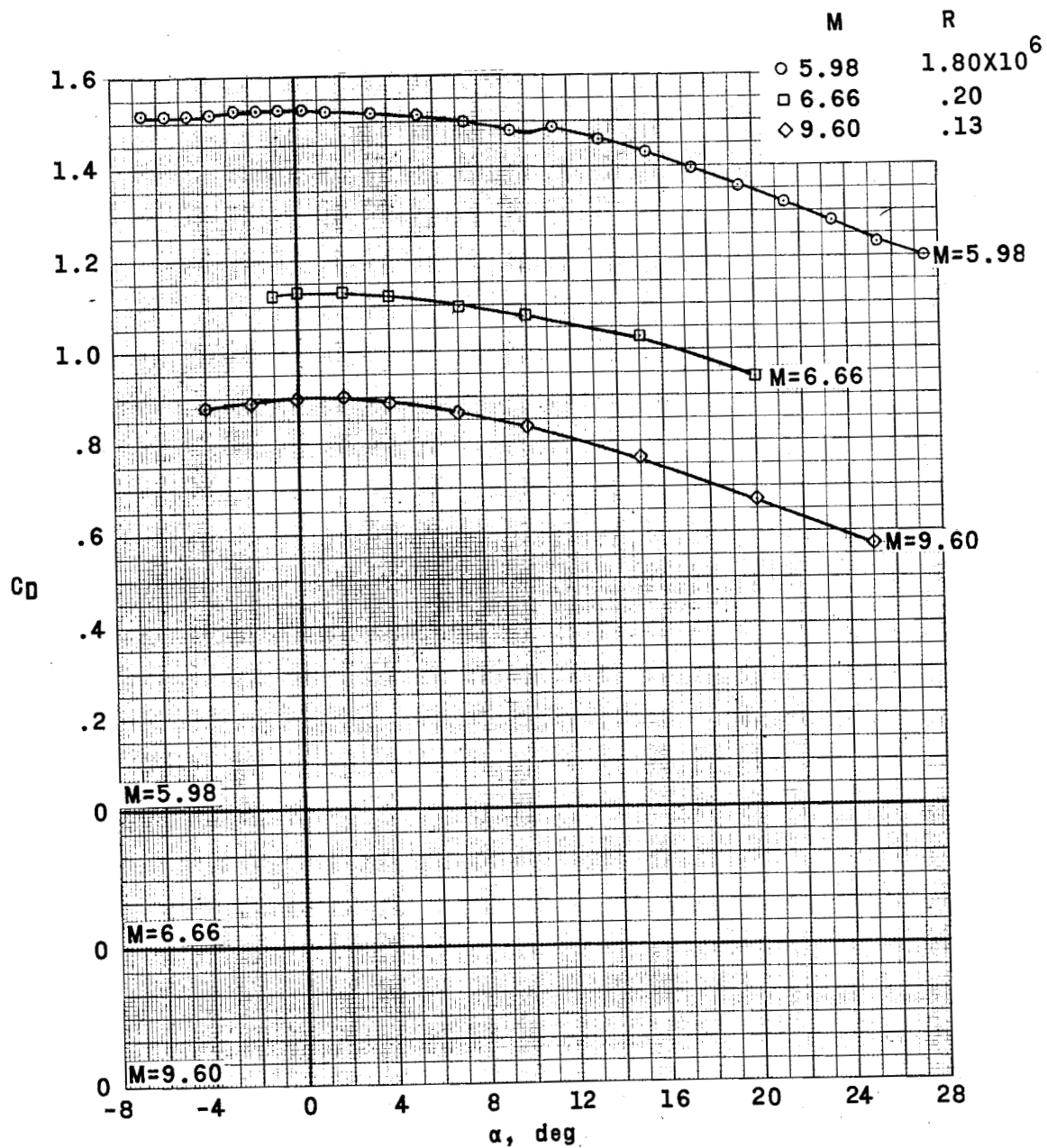
(b)  $M = 1.60$  to  $4.65$ .

Figure 19.- Continued.

REF ID: A6512

REF ID: A6512  
REF ID: A6512 UNCLASSIFIED

97



(c) M = 5.98 to 9.60.

Figure 19.- Concluded.

00191230100300

- ◊ Langley Free-Flight Tunnel
- Langley 8-foot Transonic Pressure Tunnel
- ◊ AEDC 16-foot Transonic Circuit
- Ames Unitary Plan Wind Tunnel
- Langley Unitary Plan Wind Tunnel
- ◊ 2-foot Low-Density Hypersonic Tunnel
- Basic configuration

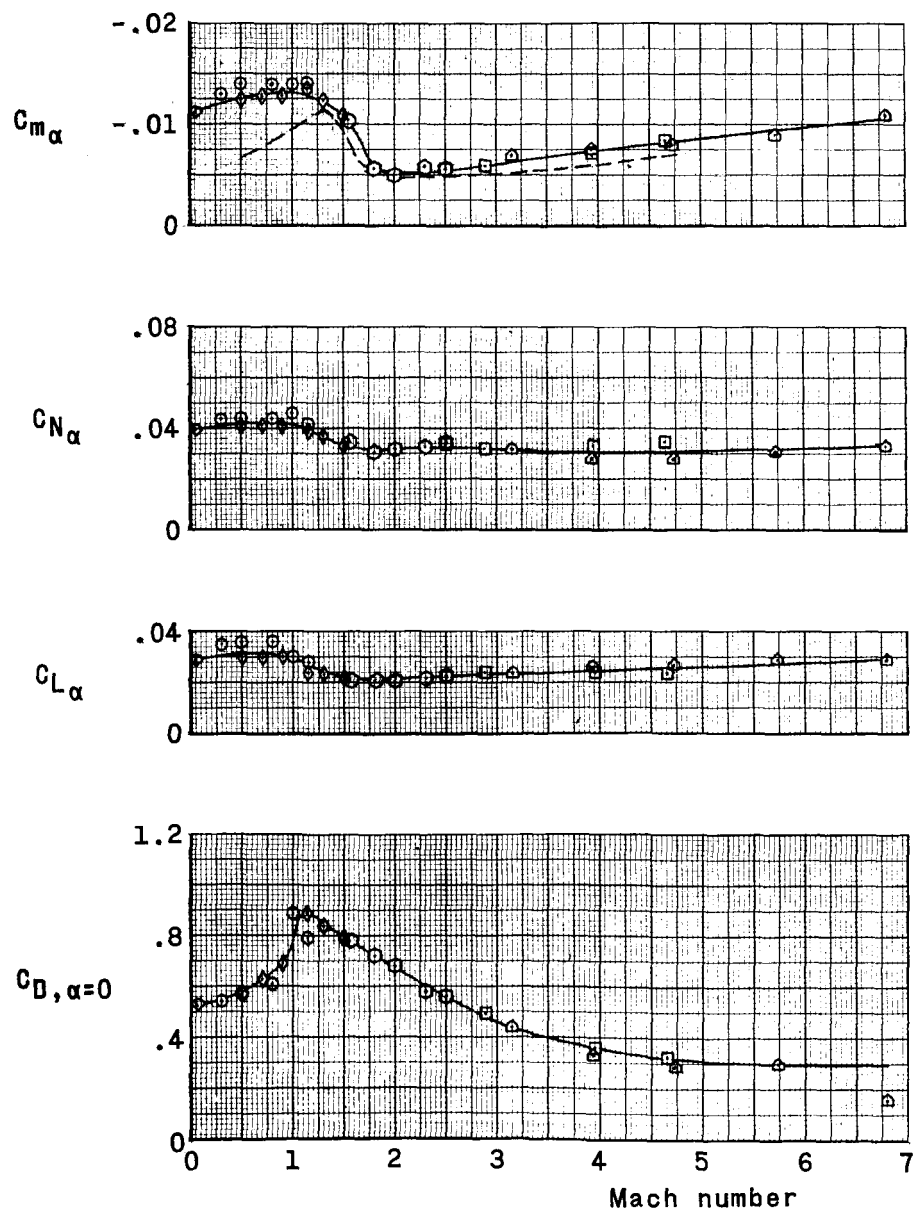


Figure 20.- Summary of longitudinal aerodynamic characteristics.  
Escape configuration.

[REDACTED]

REF ID: A6530

99

- Langley 8-foot Transonic Pressure Tunnel
- ◊ AEDC 16-foot Transonic Circuit
- Langley Unitary Plan Wind Tunnel
- △ Langley 20-inch Hypersonic Tunnel
- ◇ 2-foot Low-Density Hypersonic Tunnel

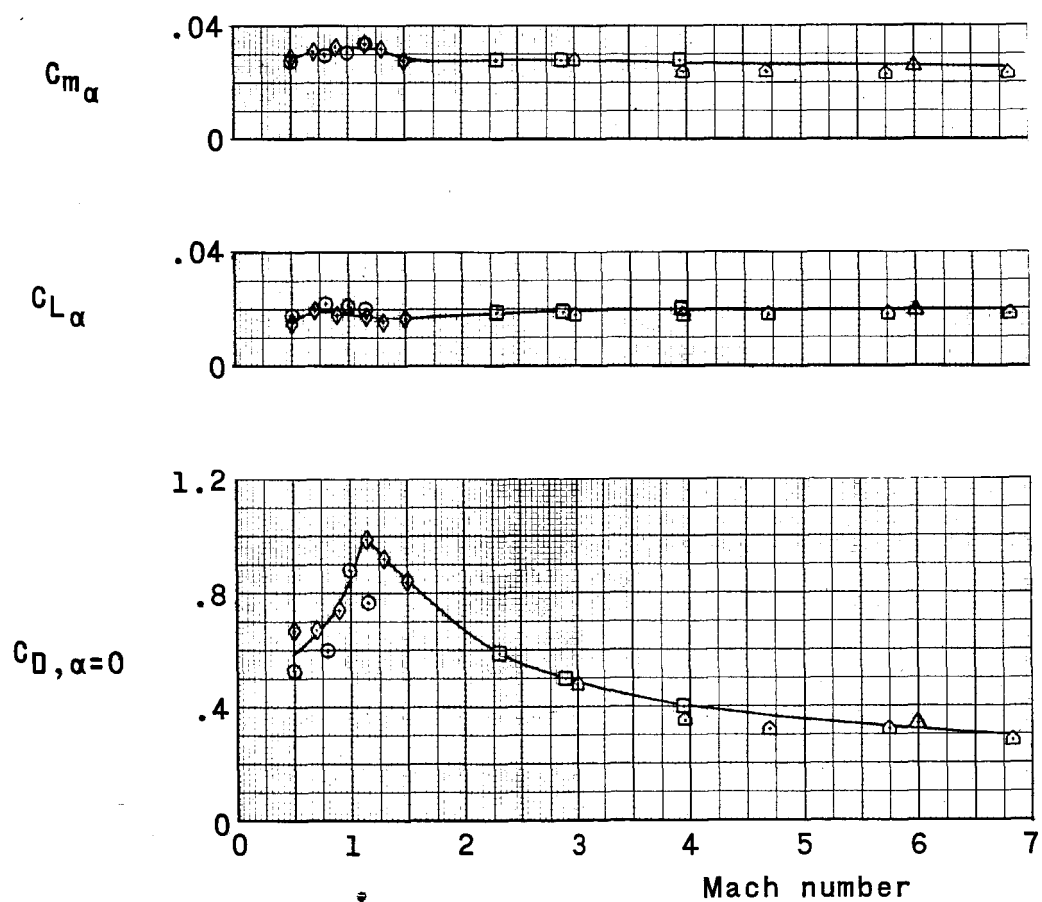


Figure 21.- Summary of longitudinal aerodynamic characteristics.  
Exit configuration.

[REDACTED]

100

- ◆ Langley Free-Flight Tunnel  
 ○ Langley 8-foot Transonic Pressure Tunnel  
 □ Langley Unitary Plan Wind Tunnel  
 ◇ Langley 11-inch Hypersonic Tunnel  
 △ Langley 20-inch Hypersonic Tunnel  
 ▽ Ames Pressurized Ballistic Range  
 ▨ Ames Supersonic Free-Flight Tunnel  
 ▨ AEDC Tunnel HS-2

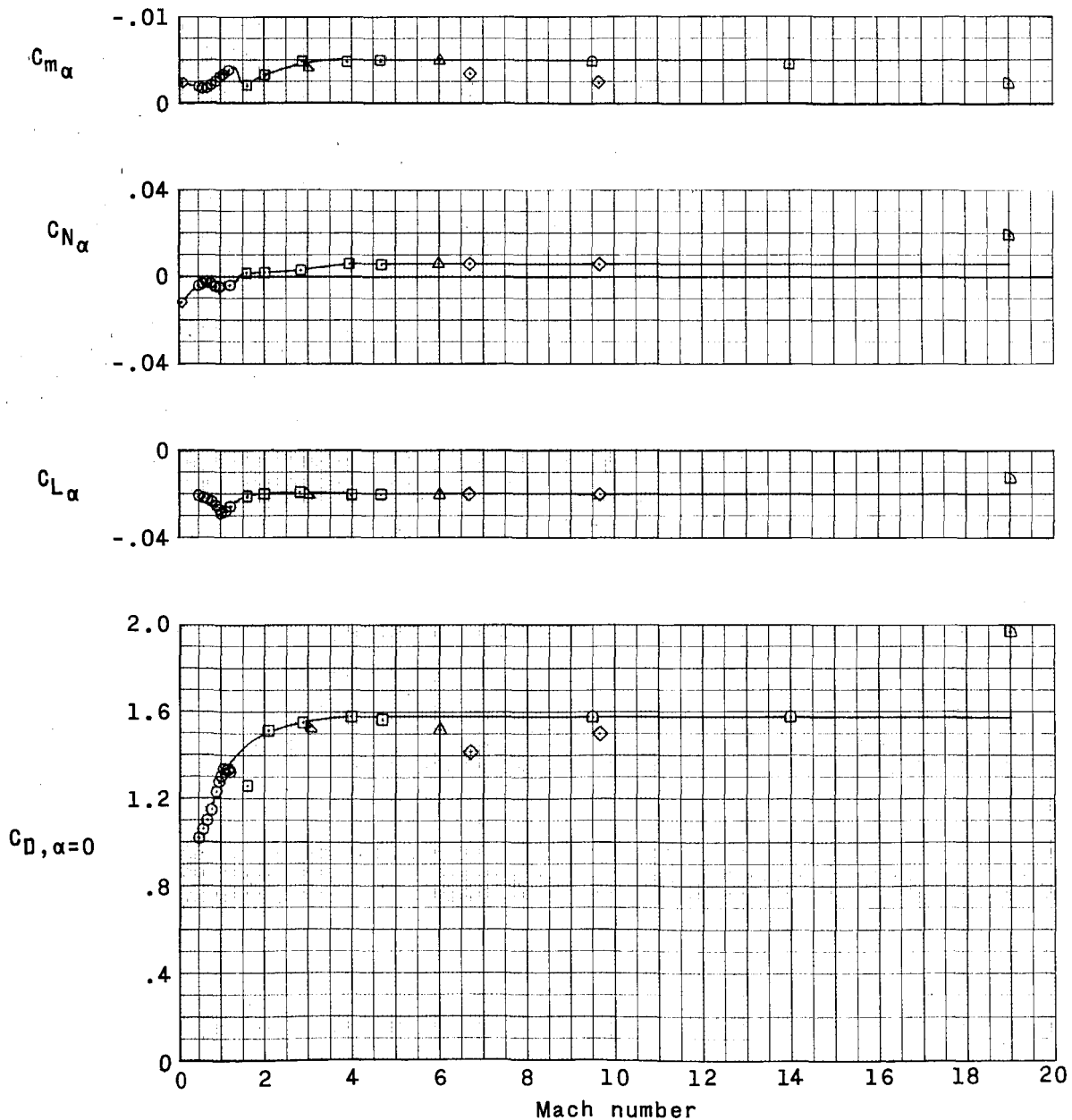
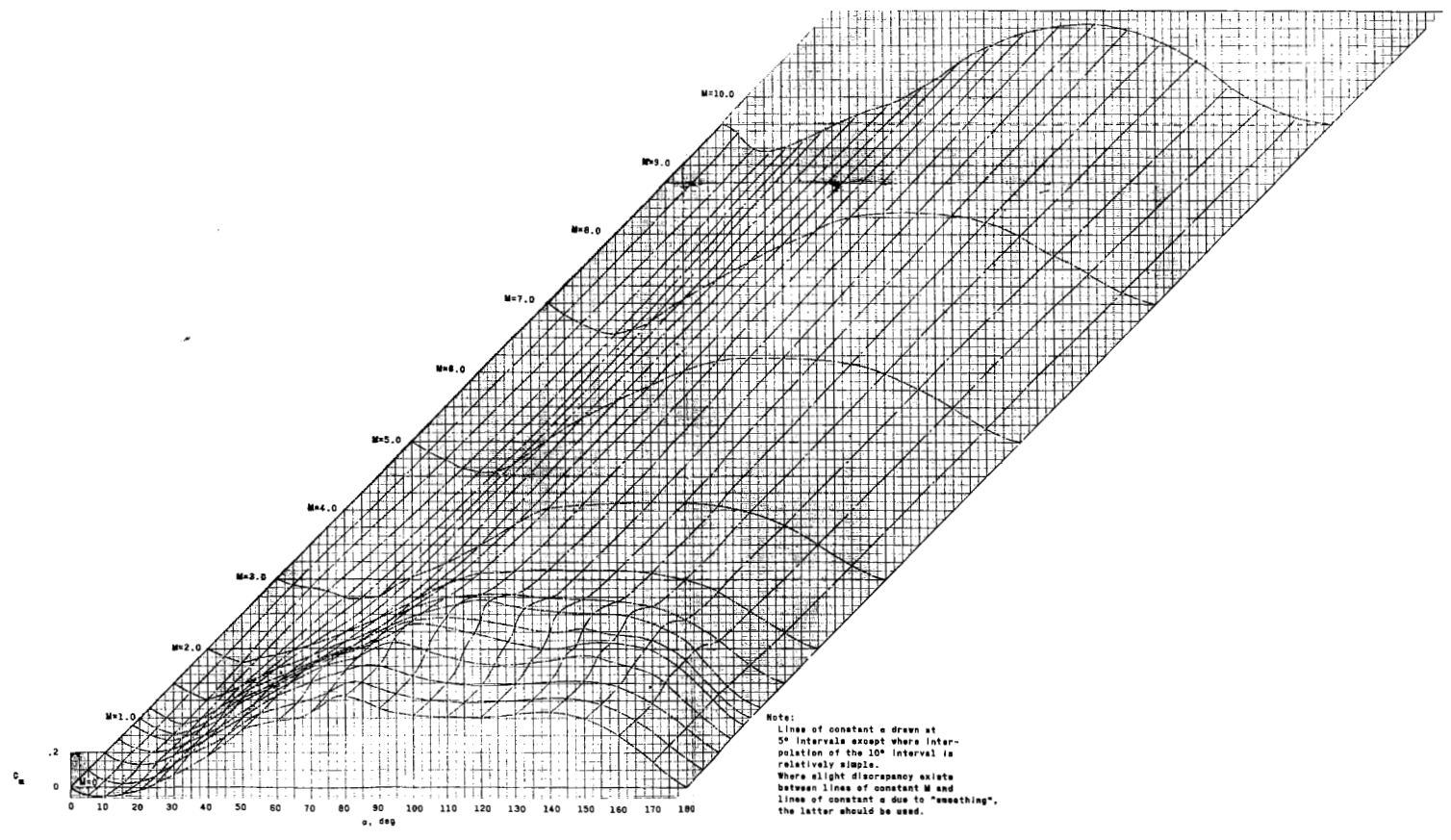


Figure 22.- Summary of longitudinal aerodynamic characteristics.  
 Reentry configuration.

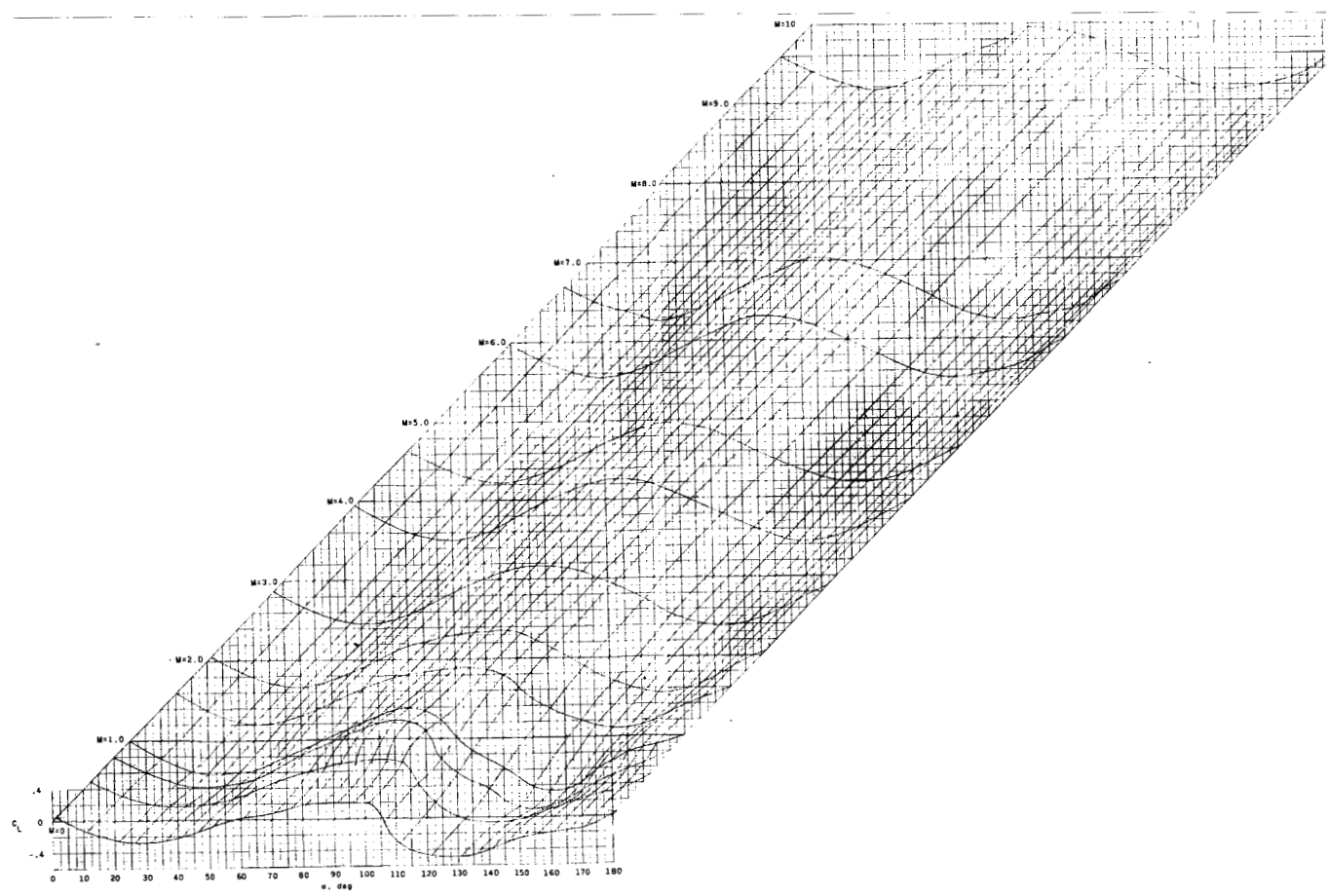


(a) Pitching-moment coefficient.

Figure 25.- Variation of aerodynamic characteristics with angle of attack and Mach number.  
 Escape configuration.

03183507030

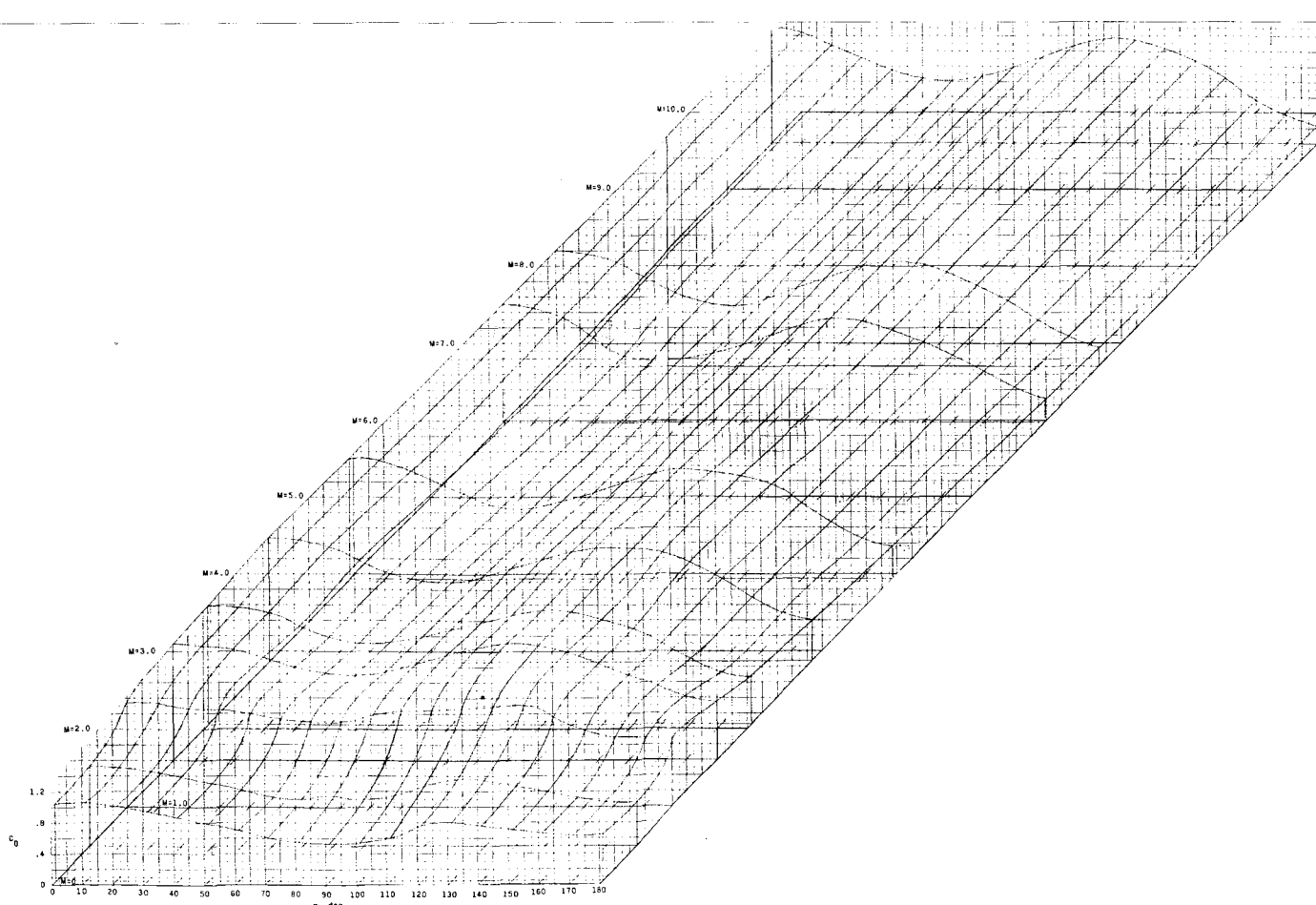
DECTUZ2HED



(b) Lift coefficient.

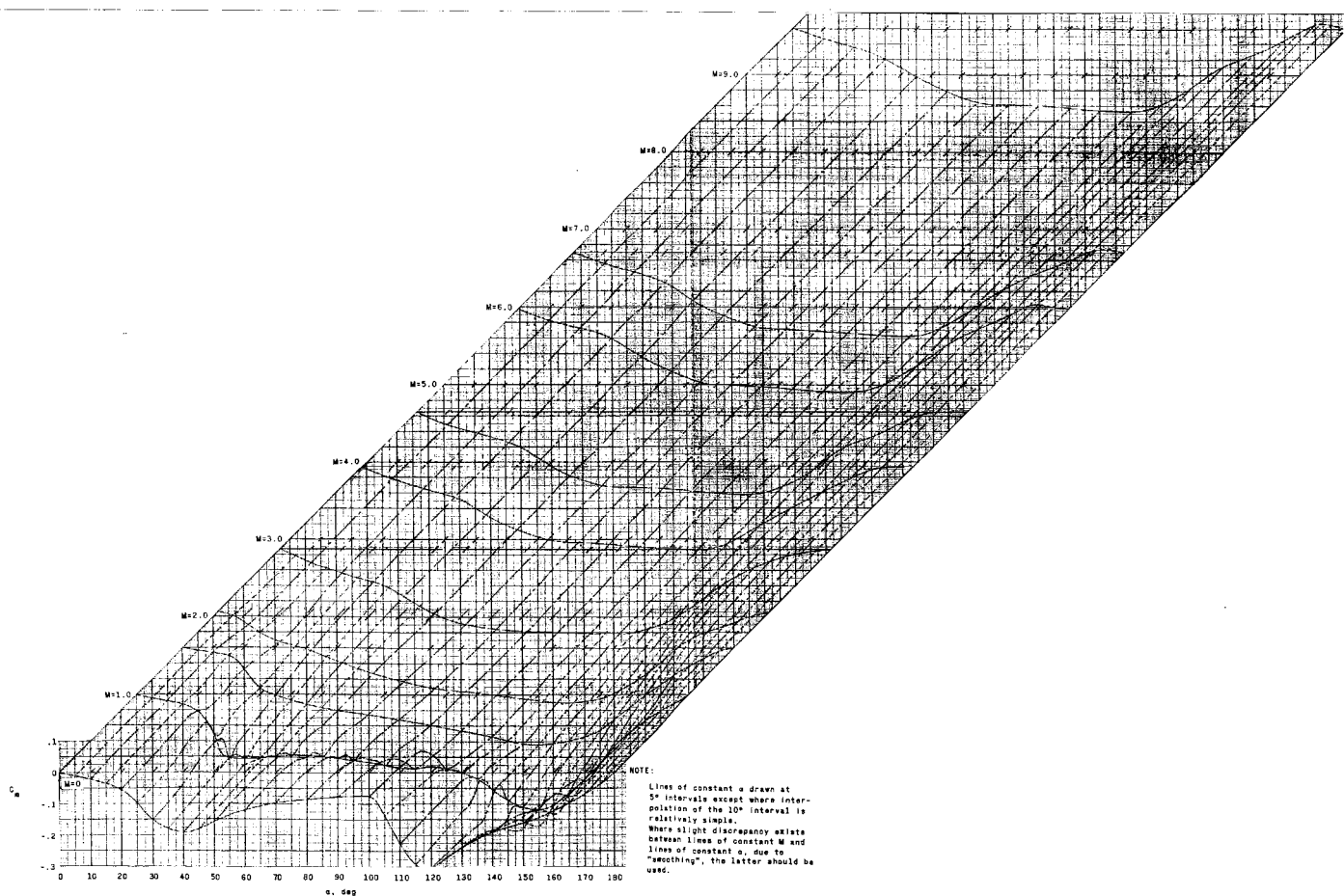
Figure 25.- Continued.

DECLASSIFIED



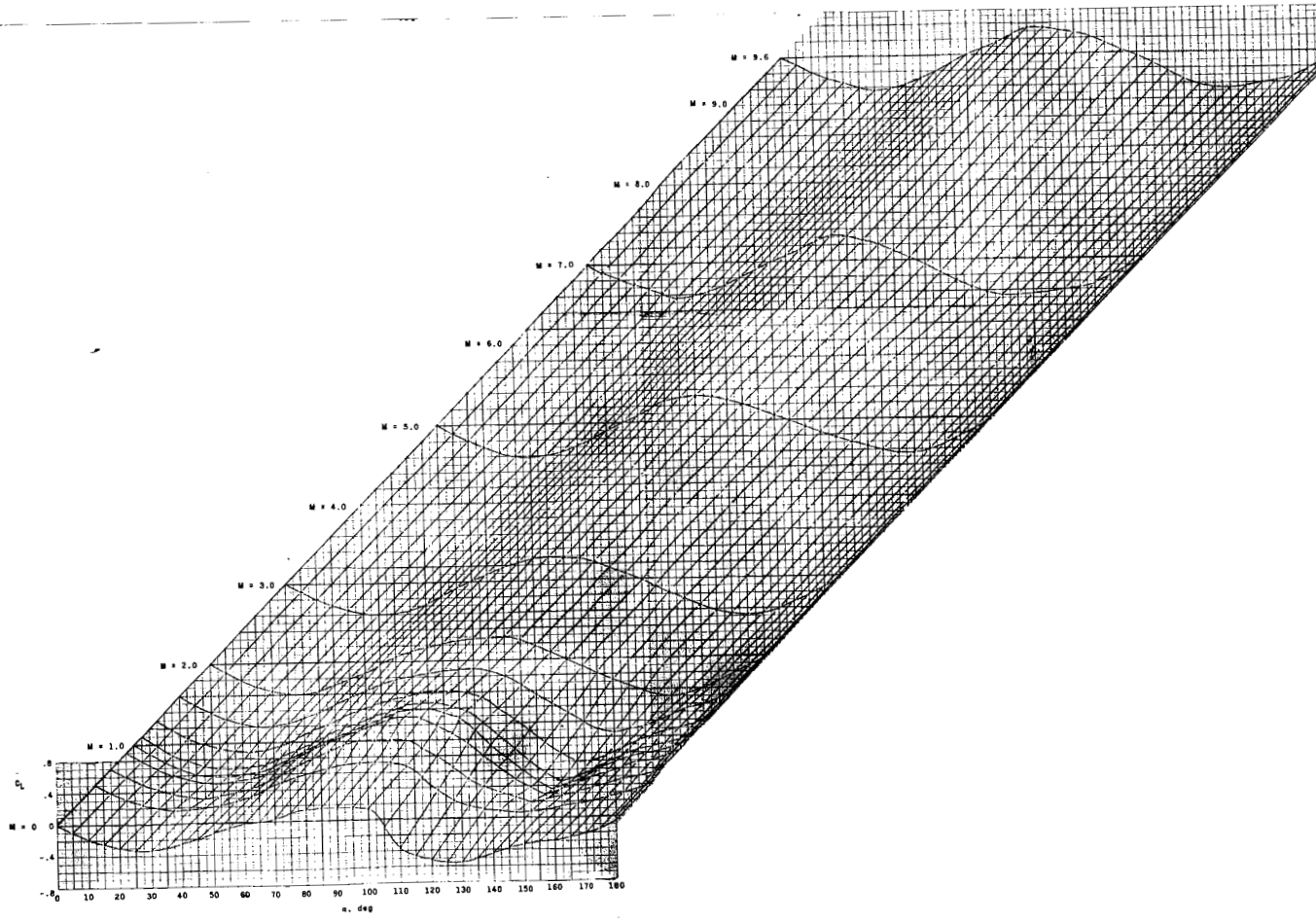
(c) Drag coefficient.

Figure 23.- Concluded.



(a) Pitching-moment coefficient.

Figure 25.- Variation of aerodynamic characteristics with angle of attack and Mach number.  
• slender configuration without de-ailabilizer flap.



(b) Lift coefficient  
Figure 24. Continued.

DECTERMINED

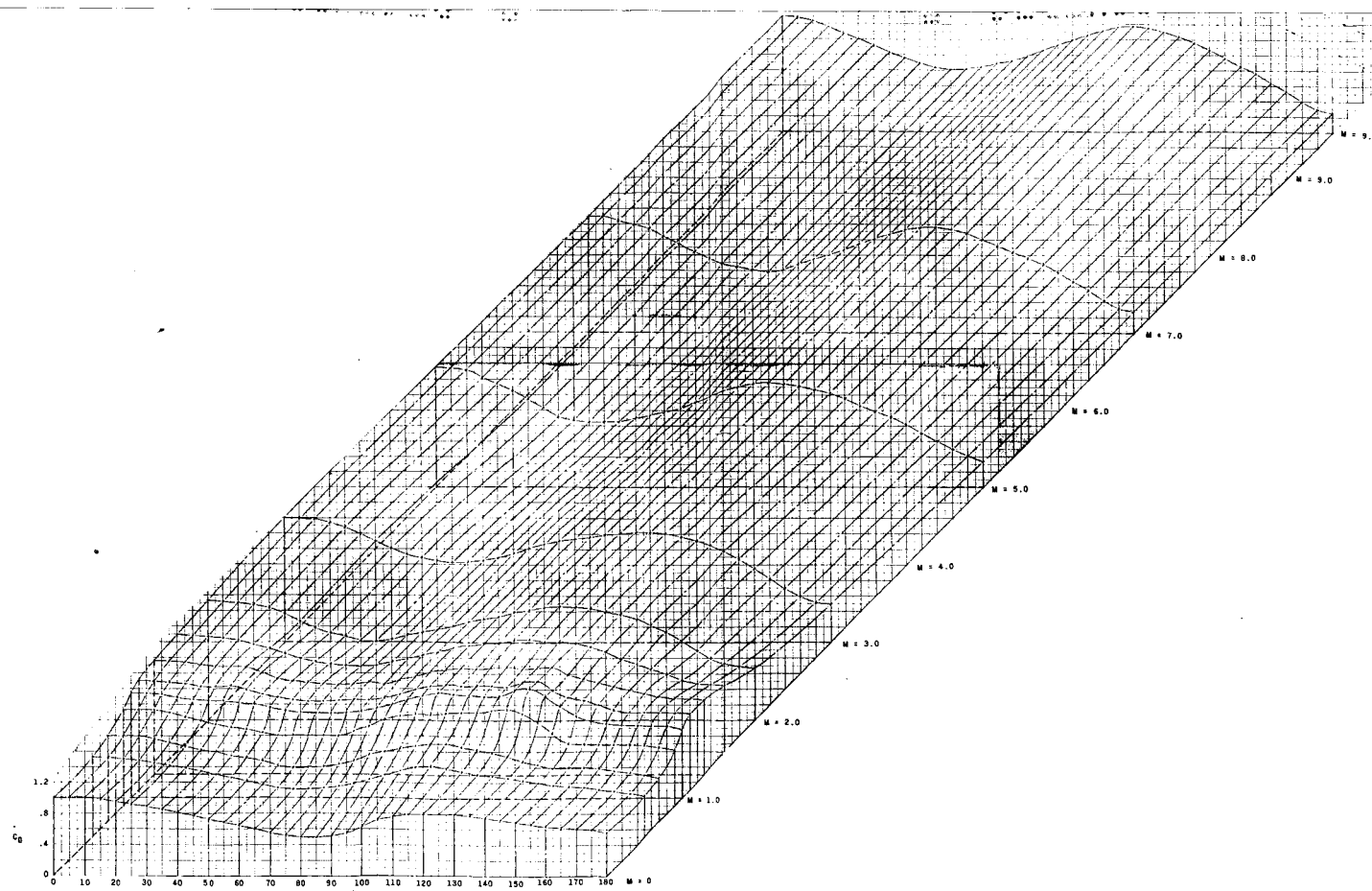
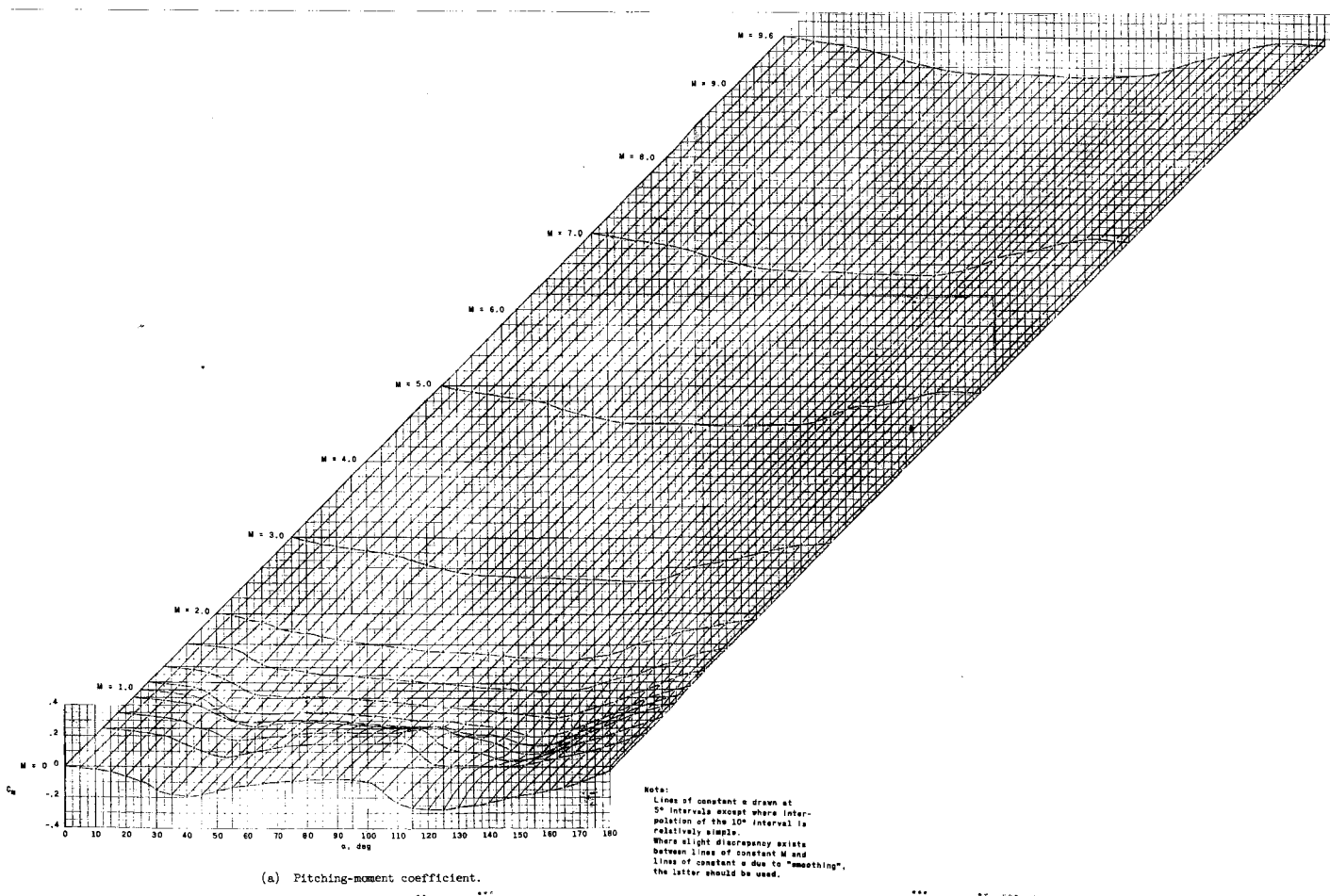


Figure 24.- Concluded.

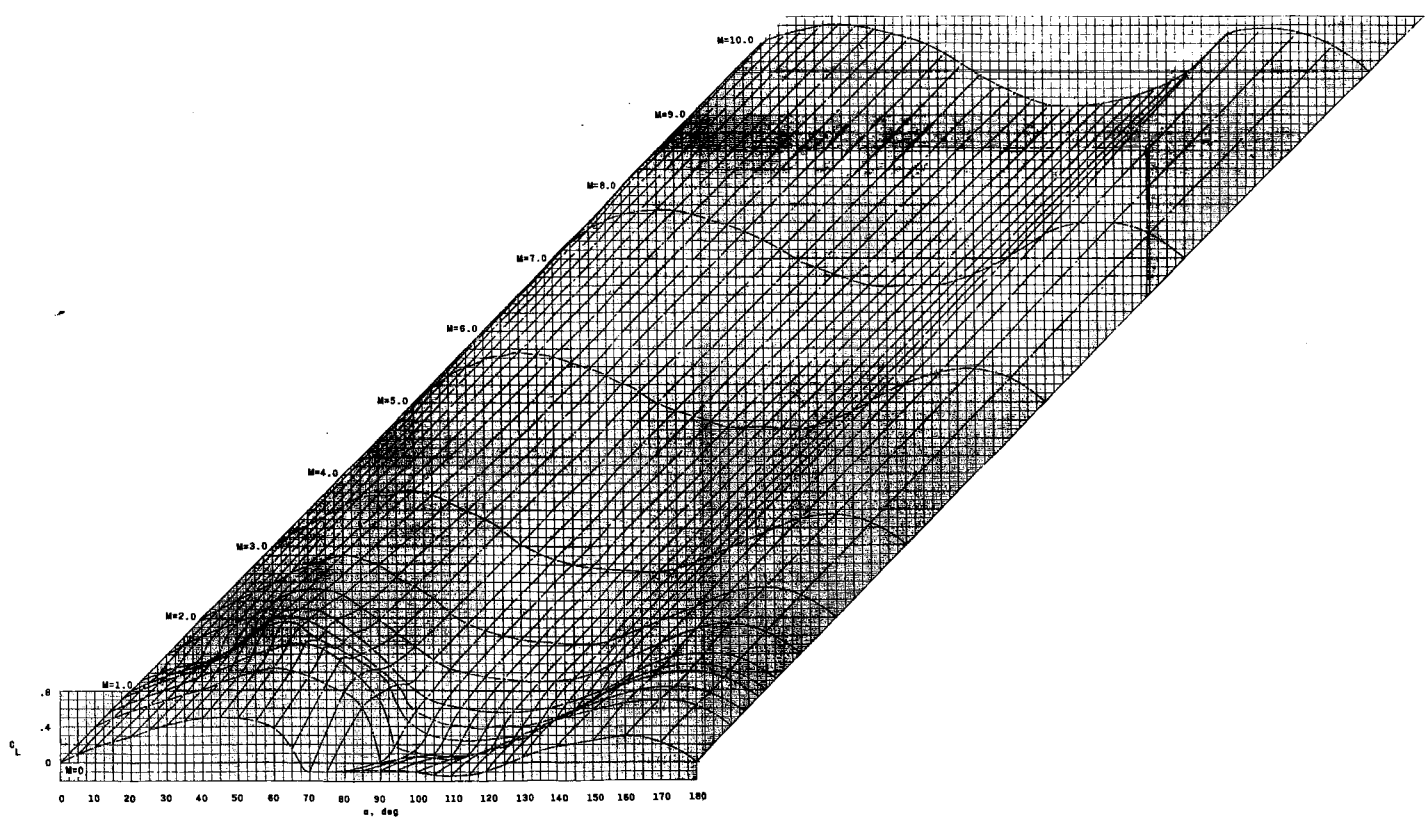
DECODED  
DECRYPTED



(a) Pitching-moment coefficient.

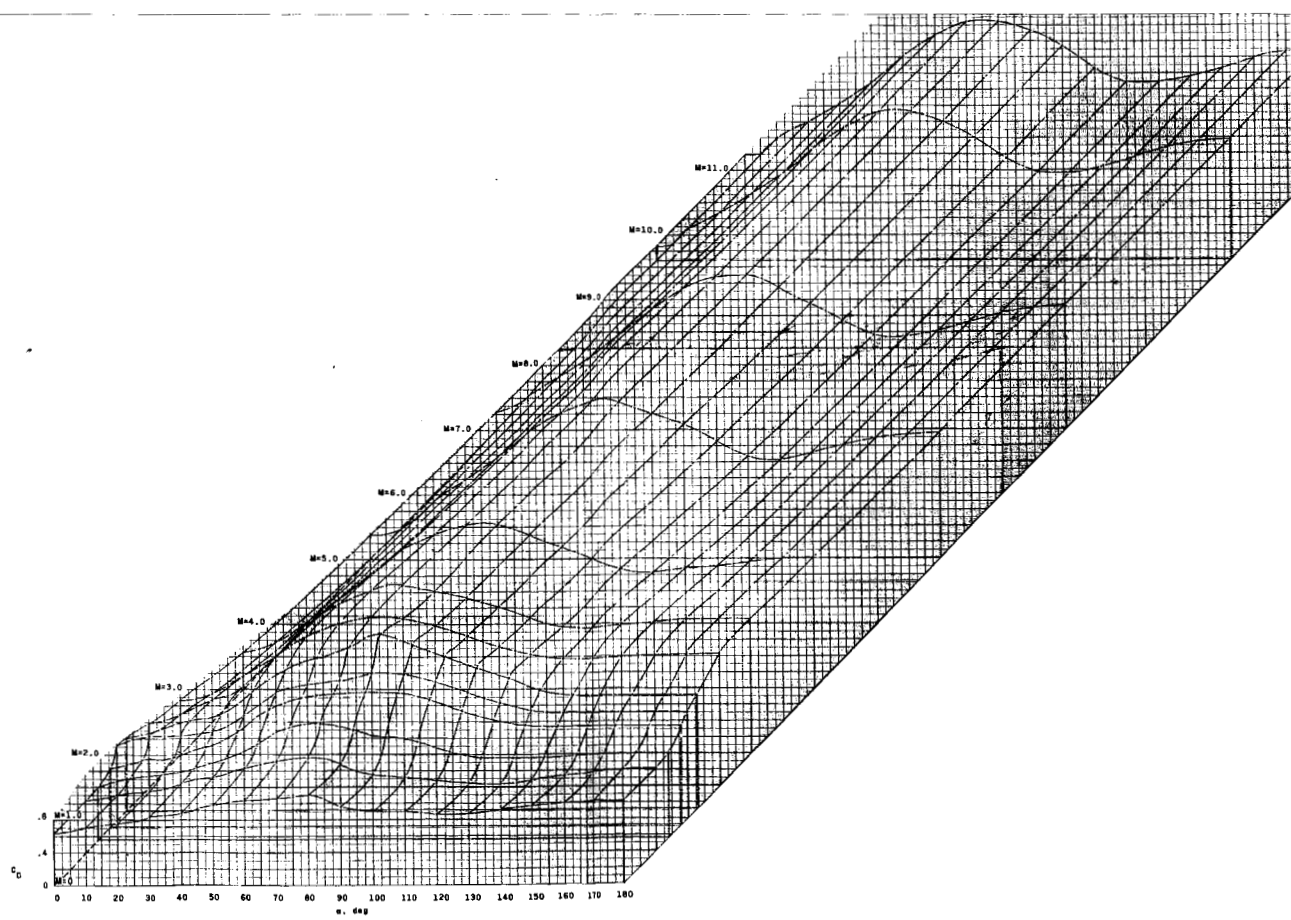
Figure 24.- Variation of aerodynamic characteristics with angle of attack and Mach number.  
Rectory configuration with stabilizer flap.

DECLASSIFIED



(b) Lift coefficient.

Figure 23.- Continued.



(c) Drag coefficient.

Figure 23.- Concluded.

REISSUED 10-30-91

DECLASSIFIED